NDP
National Development Plan 2007 - 2013

epa
Environmental Protection Agency
An Ghníomhaireacht um Chaomhnú Comhshaoil

STRIVE
Report Series No.48

An Assessment of Uncertainties in Climate Modelling at the Regional Scale: The Development of Probabilistic Based Climate Scenarios for Ireland

STRIVE

Environmental Protection Agency Programme

2007-2013

SSTI
Strategy for Science, Technology and Innovation

Comhshaol, Oidhreacht agus Rialtas Áitiúil
Environment, Heritage and Local Government

Environmental Protection Agency

The Environmental Protection Agency (EPA) is a statutory body responsible for protecting the environment in Ireland. We regulate and police activities that might otherwise cause pollution. We ensure there is solid information on environmental trends so that necessary actions are taken. Our priorities are protecting the Irish environment and ensuring that development is sustainable.

The EPA is an independent public body established in July 1993 under the Environmental Protection Agency Act, 1992. Its sponsor in Government is the Department of the Environment, Heritage and Local Government.

OUR RESPONSIBILITIES

LICENSING

We license the following to ensure that their emissions do not endanger human health or harm the environment:

- waste facilities (e.g., landfills, incinerators, waste transfer stations);
- large scale industrial activities (e.g., pharmaceutical manufacturing, cement manufacturing, power plants);
- intensive agriculture;
- the contained use and controlled release of Genetically Modified Organisms (GMOs);
- large petrol storage facilities.
- Waste water discharges

NATIONAL ENVIRONMENTAL ENFORCEMENT

- Conducting over 2,000 audits and inspections of EPA licensed facilities every year.
- Overseeing local authorities' environmental protection responsibilities in the areas of - air, noise, waste, waste-water and water quality.
- Working with local authorities and the Gardaí to stamp out illegal waste activity by co-ordinating a national enforcement network, targeting offenders, conducting investigations and overseeing remediation.
- Prosecuting those who flout environmental law and damage the environment as a result of their actions.

MONITORING, ANALYSING AND REPORTING ON THE ENVIRONMENT

- Monitoring air quality and the quality of rivers, lakes, tidal waters and ground waters; measuring water levels and river flows.
- Independent reporting to inform decision making by national and local government.

REGULATING IRELAND'S GREENHOUSE GAS EMISSIONS

- Quantifying Ireland's emissions of greenhouse gases in the context of our Kyoto commitments.
- Implementing the Emissions Trading Directive, involving over 100 companies who are major generators of carbon dioxide in Ireland.

ENVIRONMENTAL RESEARCH AND DEVELOPMENT

- Co-ordinating research on environmental issues (including air and water quality, climate change, biodiversity, environmental technologies).

STRATEGIC ENVIRONMENTAL ASSESSMENT

- Assessing the impact of plans and programmes on the Irish environment (such as waste management and development plans).

ENVIRONMENTAL PLANNING, EDUCATION AND GUIDANCE

- Providing guidance to the public and to industry on various environmental topics (including licence applications, waste prevention and environmental regulations).
- Generating greater environmental awareness (through environmental television programmes and primary and secondary schools' resource packs).

PROACTIVE WASTE MANAGEMENT

- Promoting waste prevention and minimisation projects through the co-ordination of the National Waste Prevention Programme, including input into the implementation of Producer Responsibility Initiatives.
- Enforcing Regulations such as Waste Electrical and Electronic Equipment (WEEE) and Restriction of Hazardous Substances (RoHS) and substances that deplete the ozone layer.
- Developing a National Hazardous Waste Management Plan to prevent and manage hazardous waste.

MANAGEMENT AND STRUCTURE OF THE EPA

The organisation is managed by a full time Board, consisting of a Director General and four Directors.

The work of the EPA is carried out across four offices:

- Office of Climate, Licensing and Resource Use
- Office of Environmental Enforcement
- Office of Environmental Assessment
- Office of Communications and Corporate Services

The EPA is assisted by an Advisory Committee of twelve members who meet several times a year to discuss issues of concern and offer advice to the Board.

EPA STRIVE Programme 2007–2013

An Assessment of Uncertainties in Climate Modelling at the Regional Scale: The Development of Probabilistic Based Climate Scenarios for Ireland

(2005-FS-33)

STRIVE Report

Prepared for the Environmental Protection Agency

by

Department of Geography, National University of Ireland Maynooth

Author:

Rowan Fealy

ENVIRONMENTAL PROTECTION AGENCY
An Ghníomhaireacht um Chaomhnú Comhshaoil
PO Box 3000, Johnstown Castle, Co.Wexford, Ireland

Telephone: +353 53 916 0600 Fax: +353 53 916 0699
Email: info@epa.ie Website: www.epa.ie

ACKNOWLEDGEMENTS

This report is published as part of the Science, Technology, Research and Innovation for the Environment (STRIVE) Programme 2007–2013. The programme is financed by the Irish Government under the National Development Plan 2007–2013. It is administered on behalf of the Department of the Environment, Heritage and Local Government by the Environmental Protection Agency which has the statutory function of co-ordinating and promoting environmental research. The author is grateful to Met Éireann, for providing the original observed data employed in the analysis, and Professor Rob Wilby and Dr Chris Dawson, Loughborough University, for the gridded global climate model data employed in this report. The author would also like to thank Dr Conor Murphy and Winifred Power for commenting on earlier versions of this document.

EPA STRIVE PROGRAMME 2007–2013

Published by the Environmental Protection Agency, Ireland .

Printed on recycled paper.

ISBN: 978-1-84095-345-9 **06/10/150**

Price: Free

Details of Project Partner

Rowan Fealy
Department of Geography
National University of Ireland Maynooth
Co. Kildare
Ireland
Tel. +353 1 7084562
Email: rowan.fealy@nuim.ie

Table of Contents

Executive Summary

Projected changes in future climate are inherently uncertain. This uncertainty stems largely from the fact that, even for a specified emissions scenario, global climate model (GCM) simulations result in a range of plausible scenarios being modelled. While most models do agree that the globally averaged surface temperature will increase due to increasing atmospheric concentrations of greenhouse gases, there is a significant divergence between models in both the spatial and temporal projections of changes in precipitation. These differences are most pronounced at the regional scale. For example, differences are apparent in the magnitude of projected temperature changes between GCMs; for precipitation projections, both magnitude and direction of change can vary between GCMs. Nonetheless, regional scale climate information is necessary if robust adaptation strategies are to be developed.

Until recently, the use of a single climate scenario or climate trajectory was common in the literature. However, reliance on the output from a single GCM means there is significant potential for gross under- or over-estimation of the associated risks, which may result in poor decision-making and increase the risk of maladaptation.

This report presents an overview of the uncertainties that cascade or propagate through the climate modelling framework – from emissions scenarios to subsequent climate projections. It describes a methodology that has been developed for quantifying such uncertainties at the regional scale. Initially, a methodology adopted from the dynamical modelling community was used to 'pattern scale' previously downscaled emissions scenarios for selected locations in Ireland. This enabled the quantification of projected changes in temperature and precipitation for the end of the present century across four marker emissions scenarios.

In order to produce probabilistic-based scenarios of temperature and precipitation for the selected station locations, a Monte Carlo analysis was employed in conjunction with three different estimates of future warming. The projected changes in both temperature and precipitation were found to display a considerable spread in values. For example, winter temperature at one location suggested an increase from between 0.6 and 6.6°C by the 2080s' (2070–2099) period.

While the methodology outlined should enable the rapid development of probabilistic climate projections, based on a limited availability of downscaled climate scenarios, caution needs to be expressed in the interpretation of the results outlined in this report. While they provide a basis for assessing the potential risks associated to be quantified, at least one study has illustrated that details of the level of risk are not independent of the methods employed (New et al., 2007).

1 Introduction

Future projections of anthropogenic climate change arising from increased concentrations of atmospheric CO_2 are subject to a high degree of uncertainty (Jones, 2000). This stems mainly from both aleatory ('unknowable' knowledge) and epistemic, or systematic ('incomplete' knowledge) uncertainties (Hulme and Carter, 1999; Oberkampf et al., 2002).

Aleatory uncertainties are considered to be irreducible and result from an inherent indeterminacy of the system being modelled (Hulme and Carter, 1999; Oberkampf et al., 2002). For example, future human behaviour and actions are not predictable and therefore require future emissions scenarios to be prescribed on the basis of storylines or indeterminate scenario analysis (Box 1.1) (Hulme and Carter, 1999).

Epistemic or systematic uncertainties arise primarily from a lack of complete knowledge of the system, and these are considered to be reducible as our understanding or knowledge of the particular system or environment increases. For example, the envelope of possible values of the sensitivity of the climate system may be narrowed as understanding of the key climate processes improves. Conversely, additional research could also show that a particular process, which had not been included previously, could mean an increase in the climate sensitivity envelope.

Box 1.1. Special Report on Emissions Scenarios (SRES) with four scenario 'families' illustrated.

The A1 storyline and scenario family describes a future world of very rapid economic growth, global population that peaks in mid-century and declines thereafter, and the rapid introduction of new and more efficient technologies. Major underlying themes are convergence among regions, capacity building, and increased cultural and social interactions, with a substantial reduction in regional differences in per capita income. The A1 scenario family develops into three groups that describe alternative directions of technological change in the energy system. The three A1 groups are distinguished by their technological emphasis: fossil intensive (A1FI), non-fossil energy sources (A1T), or a balance across all sources (A1B).

The A2 storyline and scenario family depicts a very heterogeneous world. The underlying theme is self-reliance and the preservation of local identities. Fertility patterns across regions converge very slowly, resulting in a continuously increasing global population. Economic development is primarily regionally oriented and per capita economic growth and technological change are more fragmented and slower than in other storylines.

The B1 storyline and scenario family describes a convergent world with the same global population that peaks in mid-century and declines thereafter, as in the A1 storyline, but with rapid changes in economic structures towards a service and information economy, with reductions in material intensity, and the introduction of clean and resource-efficient technologies. The emphasis is on global solutions to economic, social, and environmental sustainability, including improved equity, but without additional climate initiatives.

The B2 storyline and scenario family describes a world in which the emphasis is on local solutions to economic, social, and environmental sustainability. It is a world with a continuously increasing global population at a rate lower than in A2, intermediate levels of economic development, and less rapid and more diverse technological change than in the B1 and A1 storylines. While the scenario is also oriented towards environmental protection and social equity, it focuses on local and regional levels.

Source: Intergovernmental Panel on Climate Change (IPCC), 2001a after Nakicenovic et al., 2000.

In addition, the climate system is considered to be a highly dynamical, non-linear system, which is sensitive to initial conditions. For a similar forcing, a range of possible climate states or equilibria is possible. There is also evidence for the presence of thresholds in the ocean-atmosphere system, which once exceeded, can result in rapid transition between stable climate equilibrium or 'eigenstates'. The exceedence of such thresholds in the climate system is associated with abrupt climate changes as the climate system shifts from one stable state to another.

Both aleatory and epistemic uncertainties can arise from a number of sources, many of which are outside the researcher's direct control. Some sources of uncertainty that were commonly encountered by Intergovernmental Panel on Climate Change (IPCC) authors of the *Third Assessment Report* (TAR) (2001a) are:

1. Problems with data:
    a) Missing components or errors in the data;
    b) Noise in the data associated with biased or incomplete observations;
    c) Random sampling error and biases (non-representativeness) in a sample.
2. Problems with models:
    a) Known processes but unknown functional relationships or errors in the structure of the model;
    b) Known structure but unknown or erroneous values of some important parameters;
    c) Known historical data and model structure, but reasons to believe parameters or model structure will change over time;
    d) Uncertainty regarding the predictability (e.g. chaotic or stochastic behaviour) of the system or effect;
    e) Uncertainties introduced by approximation techniques used to solve a set of equations that characterize the model.
3. Other sources of uncertainty:
    a) Ambiguously defined concepts and terminology;
    b) Inappropriate spatial/temporal units;
    c) Inappropriateness of/lack of confidence in underlying assumptions;
    d) Uncertainty due to projections of human behaviour (e.g. future consumption patterns, or technological change), which is distinct from uncertainty due to 'natural' sources (e.g. climate sensitivity, chaos).

(from Moss and Schneider, 2000: 38; IPCC, 2001b)

Consequently, future projections of climate for a given emissions scenario will always result in a range of possible future scenarios being simulated (Hulme and Carter, 1999). Figures 1.1 and 1.2 illustrate the range in projected mean annual temperature and precipitation response in Europe for the 2080–2099 period, relative to 1980–1999, under the A1B emissions scenario, for each of 21 multi-model data (MMD[1]) models and the mean of all models. Despite using the same emissions scenario, A1B, in all instances, significant differences are apparent between the various model realisations. Such discrepancies in model projections present significant challenges for a policy community seeking to develop cost-effective adaptation strategies which are based on these projections. While uncertainty and confidence limits are the hallmark of science, communicating such ideas to the wider community has been less than effective.

1 The Intergovernmental Panel on Climate Change (IPCC) refers to the World Climate Research Programme (WCRP) Coupled Model Intercomparison Project phase 3 (CMIP3) experiments, with idealised climate change scenarios, as the 'multi-model data set' (MMD). This naming convention is also applied here.

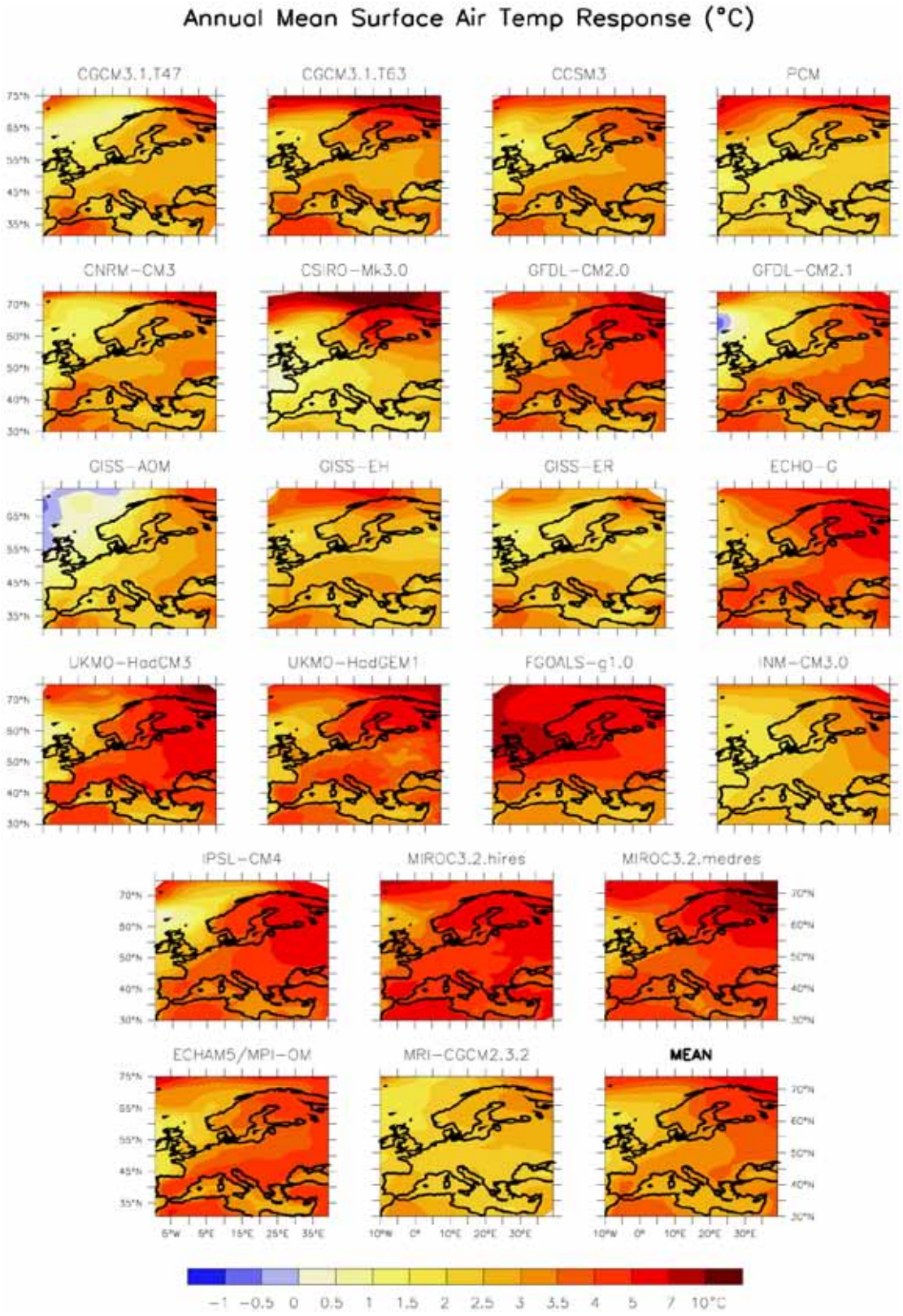

Figure 1.1. Annual mean temperature response in Europe for the years 1980–1999 to 2080–2099 under the A1B scenario, averaged over all realisations available for each of 21 multi-model data (MMD) models. The mean change, representing an average over all models is shown in the lower right-hand corner (IPCC, 2007).

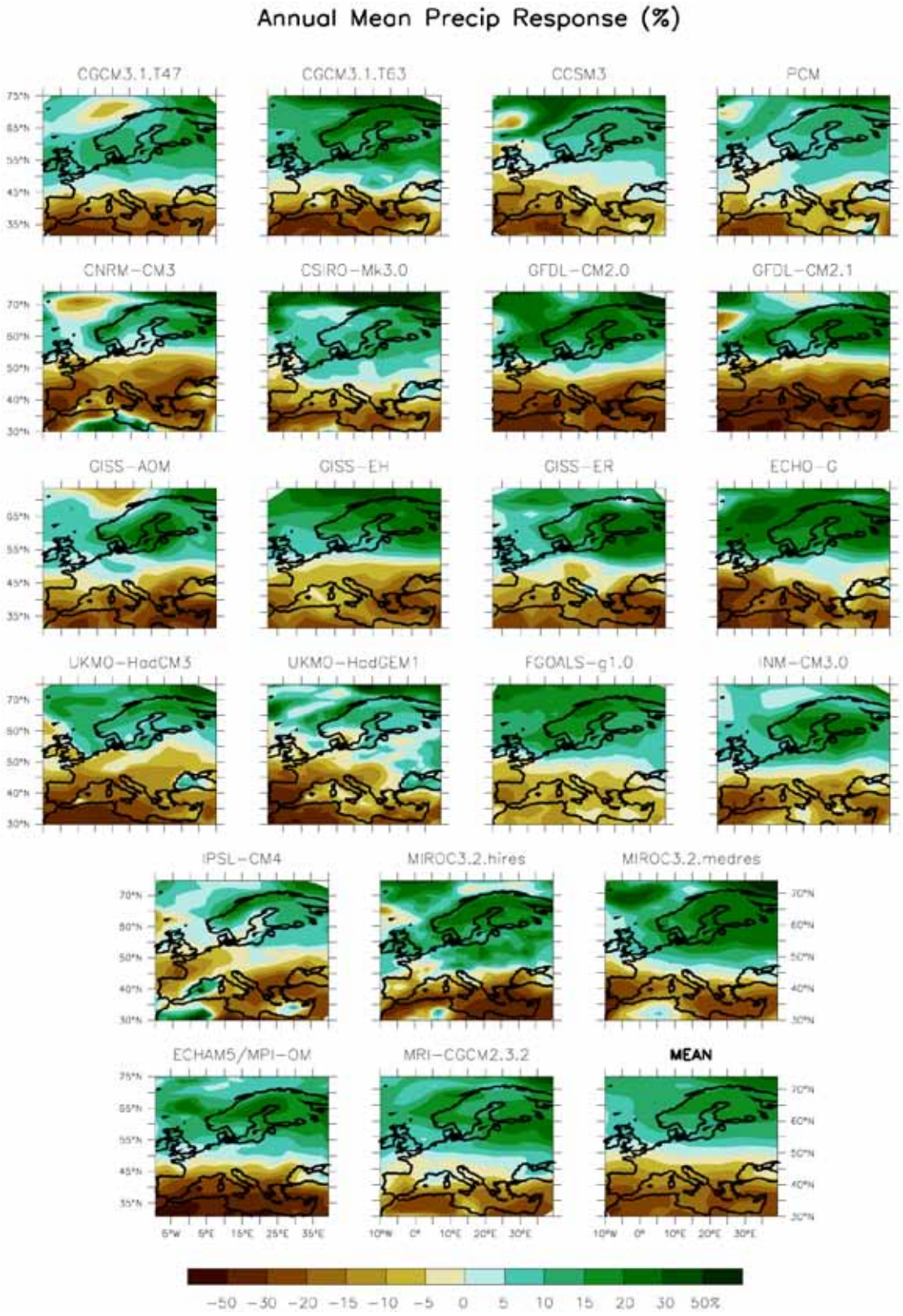

Figure 1.2. Annual mean precipitation response in Europe for the years 1980–1999 to 2080–2099 under the A1B scenario, averaged over all realisations available for each of 21 multi-model data (MMD) models. The mean change, representing an average over all models is shown in the lower right-hand corner (IPCC, 2007).

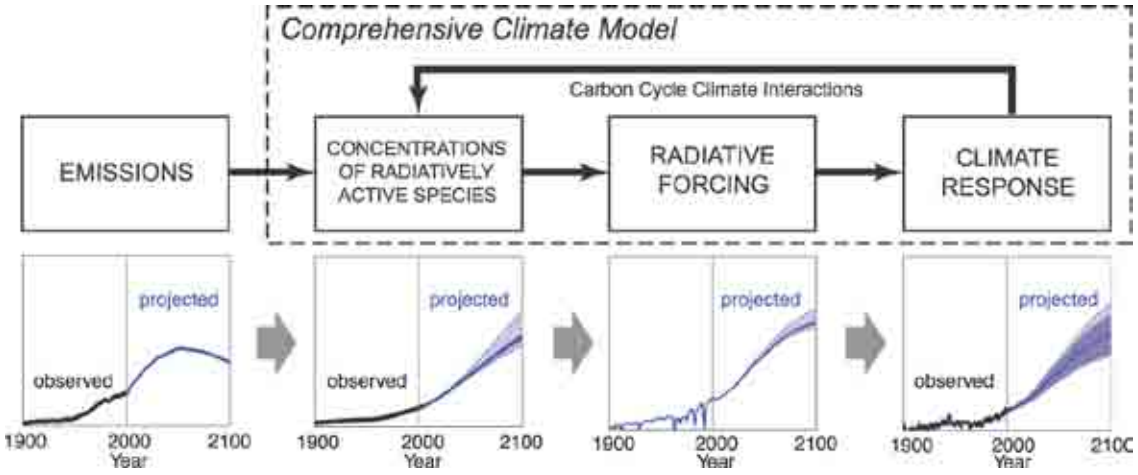

Figure 1.3. Each stage in the progression from an emissions scenario to the final climate response contributes to the uncertainty within a climate model projection due to both aleatory and epistemic uncertainties. The resulting uncertainties cascade through to the final output. (Dark shaded areas represent the mean ±1 standard deviation for 19 model tunings. The lighter shaded areas illustrate the change in the uncertainty range, if carbon cycle feedbacks are assumed to be lower or higher than in the medium setting) (Figure after IPCC, 2007).

If not accounted for adequately, the various sources of uncertainties that exist at each level in the modelling process can result in large uncertainties being associated with the model outcome (Fig. 1.3). Climate model projections are inherently uncertain because of the 'cascade of uncertainty' that results from translating future socio-economic storylines into greenhouse gas emissions and subsequent climate change scenarios (Moss and Schneider, 2000; Jones, 2000; Wilby, 2005) (Fig. 1.4). Such uncertainties need to be acknowledged at the very minimum and quantified if at all possible.

Moreover, the possibility of 'surprise' outcomes or unimaginable abrupt events that may occur because of the non-linear responses of the climate system to anthropogenic forcing must be allowed for (Hulme and Carter, 1999; Moss and Schneider, 2000). While no global climate model (GCM) to date has produced a sudden collapse in the thermohaline circulation (THC) in the North Atlantic, most GCMs do show a reduction in the THC's strength caused by increasing anthropogenic emissions, which may partially offset the resulting warming (IPCC, 2007). A reduction in the strength of the

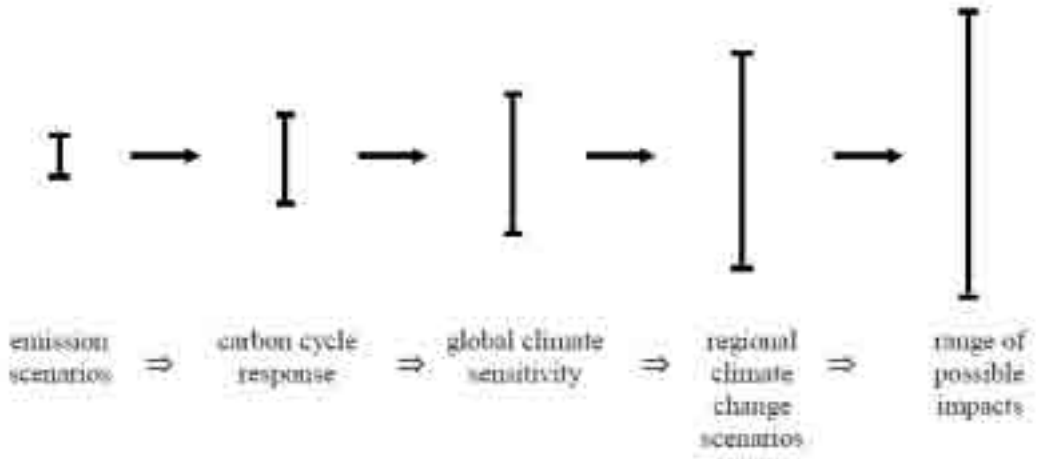

Figure 1.4. Cascade of uncertainties (IPCC, 2001a modified after Jones, 2000).

THC would have significant impacts for the development of adaptation strategies, particularly in Europe, where the rate of warming may be less than expected.

It is thought that under certain climate regimes, resulting in increased freshwater fluxes into the North Atlantic, the THC may be prone to a shift from its present 'on' state to a colder 'off' state (Broecker and Hemming, 2001; Broecker, 2006). Evidence from the Younger Dryas (~11,000 years ago) suggests that this shift could happen quite rapidly, possibly over a timescale as little as 20–50 years. While such 'surprise' events are considered to have a low probability of occurrence, their potential impact could be very large.

A number of approaches have been developed to address some of the issues that are associated with uncertainties in climate model projections, such as adopting a 'best guess' framework or taking the mean or median value from a range of scenarios (e.g. Fealy and Sweeney, 2007; 2008). Nevertheless, such top-down trajectory approaches are not considered particularly useful for subsequent use in sensitivity or risk analysis, because of an inability to attach probabilities or likelihoods to the selected climate scenario. In addition, without a clear statement on the uncertainties that have or have not been incorporated into the research, policy- and decision-makers need to exercise extreme caution as any subsequent decisions may not encompass the full range of associated risks. Such policy decisions can give rise to maladaptation (over- or under- adaptation). A further weakness of employing such top-down approaches using a single-emissions scenario is that they have tended to dismiss the possibility of local adaptation or assume only an arbitrary level of adaptation (Dessai and Hulme, 2003).

As an alternative, sensitivity analyses have been used to assess the sensitivity of a system to incremental changes in climate, and constitute a bottom-up approach to informing climate adaptation policy (Dessai and Hulme, 2003). In order to test the sensitivity of a system to changes, a single input is varied while all other inputs are held constant. More recent developments in sensitivity analysis try to account for simultaneous changes in a number of variables and can also take into account uncertainty in inputs (Katz, 2002).

A number of authors have employed analogue approaches, where present-day, or recent historic, climate variability is used as a proxy for near-term climate change (Næss et al., 2005; Pulwarty and Melis, 2001; Thomas et al., 2007). Such approaches, where adaptation measures are assessed against past climate, have also been suggested as an alternative to the probabilistic approach in impacts assessments.

However, such bottom-up approaches are not without their opponents. While sensitivity analysis can be used to generate response surfaces from which risk thresholds can be identified (such as 'dangerous' climate change), the ability to assess uncertainties in multiple inputs requires large computing power (Beven, 2001). Additionally, sensitivity analysis may not necessarily produce consistent and plausible scenarios of future changes (Jones and Mearns, 2003), nor can the timing of a projected impact be assessed. A significant weakness of the analogue approach is that it assumes that the past climate encompasses the full range of variability that is likely to occur in the future. In spite of these weaknesses, the major criticism that exponents of bottom-up approaches have of attaching probabilities to climate change projections is that the probabilistic approach takes no account of the adaptive capacity of the system being impacted (Dessai and Hulme, 2003).

Ultimately, a combination of both approaches is required, so that probabilistic-based climate scenarios and sensitivity analysis are combined to determine the vulnerability or resilience of a particular sector, community or infrastructure to climate change. Based on the vulnerability assessment, the 'local' level of resilience to a particular change in climate can be determined and, based on probabilistic scenarios, a suitable adaptation measure implemented.

While the single-trajectory top-down approach was common practice in the peer-review literature until recently, quantification of uncertainties is becoming increasingly more feasible, primarily because of increased data availability from more than one GCM modelling centre (see Figs 1.1 and 1.2 above). While a scenario represents a plausible future outcome, its usefulness is limited in that it has no degree of probability attached (Jones, 2000). In an assessment of modelling uncertainty, Murphy et al. (2004) used a pattern-scaling technique from a single GCM to estimate regional climate uncertainty according to a range of possible changes in averaged global surface temperatures. They show in one instance that the pattern-scaling approach

captured less than 10% of the variance in tropical precipitation and concluded that a single prediction from even the most sophisticated GCM will be of limited use for impact assessment. They suggest that only multi-model ensembles, which sample as wide a range of model uncertainties as possible, can reliably show the spread of possible regional changes reliably.

The use of probabilities is a well-established technique in short- and medium-range weather forecasting where uncertainty in model output is represented by the dispersion of an ensemble (Räisänen and Palmer, 2001). The incorporation of probability distribution functions (PDFs) or cumulative distribution functions (CDFs) in impact assessments is a logical development when dealing with multi-model ensembles from GCMs in order to try and quantify uncertainties of future climates at the regional scale. However, their use also presents a number of new challenges, particularly for policy-makers more familiar with the single 'best estimate' of future changes in climate (Wilby and Harris, 2006).

Increasingly, the use of probabilities in climate change impact assessments is becoming more widely accepted. As researchers move from employing single trajectory, top-down approaches towards the use of multiple scenarios from multiple GCMs in climate impact assessments, attributing likelihoods to outcomes becomes increasingly important, particularly if the outcomes are to be relevant to policy-makers. For example, if in the case of a regional projection of precipitation (a variable which is inherently difficult to simulate accurately) two GCMs produce scenarios with similar magnitude changes but opposite in sign (Giorgi and Francisco, 2000) – for instance, a 10% increase and 10% decrease – should a policy maker assume that there is going to be 0% change in precipitation.

It is likely that adaptation measures required for a 10% increase in precipitation (possibly flood defences) will be significantly different to those required for a decrease in precipitation (such as additional reservoir capacity). If probabilities could be attached to either outcome, which take account of the key uncertainties, the possibility exists for policy-makers to make 'coherent risk management decisions' and 'within resource constraints' (Paté-Cornell, 1996).

An advantage to incorporating uncertainties in the form of probabilities is that many of the potential 'end-users' of climate scenarios, such as engineers and water-resource managers, already use probabilities in estimating return periods for floods or structural reliability (Paté-Cornell, 1996; Dessai and Hulme, 2003). Strictly, probabilities employed by engineers are frequentist or classical probabilities, while climate change researchers use subjective or Bayesian probabilities (Dessai and Hulme, 2003). However, there is a significant level of understanding between both the classical and Bayesian schools, which means that probabilities associated with climate change can be communicated effectively to the user community.

2 Key Sources of Uncertainties

Uncertainties associated with GCM projections of future climate change arise from a number of sources (after Hulme and Carter, 1999; Jones, 2000). The key sources are:

1. Emissions scenarios;
2. Climate sensitivity;
3. Climate system predictability;
4. Sub-grid scale variability.

2.1 Emissions Scenarios

Due to the fact that human actions are inherently unpredictable, emissions scenarios, which are influenced by population growth, energy use, economic activity and technology, are also unpredictable in any deterministic sense. As a consequence, future emissions scenarios are prescribed according to 40 different 'storylines', which represent different rates of future world development. These are based on various scenarios of socio-economic growth, population growth, uptake of energy-efficient technologies or continued reliance on fossil fuels and regional versus global development patterns. Of the 40 scenarios developed, four marker scenarios, which are characteristic of the four scenario families (A1, A2, B1 and B2), capture the range of uncertainties associated with the emissions and driving forces spanned by the full set of the 40 scenarios (Nakicenovic et al., 2000) (see Box 1.1 in Section 1 above). Such future projections of population and development, though ultimately dependent on models and therefore subject to significant uncertainties themselves, do present a range of equally plausible future 'worlds'.

Atmospheric CO_2 concentrations levels vary significantly depending on the scenario, ranging from 540 to 970 parts per million volume (ppmv) by 2100 (IPCC, 2007), compared to present-day globally averaged atmospheric CO_2 concentration levels of just over 384 ppmv (Tans, 2009). Figure 2.1 illustrates the historical (20th century)

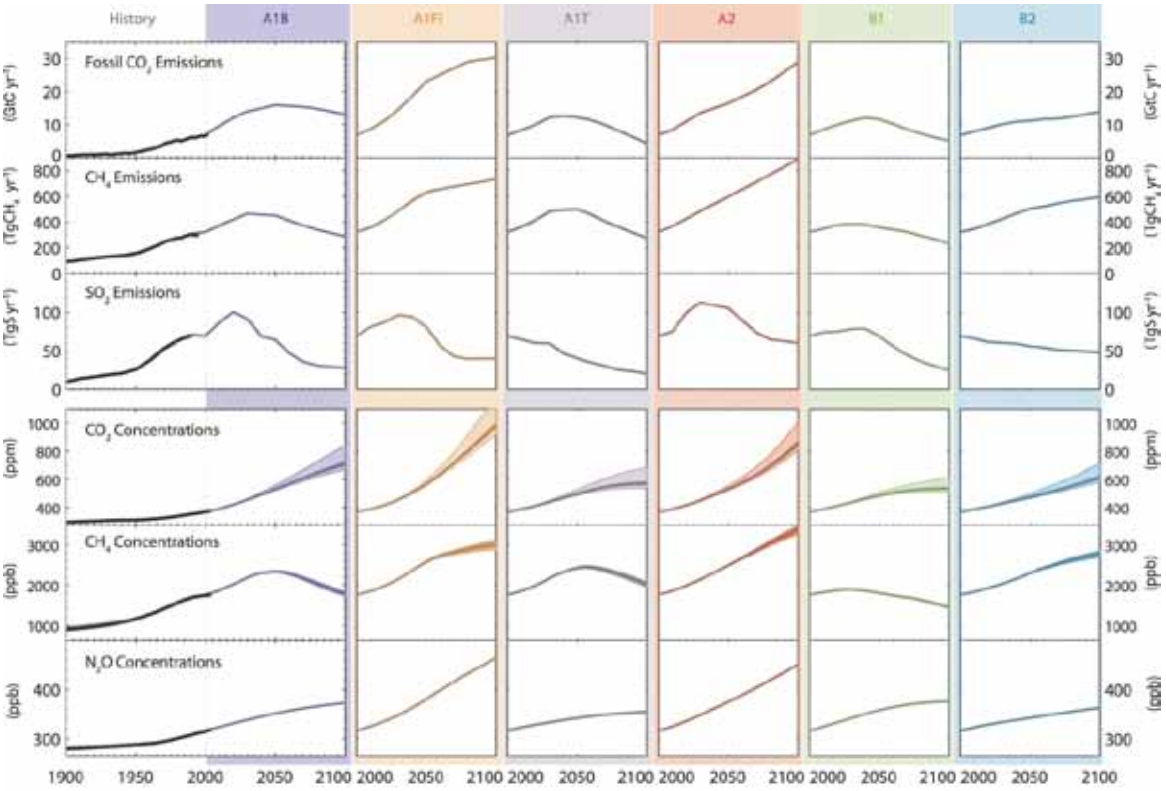

Figure 2.1. Historical (20th century) and projected (21st century) emissions of CO_2, CH_4 and SO_2 for six illustrative Special Report on Emissions Scenarios (SRES) emission scenarios (A1B, A1FI, A1T, A2, B1 and B2) and their corresponding historical and projected atmospheric concentration levels (IPCC, 2007).

and projected (21st century) emissions and resulting atmospheric concentration levels of carbon dioxide (CO_2), methane (CH_4) and sulphur dioxide (SO_2) for the six 'families' of scenarios, namely, A1B, A1FI, A1T, A2, B2 and B1.

While any particular scenario may never be realised, and hence no associated probabilities can be attached to the scenarios, they do provide an essential tool for tentatively exploring potential future changes in the climate system arising from anthropogenic activities.

2.2 Climate Sensitivity

Climate sensitivity is defined as 'the equilibrium change in global and annual mean surface air temperature, T, due to an increment in downward radiative flux, Rf, that would result from sustained doubling of atmospheric CO_2 over its pre-industrial value of ~280 ppm (2 x CO_2 ~560 ppm)' (Roe and Baker, 2007: 629).

A projected doubling of CO_2 will reduce the heat escaping from the top of the atmosphere (TOA) by approximately 3.7 Watts per square meter (Wm^{-2}). In the absence of any feedback processes, the Stefan-Boltzmann Law (which relates the amount of electromagnetic radiation emitted by a black body to its temperature), can be used to calculate the change in surface temperature of the Earth due to a change in radiative forcing arising from a doubling of CO_2 (Eqn 2.1):

$E = \varepsilon\sigma T^4$

Where

E = Energy emitted

ε = Emissivity of object

σ = 5.67 x 10-8 Wm^{-2} K^{-4} (Stefan-Boltzman constant)

T = Temperature in Kelvin

Let

E_1 = 240 W/m^2 (net outgoing radiation)

E_2 = 243.7 W/m^2 (net outgoing radiation due to a doubling of CO_2)

T_1 = 288 K (approximate present day temperature of the Earth's surface)

T_2 = Earth's surface temperature due to an increase in radiative forcing arising from a doubling of CO_2.

$$\varepsilon\sigma = \frac{E_1}{T_1^4} = \frac{E_2}{T_2^4}$$

Solving for T_2

T_2 = 289.1

T_2-T_1 = 289.1 – 288 = 1.1 K

Equation 2.1. The Stephan-Boltzmann equation, which relates the amount of electromagnetic radiation emitted by a black body to its temperature, employed to calculate the change in surface temperature of the Earth due to a change in radiative forcing arising from a doubling of CO_2. Feedbacks are not included.

While Equation 1, which includes a number of simplifying assumptions, illustrates the climate response to a doubling of pre-industrial CO_2 levels based on current understanding, it does not take account of feedbacks within the climate system, which act to amplify or dampen the climate response.

Estimates of the equilibrium climate sensitivity are dependent on the sensitivity of the climate response to radiative feedbacks associated with water vapour, lapse rates (Bony et al., 2006), clouds, snow cover and sea ice extent (Fig. 2.2). As various climate models differ in their representation of the physical process (cloud amount, cloud type, optical properties, quantity of water vapour, sea ice extent, etc.), parameterisations schemes and interactions or feedbacks between processes (after Bates, unpublished), the result is an envelope of values representing equilibrium climate sensitivity.

The TAR (IPCC, 2001a) estimated that the likely range for equilibrium climate sensitivity, including feedbacks, was 1.5 to 4.5°C. This estimate was based on expert assessments of climate sensitivity as simulated by atmospheric GCMs coupled to non-dynamic slab-oceans (IPCC, 2007). However, the TAR did not attribute probabilities to the climate sensitivity range, with the implication that all values within the quoted range were equally plausible.

A significant contribution to inter-model differences in estimating the equilibrium climate sensitivity arises from

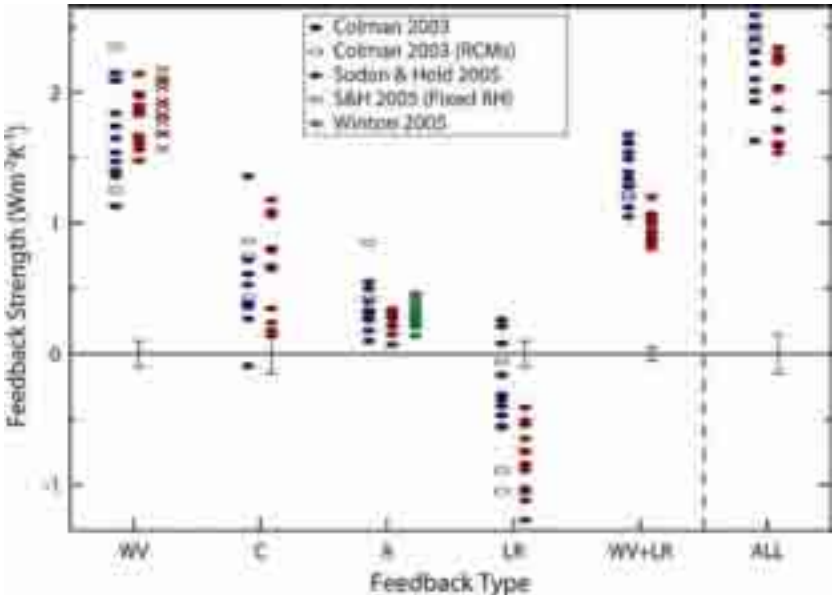

Figure 2.2. Comparison of global climate model (GCM) climate feedback parameters (W m^{-1} K^{-1} = watts per meter-kelvin) for water vapour (WV), cloud (C), surface albedo (A), lapse rate (LR) and the combined water vapour lapse rate (WV LR). ALL represents the sum of all feedbacks. Vertical bars indicate estimated uncertainty ranges in the calculation of feedbacks (Bony et al., 2006).

differences in model representations of cloud feedbacks, with low cloud amount making the largest contribution to the associated uncertainty (Fig. 2.3) (Webb et al., 2006; Williams et al., 2006; IPCC, 2007). However, Williams et al. (2006) suggest that the relationship between cloud radiative forcing and local climate response may not be model specific, as a relationship was found to exist in models that had significantly different structural elements, and therefore the uncovered relationship may have relevance in the real world. The advent of improved cloud radiative parameterisation schemes based on ongoing research into cloud feedbacks, though computationally expensive, should mean improved GCM simulations of the associated radiative forcings and result in a narrowing of the climate sensitivity envelope (Bates, unpublished; Bony, 2006).

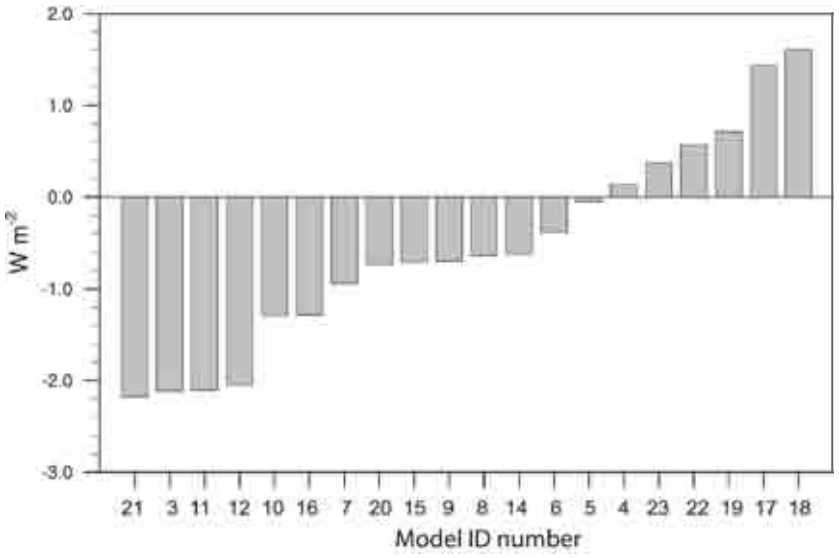

Figure 2.3. Projected changes in the global mean cloud radiative forcing (W m^{-2}) from 20 atmosphere ocean global climate models (AOGCMs) employed in the Fourth Assessment Report. Numbers correspond to the model ID number (IPCC, 2007).

In an effort to provide probabilistic-based estimates of the climate sensitivity, Wigley and Raper (2001) employed a Bayesian type approach in which five sources of uncertainty were considered – (i) emissions, (ii) climate sensitivity, (iii) carbon cycle, (iv) aerosol forcing and (v) ocean mixing – with a climate sensitivity range of 1.7 to 4.2°C derived from 7 atmosphere ocean global climate models (AOGCMs). They made the assumption that the 1.5 to 4.5°C range quoted in the TAR corresponded to the 90% confidence interval, as no confidence intervals had been attached to this range originally. They concluded that the warming rate at the upper-limit of that quoted in the TAR (0.5°C/decade), was less likely than warming towards the centre (0.3°C/decade) (Wigley and Raper, 2001).

Based on a review of recent research on assessing the equilibrium climate sensitivity in the *Fourth Assessment Report* (IPCC, 2007), the likely range of equilibrium climate sensitivity was estimated to lie between 2.0 and 4.5°C (5 to 95% probability), with a most likely value of 3°C for a normal distribution or between 2.1 and 4.6°C (5 to 95% probability) with a median value of 3.2°C for a lognormal distribution (Fig. 2.4) (IPCC, 2007). A number of different methods were employed to constrain the likely range of the climate sensitivity, including the present-day climatology and the relationship between tropical sea surface temperatures (SSTs) and climate sensitivity during the Last Glacial Maximum (LGM), which incorporated proxy records of SSTs (Fig. 2.4) (IPCC, 2007). Based on the various methods for determining the likely range of equilibrium climate sensitivity, values above 4.5°C could not be excluded, largely due to feedback processes, while the lower limit of equilibrium climate sensitivity is very likely to be larger than 1.5°C (IPCC, 2007).

2.3 Climate System Predictability

While all current GCMs suggest increasing global mean temperatures as a consequence of increased atmospheric concentrations of radiatively active species of gases, significant differences are apparent in the magnitude of the projected changes. Similarly, while all GCMs project changes to occur in the temporal and spatial distribution of precipitation, both the magnitude and direction vary significantly between GCMs.

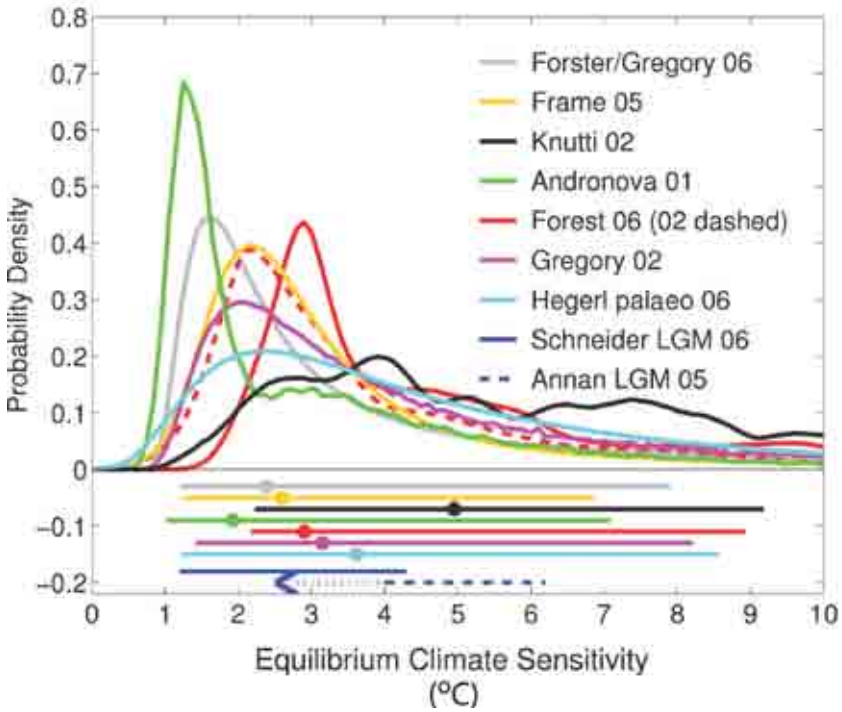

Figure 2.4. Probability distribution functions (PDFs) representing estimates of the equilibrium climate sensitivity based on various techniques, including two estimates from the Last Glacial Maximum (LGM) (IPCC, 2007).

A range of components of the climate system vary over different time horizons and spatial scales. For example, while the atmosphere is very unstable and can respond to a forcing very rapidly, the oceanic response tends to be more conservative. Even without a change in the external forcing, the natural variability of the climate system, because of natural variations in the climate system such as El Niño or the North Atlantic Oscillation (NAO), has a fundamental role in influencing the interannual to millennial scale variability of the system (IPCC, 2001b). A GCM's ability to capture such modes of variability and how they are likely to respond in a warmer world will have a significant impact on the resulting projections.

Feedback processes also play an important role in determining a climatic response to a perturbation; in complex, non-linear systems, such as the climate system, small perturbations can result in chaotic behaviour. Both the climate system and climate models are sensitive to initial conditions.

Despite the inherently chaotic behaviour of the climate, its quasi-linear response, reproduced in many GCMs, to a change in forcing suggests that some elements of the large-scale changes can be modelled with reasonable confidence. In a study of climate models' capability to reproduce the large-scale forcing of NAO, Stephenson and Pavan (2003) found that 13 out of 17 models were able to capture the key large-scale patterns of surface temperature, with 10 models producing similar indices to the observed NAO. It is likely therefore that, while evidence suggests that certain elements of the climate system may be partly predictable (IPCC, 2001b; Lambert and Boer, 2001; Stephenson and Pavan, 2003), not all the key processes are adequately captured or modelled within a particular GCM, giving rise to differences between models, and between models and observations (Fig. 2.5 (a) and (b)).

To intercompare climate model output and observations, a number of intercomparison studies have been undertaken, including the Atmospheric Model Intercomparison Project (AMIP) and the Coupled Model Intercomparison Project (CMIP1–5). These studies suggest that (i) different models reproduce different components of the climate system with varying levels of success, with no single model being the most skilful at reproducing all the components; and (ii) mean model output or averaging of ensembles provides a better fit to observations than any one individual model (Lambert and Boer, 2001).

2.4 Sub-grid Scale Variability

Owing to computational limitations, the typical spatial resolution of many AOGCMs is currently in the order of greater than 100 square kilometres (T21 ~500km; T42 ~250km; T63 ~180km and T106 ~110km). While this has been demonstrated as adequate to capture large-scale variations in the climate system, many important processes occur at much smaller spatial scales (such as processes associated with convective cloud formation and precipitation), and thus are too fine to be resolved in the modelling process.

Many climate processes therefore require parameterisation, or empirical approximation, and as such their effects can only be estimated, rather than calculated on a physical basis, within a climate model. The use of parameterisation schemes, which contribute to model uncertainty, assume that present-day parameterisations are valid under conditions of a changed climate. Such parameterisations, reflecting complex processes which are unable to be resolved, represent a simplification of such processes and ultimately lead to model errors (Tebaldi and Knutti, 2007).

A number of approaches have been employed to estimate the impact of parameter uncertainty within a GCM. One such approach is the perturbed physics ensemble (PPE) method, which seeks to quantify uncertainties associated with parameterisation schemes (Murphy et al., 2004; Tebaldi and Knutti, 2007). The PPE approach varies the uncertain model parameters, and their uncertainty ranges, systematically based on expert knowledge of the physical processes, within the model to produce multiple ensemble members from which a probability distribution of future change can be derived.

For conservatively changing large-scale features of the climate system, such as mean sea-level pressure or geopotential height (height in metres of a pressure field), sub-grid scale processes are unlikely to unduly influence the variable being modelled. However, variables such as humidity, which operate at sub-grid spatial scales, and are therefore parameterised, are

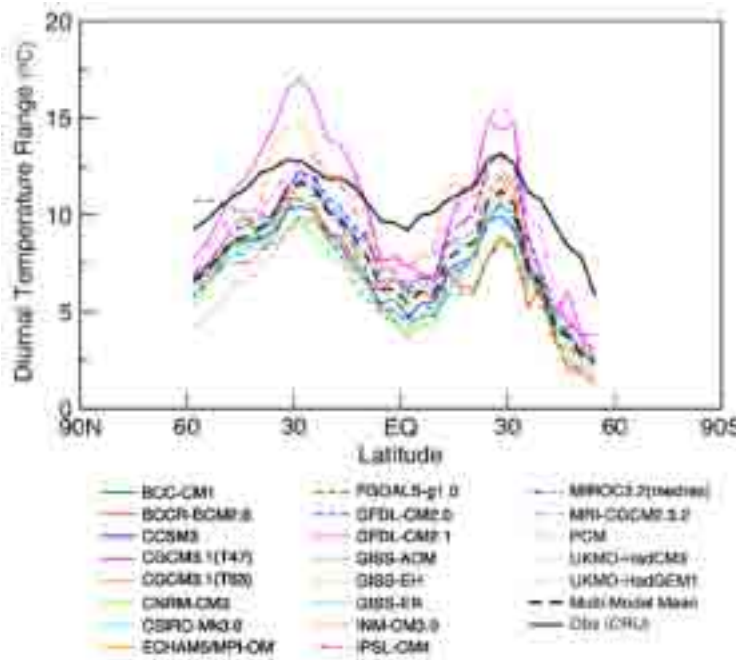

(a)

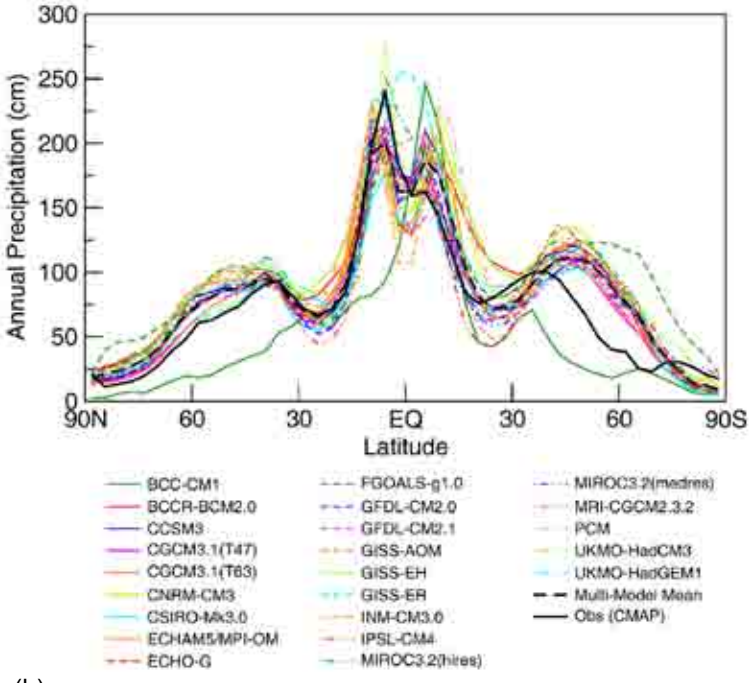

(b)

Figure 2.5 (a) and (b). Coupled Model Intercomparison Project 3 (CMIP3) 20th century model simulations for (a) Diurnal temperature range and (b) annual precipitation zonally averaged. Model data represents the period 1980–1999, while observed data for diurnal temperature is for the period 1961–1990 (Climate Research Unit [CRU]) and for precipitation, the period 1980–1999 (Climate Modelling, Analysis and Prediction [CMAP]) (IPCC, 2007).

not likely to be accurately simulated within a GCM, particularly at the regional scale.

For a location such as Ireland, where the total land area is represented by a single GCM grid box, the impacts of sub-grid scale variability are particularly relevant for a number of reasons. Differences in elevation or orography, and the morphology of the orography, between the west and east coasts, play a significant role in determining the distributional characteristics of precipitation, yet a single value for elevation is employed to represent the land area of Ireland in climate models, due to the coarse spatial resolution employed by many GCMs. Similarly, land use types, vegetation and soil characteristics, all of which influence climate processes at the regional scale, vary significantly across the country, yet are represented within the climate model by a single approximated value.

As a consequence of the coarse spatial resolution of most GCMs, there is a mismatch between the spatial scale at which GCMs operate and that required by impact modellers and policy-makers, who are faced with decision-making at city or town scale in developing appropriate and suitable adapting strategies. To address this scale mismatch, a number of techniques have been developed to 'downscale' GCM output to finer spatial and temporal scales. Regional climate models (RCMs) and statistical downscaling are two such techniques that have become the primary means by which regional- or local- scale information is derived from a parent GCM(s). This additional step, in downscaling GCM output to the regional scale, also contributes to the cascade of uncertainty within the climate modelling framework, as uncertainties in the parent GCM can propagate through to the downscaled climate projections.

Figure 2.6 shows a comparison between the percentiles of standardised monthly reanalysis data (an analysis system to perform data assimilation of observed data in a consistent framework) from the National Centres for Environmental Prediction (NCEP) and model output data from three GCMs, namely, the Canadian Centre for Climate Modelling and Analysis (CCCma-CGCM2), Australia's Commonwealth Scientific and Industrial Research Organisation (CSIRO-Mk2, referred to in figures as CSIRO) and the United Kingdom's Hadley Centre Coupled Model (HadCM3). These GCMs were previously employed to statistically downscale climate model data for Ireland (Fealy and Sweeney, 2007; 2008a; 2008b). The percentile plots show good agreement between the observed and GCM modelled atmospheric fields of sea-level pressure, vorticity (calculated variable) and geopotential height at 500 hPa. However, for the atmospheric and surface moisture variables, relative humidity at 500 hPa, near surface 2-metre relative humidity and specific humidity, the GCMs are shown to systematically over-estimate below-average humidity and under-estimate above-average humidity. Such moisture variables are often crucial for determining changes in sub-grid scale precipitation (both dynamically, through parameterisation schemes, and empirically, as a candidate predictor variable), which is an important impacts relevant variable.

Differences between model output and observed data at the regional and grid scale also arise due to an offset in temporal variability between the modelled and observed data. All GCMs appear to capture the shape of the annual cycle of near surface 2-metre temperature adequately (Fig. 2.7 (a)), while two models, CSIRO Mk2 and CGCM2, show a temporal offset in the peak in the annual temperature cycle when compared to the observations. For near surface 2-metre relative humidity, all models are shown to be much less skilful in reproducing either the shape of the annual cycle or timing of minimum humidity (Fig. 2.7 (b)). Indeed, one model simulation (CSIRO Mk2), fails to reproduce either the magnitude or direction of change in humidity for particular months.

As a consequence of the various sources of uncertainty outlined above, significant regional variations occur between model projections, even when forced with the same emissions scenario. Model structure, representation of physical processes, parameterisation schemes and sub-grid scale variability all contribute to differences between GCMs at the global, regional and grid scale (Fig. 2.8). While a particular model's ability to reproduce the statistics of the observed climate should provide a degree of confidence in a model's skill to simulate future climate, it does not guarantee that a model simulates key processes and feedbacks correctly as compensating errors may hide potential problems (Räisänen, 2001). In an analysis of GCMs from CMIP2, Räisänen (2001) found that when climate changes are averaged over areas larger than individual grid boxes, the relative agreement between models was found to improve. Model internal variability was also found to increase over a decreasing grid domain size (Räisänen, 2001).

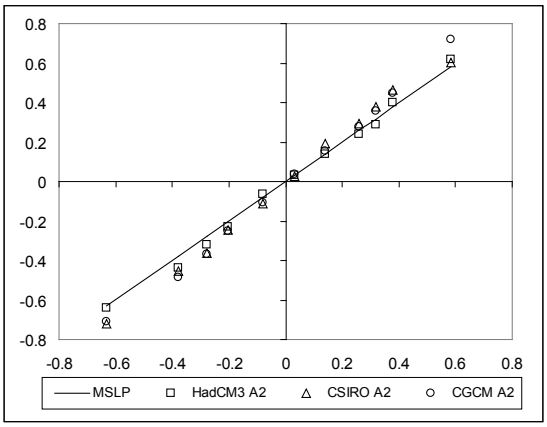

(a)

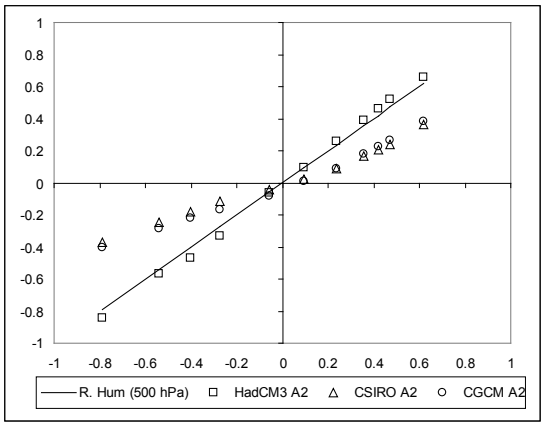

(b)

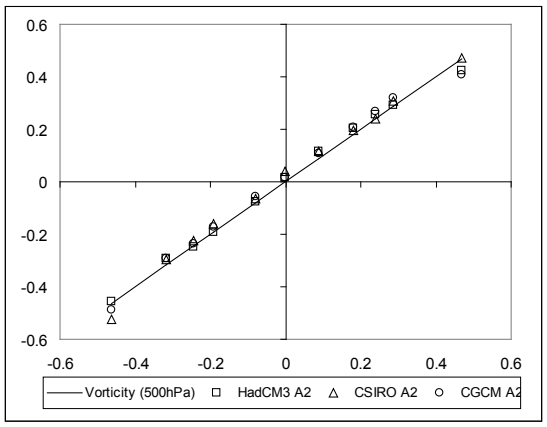

(c)

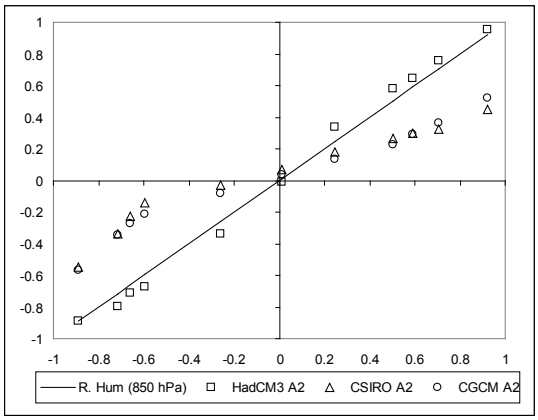

(d)

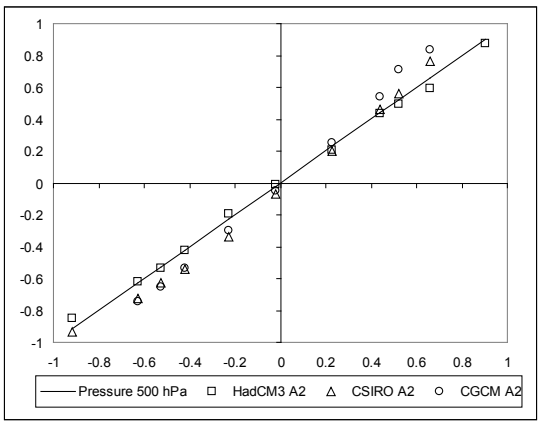

(e)

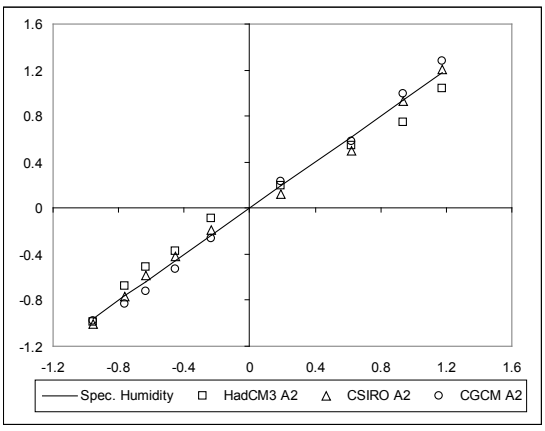

(f)

Figure 2.6. Percentile plots comparing National Centers for Environmental Prediction (NCEP) reanalysis and global climate model (GCM) model predictors (A2 emissions scenario) for a selection of atmospheric and surface variables for the baseline/control period of 1961–1990 for the grid box representing Ireland. (a) MSLP = mean sea-level pressure (surface); (b) vorticity (500 hPa), (c) geopotential height (500 hPa), (d) relative humidity (500 hPa) and (e) specific humidity (surface) (data after Wilby and Dawson, 2007).

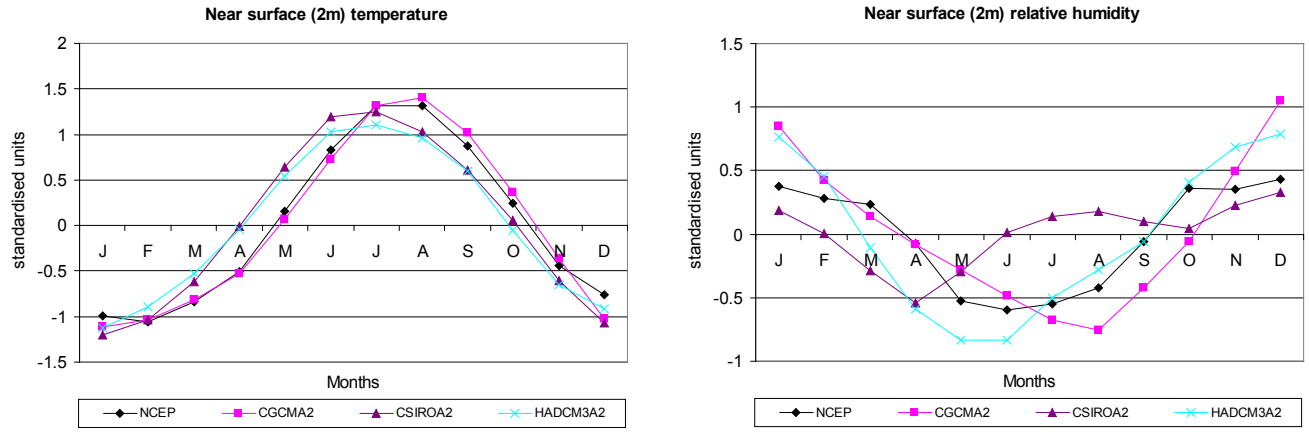

(a) (b)

Figure 2.7. Monthly near surface (2m) temperature (a) and relative humidity (b) from NCEP, CGCM2, CSIRO Mk2 and HadCM3 models for the observed baseline and model control period of 1961–2000. Global climate model (GCM) predictor values are based on the A2 emissions scenario. All values were standardised relative to their 1961–1990 mean and standard deviation and regridded to a common spatial resolution of 2.5° x 3.75° (data after Wilby and Dawson, 2007).

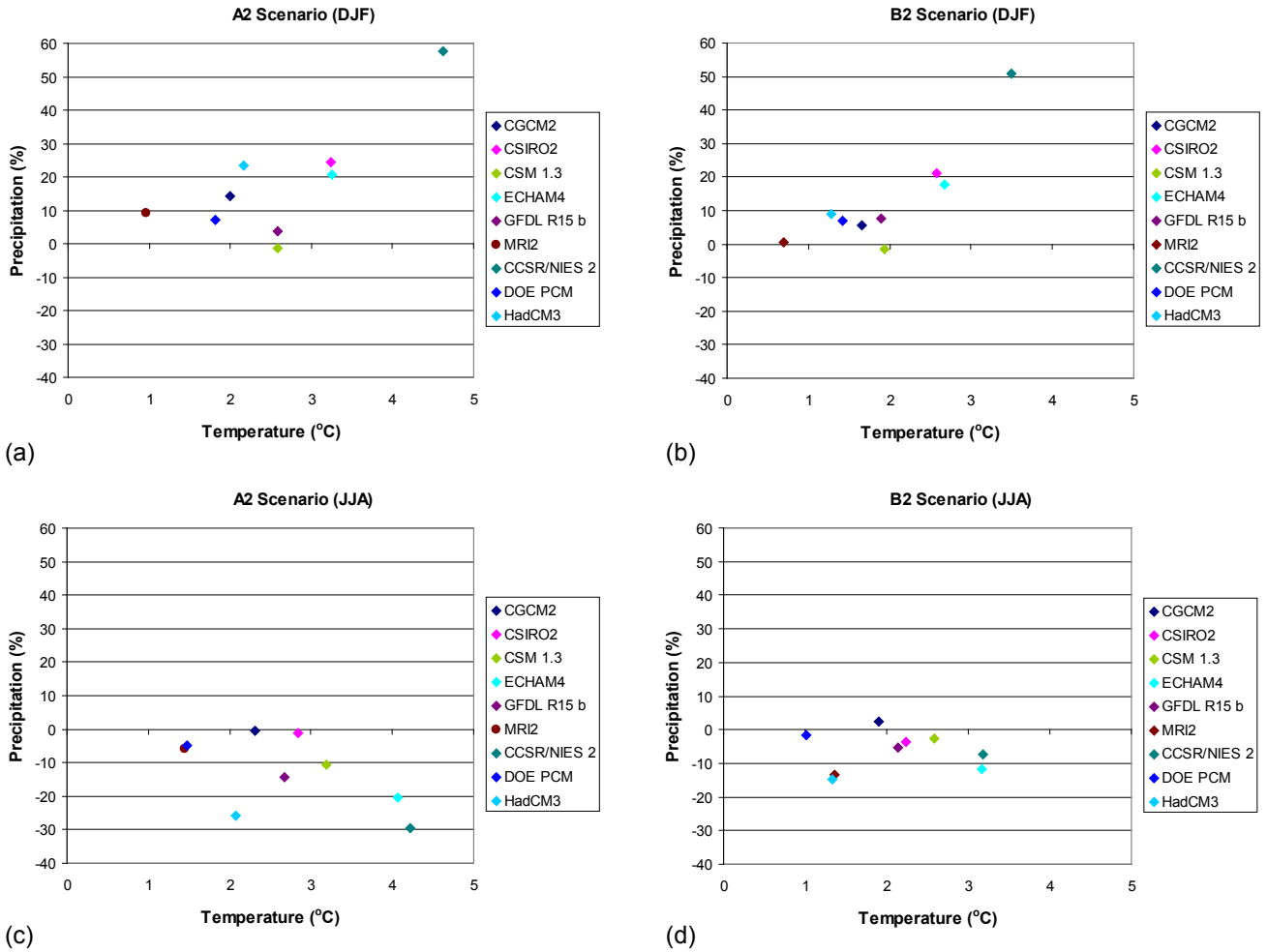

(a) (b)

(c) (d)

Figure 2.8. Projected change in mean temperature (˚C) and precipitation (%) for a grid box representing Ireland for the 2070–2099 period relative to 1961–1990 based on 9 global climate models and the A2 and B2 emissions scenarios. (a = A2 scenario for December, January and February; b = B2 scenario for December, January and February; c = A2 scenario for June, July and August; d = B2 scenario for June, July and August) (data after Mitchell et al., 2002).

3 Approaches to Quantifying Uncertainties in Regional Climate Projections for Ireland

To estimate how much confidence it is possible to have in regional climate change projections for Ireland, the various sources of uncertainty outlined in Section 2 above need to be accounted for. One method for incorporating uncertainties into downscaled projections is to use several different GCMs when constructing a climate change scenario (Table 3.1). However, differences in model reliability need to be addressed when constructing ensembles. Murphy et al. (2004) proposed a Climate Prediction Index (CPI), which is an objective means of measuring model reliability that can be used to weight different GCMs according to their relative ability to simulate the observed climate based on a broad range of observed variables. This technique has been refined by Wilby and Harris (2006), based on a narrower suite of GCM outputs relevant to statistical downscaling, to produce an Impacts Relevant Climate Prediction Index (IR-CPI). This attributes weights to each GCM based on the root-mean-square difference between the standardised modelled and observed climatological means.

Other studies have employed a Monte Carlo (MC) approach (Hulme and Carter, 1999; Jones, 2000; New and Hulme, 2000; Wilby and Harris, 2006) to quantifying uncertainties at various stages in the model framework. Hulme and Carter (1999) considered four sources of uncertainty – (i) future emissions trajectories, (ii) climate sensitivity, (iii) climate predictability and (iv) sub-grid scale variability – to allow them to examine the uncertainties that affect regional climate change for two locations in the UK for both the summer and winter seasons. They simulated the effects of different emissions scenarios and climate sensitivities on global mean temperature change using the Model of the Assessment of Greenhouse gas Induced Climate Change (MAGICC) climate model.

Hulme and Carter (1999) employed the MC approach in conjunction with the outputs from 14 different GCMs as input into a pseudo-ensemble. In the MC simulation, equal weight was given to all 14 model outcomes, in which the climate change space was sampled by 25 000 climate simulations (Hulme and Carter, 1999). Their results demonstrated not only the wide range in the regional response as simulated by the GCMs but also that the effect of different emissions scenarios only becomes apparent in the second half of the present century. In a similar analysis, New and Hulme (2000) applied their results to a response surface of annual river flow to derive PDFs for future flow changes in order to quantify a number of key uncertainties on an impact system.

Table 3.1. A simple typology of uncertainties.

Type	Indicative examples of sources	Typical approaches or considerations
Unpredictability	Projections of human behaviour not easily amenable to prediction (e.g. evolution of political systems). Chaotic components of complex systems.	Use of scenarios spanning a plausible range, clearly stating assumptions, limits considered, and subjective judgements. Ranges from ensembles of model runs.
Structural uncertainty	Inadequate models, incomplete or competing conceptual frameworks, lack of agreement on model structure, ambiguous system boundaries or definitions, significant processes or relationships wrongly specified or not considered.	Specify assumptions and system definitions clearly, compare models with observations for a range of conditions, assess maturity of the underlying science and degree to which understanding is based on fundamental concepts tested in other areas.
Value uncertainty	Missing, inaccurate or non-representative data, inappropriate spatial or temporal resolution, poorly known or changing model parameters.	Analysis of statistical properties of sets of values (observations, model ensemble results, etc.); bootstrap and hierarchical statistical tests; comparison of models with observations.

Source: IPCC, 2001b: 1.

The application of a simple scaling methodology has become more prevalent in recent years due to the widespread availability of RCM output through projects such as Prediction of Regional scenarios and Uncertainties for Defining EuropeaN Climate change risks and Effects (EU FP5 PRUDENCE) and ENSEMBLE-based Predictions of Climate Changes and their Impacts (EU FP6 ENSEMBLES). Owing to computational restrictions, RCMs are still limited to producing climate projections for a limited number of emissions scenarios, most commonly the A2 or B2 scenario, or for limited time periods. To overcome these limitations, a pattern-scaling technique, originally postulated by Santer (1990), to overcome the scarcity of GCM experiments can be applied. Indeed, this technique has found widespread use in the climate modelling community (Mitchell et al., 1999; Hulme and Carter, 2000; Kenny et al., 2000; Hulme et al., 2002).

The pattern-scaling technique allows for the rapid development of numerous climate scenarios, based on different GCM-emissions scenario combinations which sample a subset of the uncertainty range, which can then be employed in subsequent impacts analyses. For example, if the regional temperature change for the 2070–2099 period, from a particular GCM and emissions scenario is known, then a normalised 'response pattern' can be calculated by dividing by the global mean temperature change for that GCM-emissions combination (ΔT_{A2}). Employing a simple climate model, such as MAGICC, the global mean surface temperature change for the A1 scenario could be calculated for a particular model. Employing the ratio of the global mean surface temperature change for the A1 scenario to the global mean surface temperature change for the A2 scenario ($\Delta T_{A1}/\Delta T_{A2}$), the projected temperature change for the 2070–2099 period based on the A2 emissions scenario can be rescaled to produce a scaled temperature change for the A1 scenario (ΔT_{A1}) (Eqn 3.1):

$$\Delta T_{A1} = \left\langle \frac{\Delta T_{A1}}{\Delta T_{A2}} \right\rangle \Delta T_{A2}$$

Equation 3.1. Pattern scaling approach to calculate the change in surface temperature for the A1 emission scenario from the surface temperature of the A2 emissions scenarios.

The approach assumes the geographical pattern of change is independent of the forcing and that the amplitude of response is related linearly to the global mean surface temperature (Ruosteenoja et al., 2003). The assumption of a linear response, proportional to the global mean surface temperature, appears to hold in many cases, particularly for temperature, but less so for precipitation (Mitchell et al., 1999; Mitchell, 2003) as highlighted by Murphy et al. (2004). While the technique can produce a wide range of scenarios (which are useful for examining the range in projected climate response at the regional scale), the resultant scenarios are considered as being equally plausible and have no associated likelihood of occurrence.

In a study that compared seasonal-based GCM temperature and precipitation projections with RCM output for five European regions, Ruosteenoja et al. (2007) employed linear regression to relate the regional GCM response to the global mean temperature simulated by a simple climate model. The resultant 'super-ensemble' method was found to be advantageous when only a limited number of experiments were available from an individual GCM (A2 and B2) due to the reduction of random noise within the ensemble. Ruosteenoja et al. (2007) constructed 95% confidence intervals for both temperature and precipitation, for the derived pattern-scaled scenarios which could then be compared with the RCM output.

A number of authors have undertaken probabilistic-based assessments of climate change projections based on scaling the outputs from a number of RCMs with various PDFs of future warming, drawn from a number of GCMs (Hingray et al., 2007a; 2007b; Ekström et al., 2007). Rowell (2006) found that the uncertainty in the formulation of the RCM contributed a relatively small, but non-negligible, impact on projected seasonal mean climate for the UK, with the greatest contribution arising from the parent GCM, while Hingray et al. (2007b) indicate that uncertainties associated with inter-RCM variability contribute as much of the total uncertainty to the projected climate, similar in magnitude to that induced by the global mean warming.

As an alternative to a probabilistic approach to assessing GCM reliability, Giorgi and Mearns (2002) demonstrate a procedure for calculating average uncertainty range

and collective reliability of a range of regional climate projections from ensembles of different AOGCM simulations. The Reliability Ensemble Averaging (REA) method weights GCMs based on individual model performance and criteria for model convergence. In a later development, Nychka and Tebaldi (2003) demonstrate how the REA method can be 'recast' in a 'rigorous statistical framework'.

Irrespective of the approach adopted, transparency in method is considered crucial, with the onus on the individual researcher to state explicitly the approach adopted and the assumptions made to represent uncertainty (Hulme and Carter, 1999; Moss and Schneider, 2000; Dessai and Hulme, 2003).

,

4 An Assessment of Statistically Downscaled Climate Projections for Ireland

In spite of the fact that it has long been recognised that different GCMs produce significantly different regional climate responses even when forced with the same emissions scenario (Hulme and Carter, 1999), a number of previous studies have attempted to produce future climate scenarios for Ireland based on a single GCM and/or emissions scenario (McWilliams, 1991; Hulme et al., 2002; Sweeney and Fealy, 2002; Sweeney and Fealy, 2003a; 2003b; McGrath et al., 2005). These studies have acknowledged and inherent weaknesses, and Hulme and Carter (1999: 19) consider this practice, which ultimately results in the suppression of crucial uncertainties, as 'dangerous' due to any subsequent policy decisions which may only reflect a partial assessment of the risk involved (Parry et al., 1996; Risbey, 1998; New et al., 2007).

Figures 4.1 (a) and (b) illustrate GCM projected changes in monthly temperature (a) and precipitation (b) for Ireland based on four GCMs (CGCM2, CSIRO Mk2, HadCM3 and PCM) and four emissions scenarios (A1FI, A2, B2, B1) for the 2080s (2070–2099) relative to the 1961–1990 baseline. Large differences are apparent between individual GCMs and emissions scenarios. For example, in August, monthly temperature change scenarios range from 0.9 to 3.8°C, while for the month of July precipitation changes (%) are suggested to lie between -48% and +12%. In the face of such differences, paralysis in the decision-making process may be the most likely outcome.

In an attempt to produce climate ensembles for Ireland, Fealy and Sweeney (2007; 2008a; 2008b) applied the IR-CPI method after Wilby and Harris (2006) to statistically downscaled climate projections derived from the A2 and B2 emissions scenario for a range of impacts-relevant climate variables. The authors attributed an equal likelihood to both the A2 and B2 emissions scenarios. However, subjective likelihoods can easily be incorporated into this method, with relevant weightings applied to the individual emissions scenarios when combining the GCM scenarios (Wilby and Harris, 2006). While this approach considered the ability of the GCMs used in their study to reproduce the statistics of the observed climate when compared over the baseline period, the authors neglected to attach probabilities to the resultant ensembles.

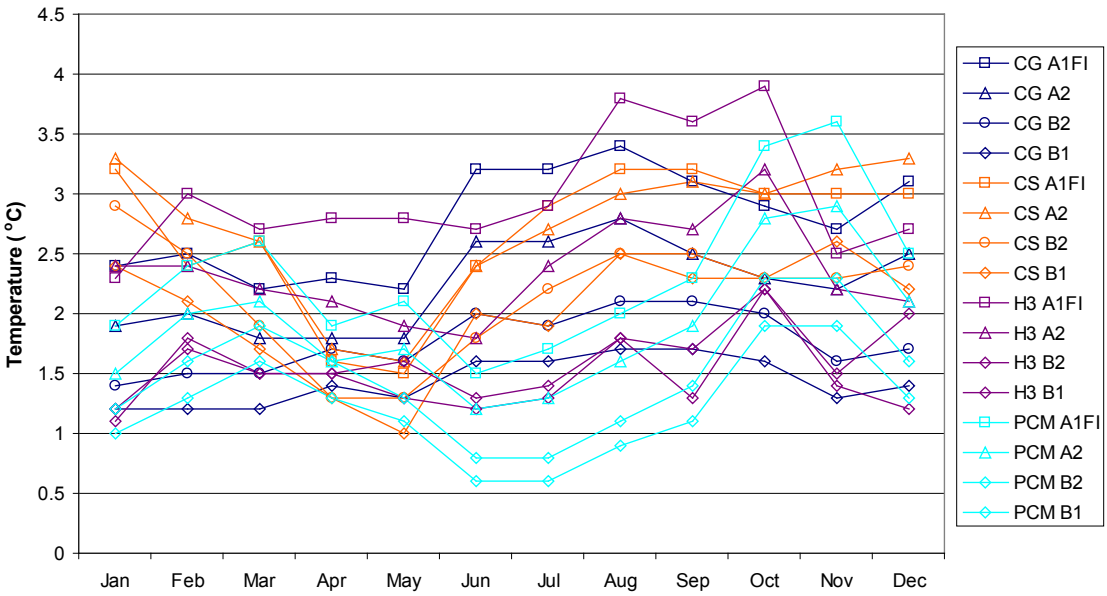

(a)

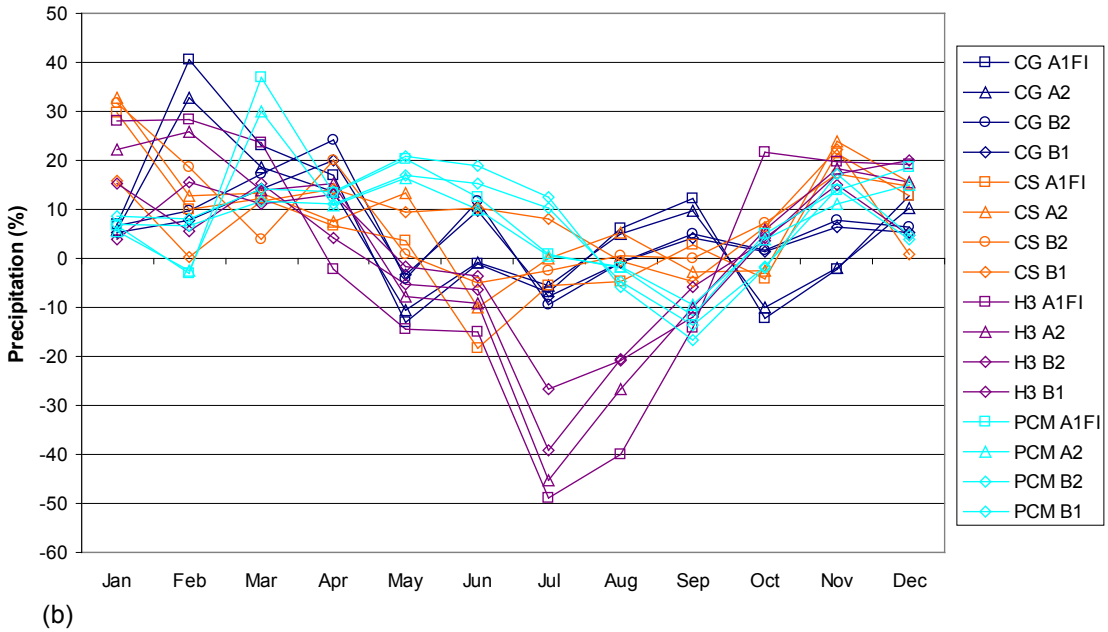

Figure 4.1. Projected changes in monthly (a) mean temperature and (b) precipitation for Ireland for the 2070–2099 period based on four global climate models (GCMs) and four emissions scenarios. CG = CGCM2 (CCCma); CS = CSIRO Mk 2 (CSIRO); H3 = HadCM3 and PCM = Parallel Climate Model (data after Mitchell et al., 2002).

The use of an additional downscaling 'layer', such as statistically downscaling a GCM to a surface environmental variable of interest, will also act to propagate the uncertainty from the driving GCM and does not account for model biases (random or systematic: see Fig. 4.2), which exist in the GCM used (Rowell, 2006; Gachon and Dibike, 2007). However, the incorporation of such an additional downscaling 'layer' can add significant value to the associated climate projection for deriving sub-grid scale information, when compared to GCM output at the grid scale. While areally averaged GCM output, such as grid scale temperature or precipitation, and point scale station level data are not directly comparable, such comparisons provide an indication of the added value of the downscaling layer, when assessed with site-specific observations.

A comparison of observed and GCM modelled (directly output from the GCM) and observed and statistically downscaled mean monthly temperatures for current (1961–1990) and future (2070–2099) periods for station locations at Valentia, Casement Aerodrome, Kilkenny and Malin Head is shown in Fig. 4.3 (a–d). Differences between observed station data (obtained from Met Éireann) and GCM output (data after Wilby and Dawson, 2007) are apparent at all stations. While differences are also evident between the observed station and statistically downscaled data (after Fealy and Sweeney, 2007; 2008a; 2008b), when averaged over calendar months, the statistically downscaled GCM data are found to lie within ±0.1°C of the observed values. In comparison, differences between the direct GCM output and observed station data range from ±0.1 to 2.5°C.

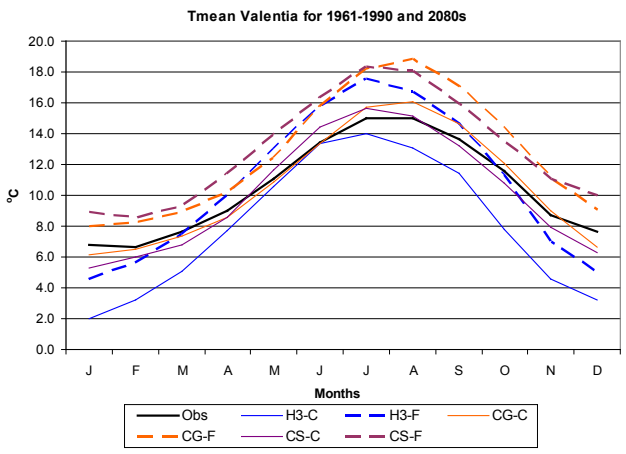
Tmean Valentia for 1961-1990 and 2080s
°C
Months
J F M A M J J A S O N D
Obs
H3-C
H3-F
CG-C
CG-F
CS-C
CS-F

(a)

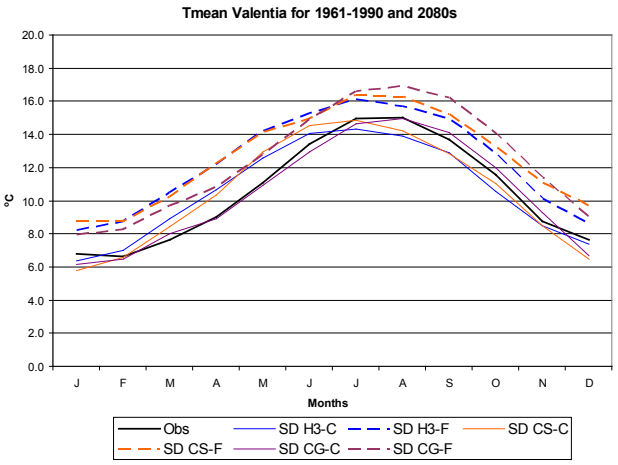
Tmean Valentia for 1961-1990 and 2080s
°C
Months
J F M A M J J A S O N D
Obs
SD H3-C
SD H3-F
SD CS-C
SD CS-F
SD CG-C
SD CG-F

(b)

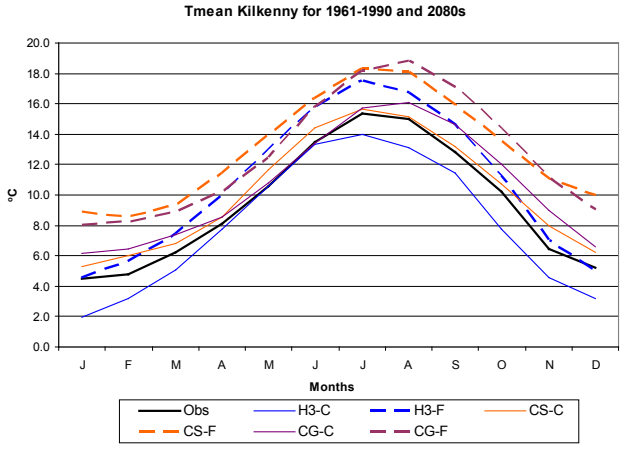
Tmean Kilkenny for 1961-1990 and 2080s
°C
Months
J F M A M J J A S O N D
Obs
H3-C
H3-F
CS-C
CS-F
CG-C
CG-F

(c)

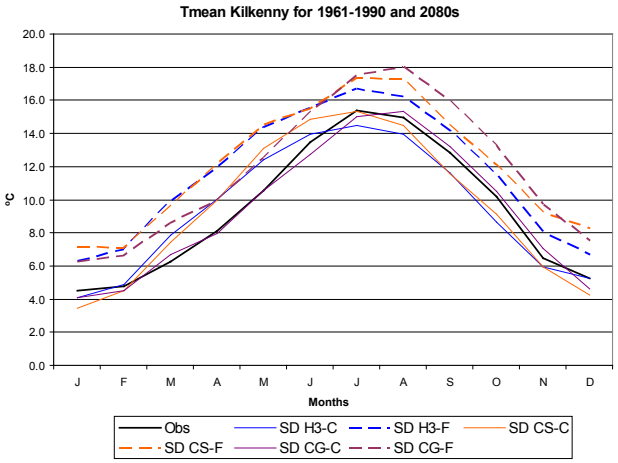
Tmean Kilkenny for 1961-1990 and 2080s
°C
Months
J F M A M J J A S O N D
Obs
SD H3-C
SD H3-F
SD CS-C
SD CS-F
SD CG-C
SD CG-F

(d)

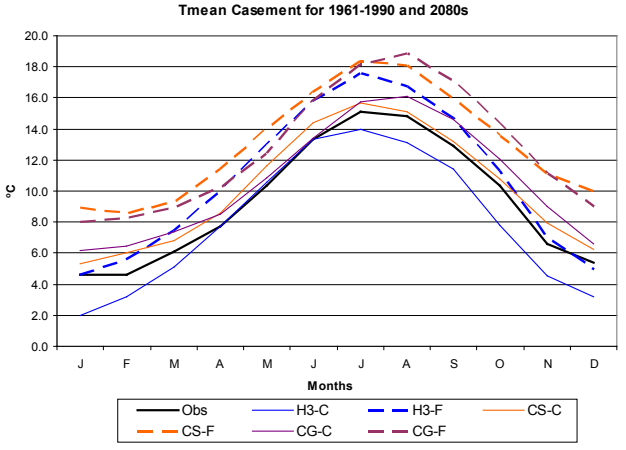
Tmean Casement for 1961-1990 and 2080s
°C
Months
J F M A M J J A S O N D
Obs
H3-C
H3-F
CS-C
CS-F
CG-C
CG-F

(e)

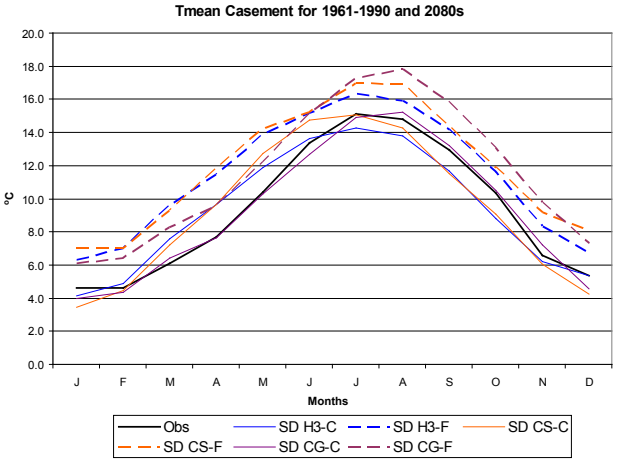
Tmean Casement for 1961-1990 and 2080s
°C
Months
J F M A M J J A S O N D
Obs
SD H3-C
SD H3-F
SD CS-C
SD CS-F
SD CG-C
SD CG-F

(f)

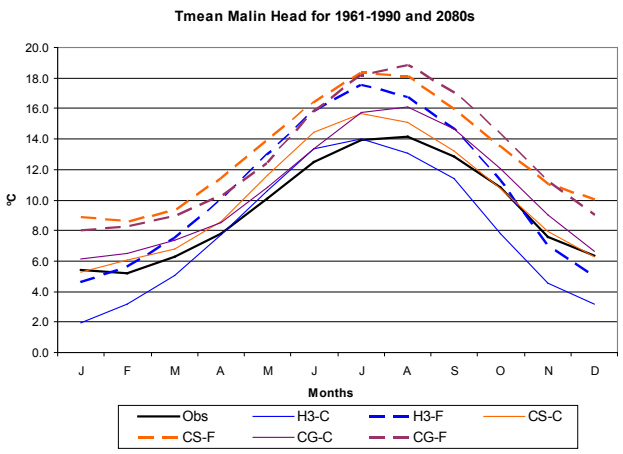

(g)

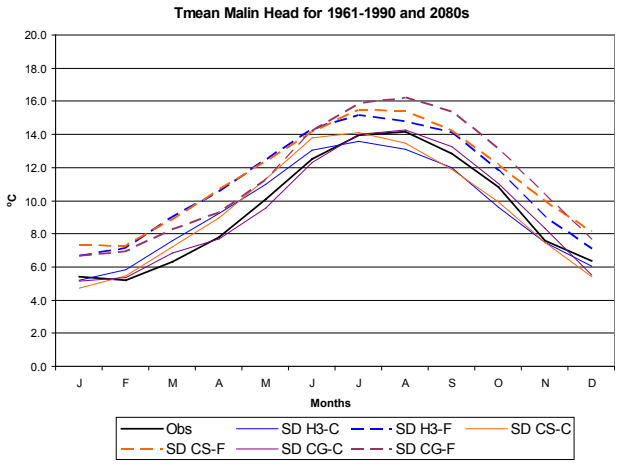

(h)

Figure 4.2. Comparison of observed and global climate model (GCM) modelled (direct global climate model (a, c, e, g) and statistically downscaled (b, d, f, h) mean monthly temperature for current (1961–1990) and future (2070–2099) periods for Valentia (a, b), Kilkenny (c, d), Casement Aerodrome (e, f) and Malin Head (g, h). The statistically downscaled data has not been bias corrected. All modelled scenarios are based on the A2 emissions scenario. Obs = observed station data, H3 = HadCM3, CS = CSIRO Mk2, CG = CGCM2, SD indicates statistically downscaled from parent global climate model, C = current or model baseline (1961–1990) and F = future (2070–2099) (GCM data after Wilby and Dawson, 2007; observed data from Met Éireann; statistically downscaled data after Fealy and Sweeney, 2007; 2008a; 2008b; modified after Gachon and Dibike, 2007).

An additional step, employed by Fealy and Sweeney (2007; 2008b), corrected the bias in the statistically downscaled data which resulted in an improvement in the correspondence between the downscaled scenarios and observed data (Fig. 4.4). This bias correction was also applied to the future projections, under the assumption that it was a systematic bias.

A comparison of PDFs between the observed GCM output and statistically downscaled data demonstrates a better correspondence between the observed and statistically downscaled data than with the GCM output. Seasonal PDFs of temperature are shown in Fig. 4.4 for Valentia (a coastal maritime-influenced station) and in Fig. 4.5 for Kilkenny (an interior, continental station). At both stations, the statistically downscaled data are shown to reproduce the mean and standard deviation of the observed data more faithfully than the PDFs derived from the GCM output (Tables 4.1 and 4.2).

Table 4.1. Seasonal means ($\bar{x}$) and standard deviations (s) for mean seasonal temperature at Valentia (observed), direct global climate model output (global climate model [GCM]) from HadCM3 (H3), CSIRO Mk2 (CS) and CGCM2 (CG), statistically downscaled (SD) and bias corrected statistically downscaled for the 1961–1990 period.

	Season	Obs.	GCM			No bias correction			Bias correction		
		Valentia	H3	CG	CS	H3-SD	CG-SD	CS-SD	H3-SD	CG-SD	CS-SD
$\bar{x}$	DJF	*7.0*	2.8	6.4	5.9	6.9	6.4	6.3	*7.0*	*7.1*	*7.0*
	MAM	*9.2*	7.8	8.9	9.0	10.7	9.3	10.6	*9.3*	*9.2*	*9.2*
	JJA	*14.5*	13.5	15.1	15.1	14.1	14.2	14.6	*14.4*	*14.4*	*14.5*
	SON	*11.3*	7.9	11.9	10.6	10.7	11.8	10.8	*11.3*	*11.3*	*11.3*
s	DJF	*2.6*	4.4	1.8	2.9	3.3	1.8	2.1	*2.8*	*2.7*	*2.8*
	MAM	*2.6*	3.5	2.1	2.8	2.4	2.0	2.5	*2.7*	*2.8*	*2.7*
	JJA	*1.9*	2.2	1.8	1.6	1.3	1.4	1.3	*2.0*	*2.2*	*2.0*
	SON	*3.0*	4.3	3.0	2.9	2.9	2.6	2.4	*3.3*	*3.2*	*3.2*

Italic shows observed data. DJF = December, January, February; MAM = March, April, May; JJA = June, July, August; SON = September, October, November. (Observed data after Met Éireann; GCM outputs after Wilby and Dawson, 2007; statistically downscaled data after Fealy and Sweeney, 2007; 2008b.)

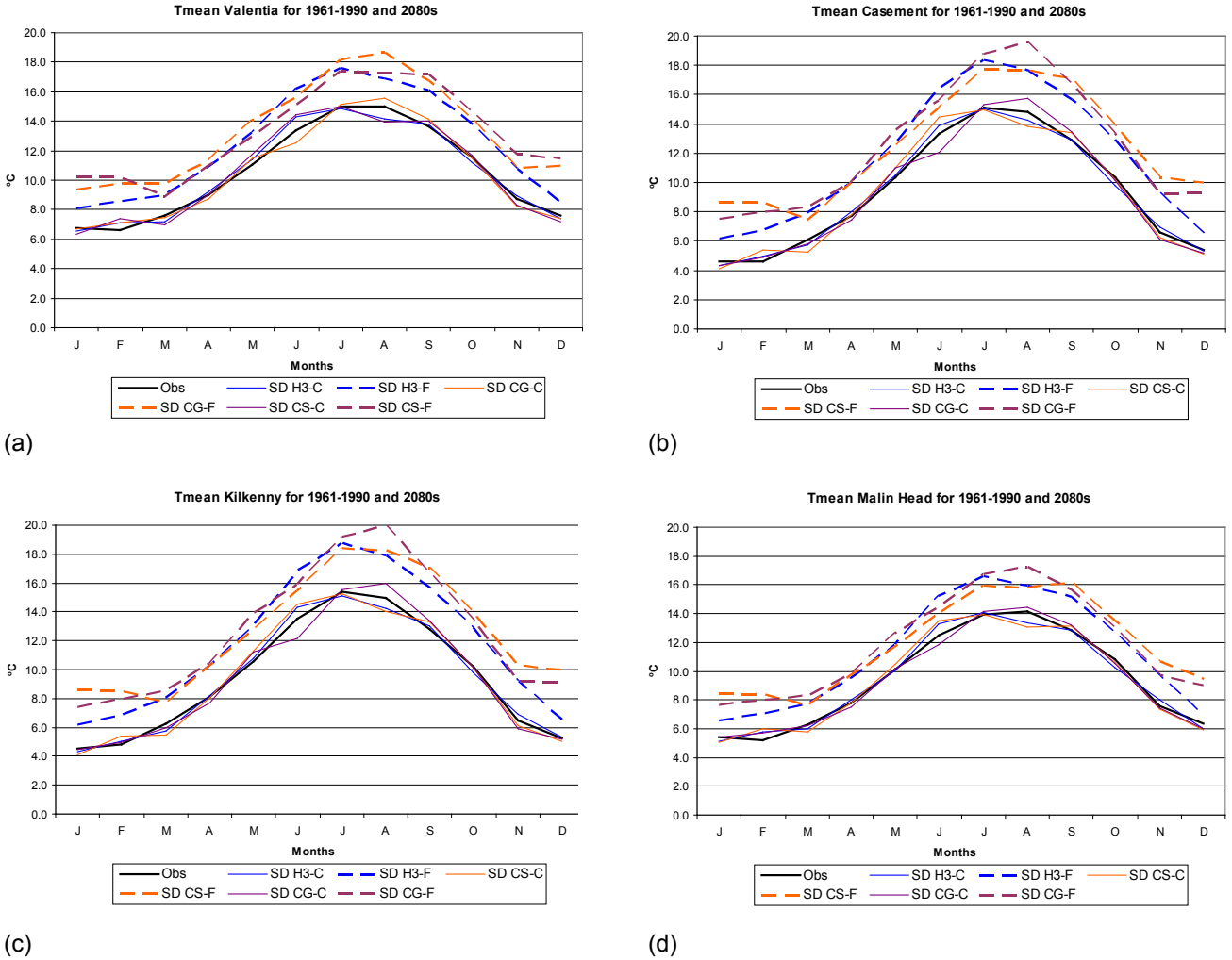

Figure 4.3. Comparison of observed and bias corrected statistically downscaled mean monthly temperature for current (1961–1990) and future (2070–2099) periods for (a) Valentia, (b) Casement Aerodrome, (c) Kilkenny and (d) Malin Head. All global climate model (GCM) modelled scenarios are based on the A2 emissions scenario. Obs = observed station data, H3 = HadCM3, CS = CSIRO Mk2, CG = CGCM2, SD indicates statistically downscaled from parent global climate model , C = current or model baseline (1961–1990) and F = future (2070–2099) (GCM data after Wilby and Dawson, 2007; observed data from Met Éireann; statistically downscaled data after Fealy and Sweeney, 2007; 2008a; 2008b; modified after Gachon and Dibike, 2007).

Table 4.2. Seasonal means ($\bar{x}$) and standard deviations (s) for mean seasonal temperature at Kilkenny (observed), direct global climate model output (global climate model [GCM]) from HadCM3 (H3), CSIRO Mk2 (CS) and CGCM2 (CG), statistically downscaled (SD) and bias corrected statistically downscaled for the 1961–1990 period.

	Season	Obs	GCM			No bias correction			Bias correction		
		Kilkenny	H3	CG	CS	H3-SD	CG-SD	CS-SD	H3-SD	CG-SD	CS-SD
$\bar{x}$	DJF	*4.9*	2.8	6.4	5.9	4.7	4.4	4.0	*4.9*	*4.9*	*4.8*
	MAM	*8.3*	7.8	8.9	9.0	10.1	8.4	10.2	*8.3*	*8.3*	*8.3*
	JJA	*14.6*	13.5	15.1	15.1	14.1	14.4	14.9	*14.6*	*14.6*	*14.6*
	SON	*9.8*	7.9	11.9	10.6	8.7	10.3	8.9	*9.9*	*9.8*	*9.9*
s	DJF	*3.1*	4.4	1.8	2.9	3.9	2.4	2.8	*3.3*	*3.2*	*3.4*
	MAM	*3.0*	3.5	2.1	2.8	2.9	2.4	3.0	*3.3*	*3.3*	*3.1*
	JJA	*2.4*	2.2	1.8	1.6	1.6	1.8	1.6	*2.6*	*2.7*	*2.4*
	SON	*3.9*	4.3	3.0	2.9	3.8	3.4	3.1	*4.1*	*4.1*	*4.0*

Italic shows observed data. DJF = December, January, February; MAM = March, April, May; JJA = June, July, August; SON = September, October, November. (Observed data after Met Éireann; GCM outputs after Wilby and Dawson, 2007; statistically downscaled data after Fealy and Sweeney, 2007; 2008b.)

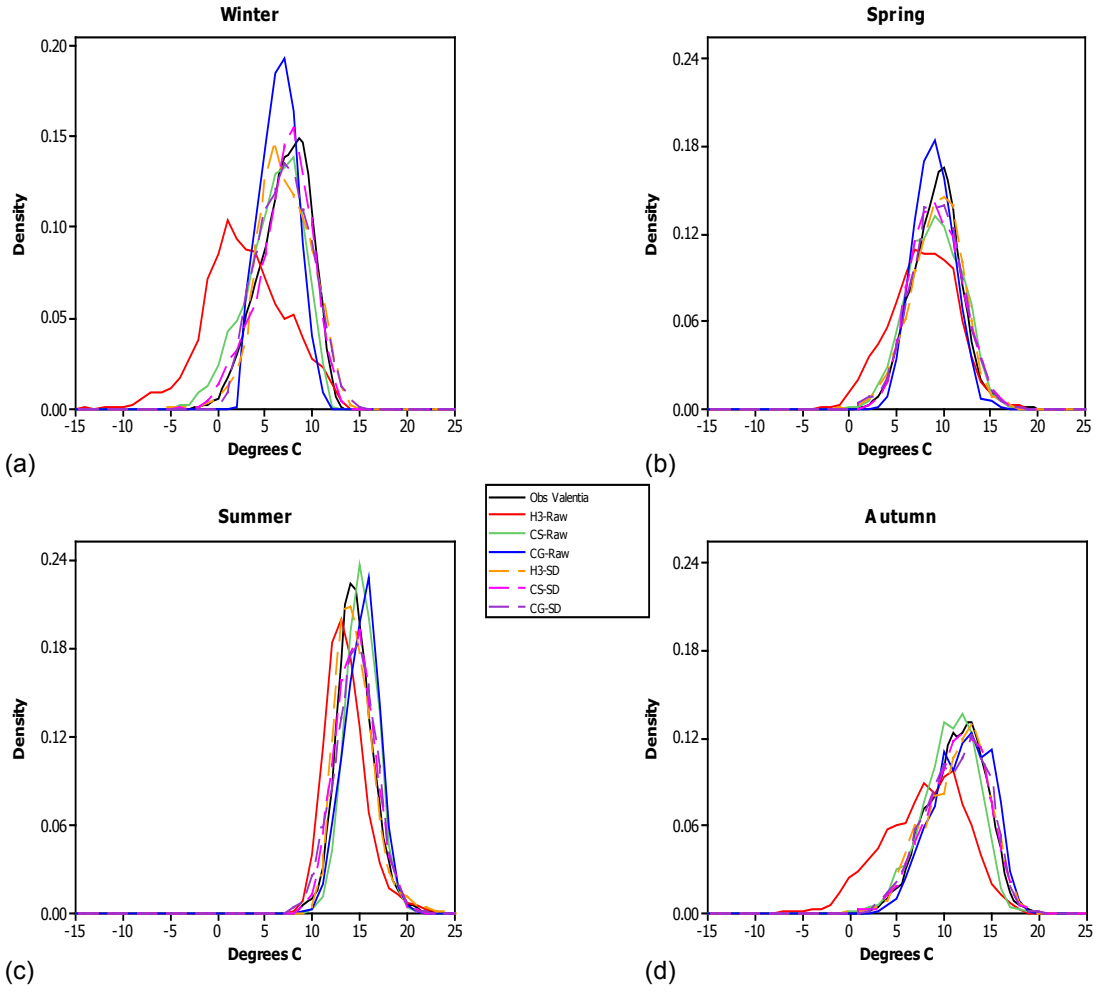

Figure 4.4. Probability distribution functions (PDFs) of mean daily observed temperature at Valentia, direct global climate model (GCM) mean temperature (Raw) and bias corrected statistically downscaled (SD) mean temperature for the 1960–1990 period for the A2 emissions scenario (a = December, January, February; b = March, April, May; c = June, July, August; d = September, October, November.) (Observed data from Met Éireann; GCM data after Wilby and Dawson, 2007; statistically downscaled data after Fealy and Sweeney, 2007; 2008b.)

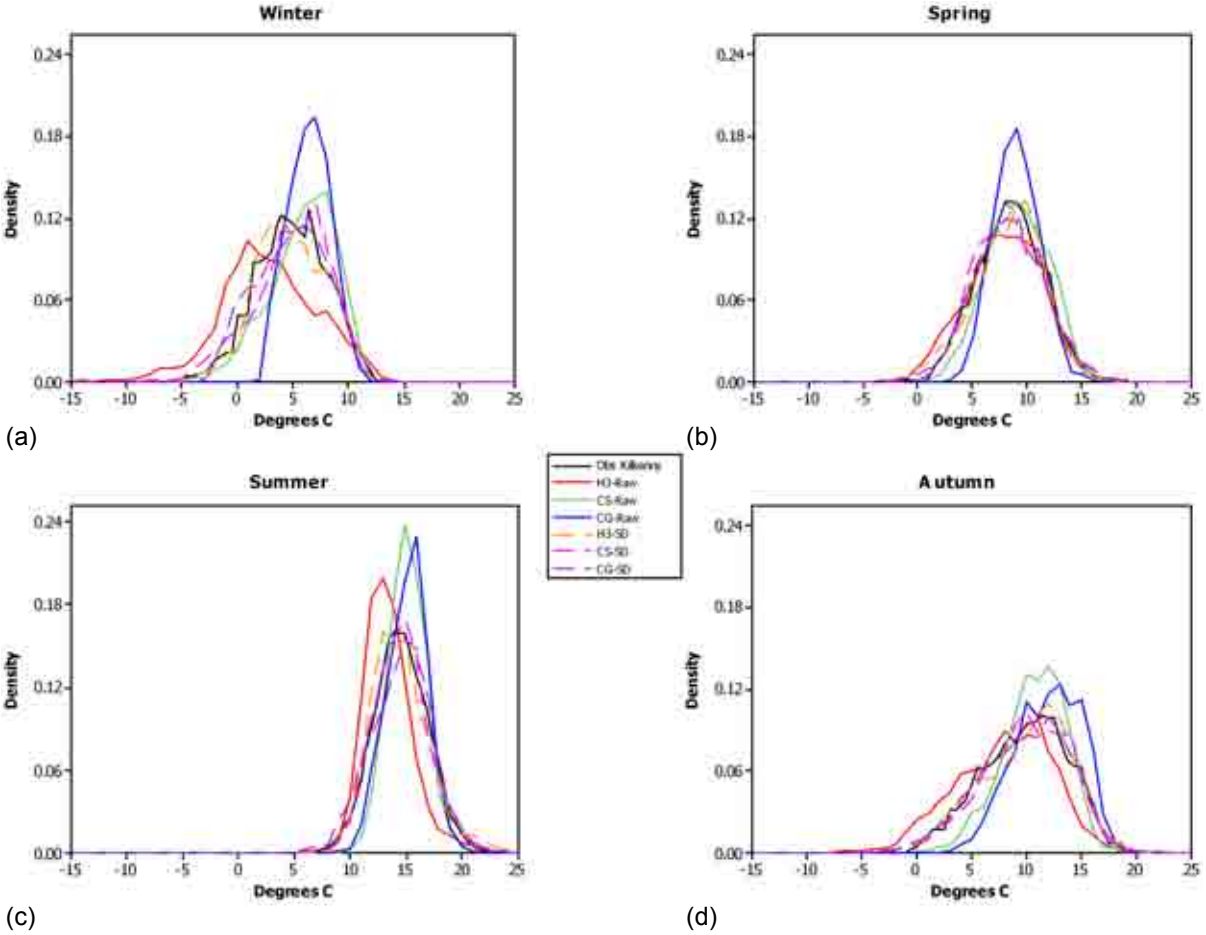

Figure 4.5. Probability distribution functions (PDFs) of mean daily observed temperature at Kilkenny, direct global climate model mean temperature (Raw) and bias corrected statistically downscaled (SD) mean temperature for the 1960–1990 period for the A2 emissions scenario. a = December, January, February; b = March, April, May; c = June, July, August; d = September, October, November. (Observed data from Met Éireann; global climate model data after Wilby and Dawson, 2007; statistically downscaled data after Fealy and Sweeney, 2007; 2008b.)

Figures 4.6 and 4.7 show the empirical quantile-quantile plots for daily precipitation at Valentia (Fig. 4.6) and Kilkenny (Fig. 4.7) with observed, GCM modelled and statistically downscaled data. At both stations, GCM and statistically downscaled simulations underestimate observed precipitation over the 1961–1990 period. The statistically downscaled data at Valentia, while underestimating observed values, offers a significant improvement over the GCM output. At Kilkenny, the skill level of both simulated datasets would appear to be comparable, with statistical downscaling offering no obvious improvement over the GCM output. Seasonal PDFs of observed, GCM output and statistically downscaled precipitation for Valentia and Kilkenny for the period 1961–1990 can be found in Appendix I.

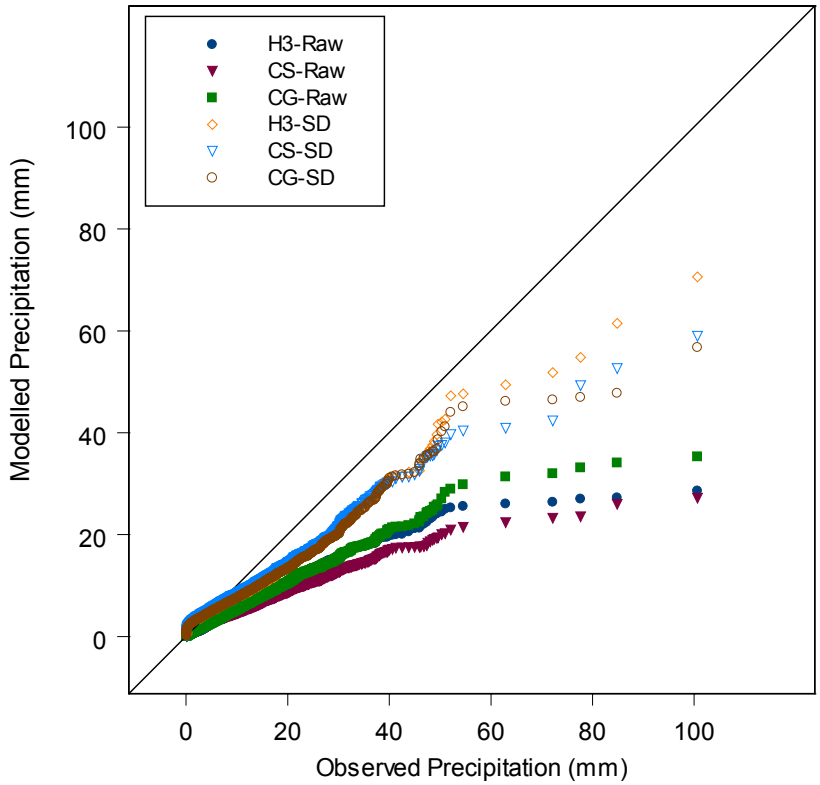

Figure 4.6. Empirical quantile-quantile plots for observed, direct global climate model (GCM) output (Raw) and statistically downscaled (SD) precipitation at Valentia for the period 1961–1990. H3 = HadCM3, CS = CSIRO Mk2 and CG = CGCM2.

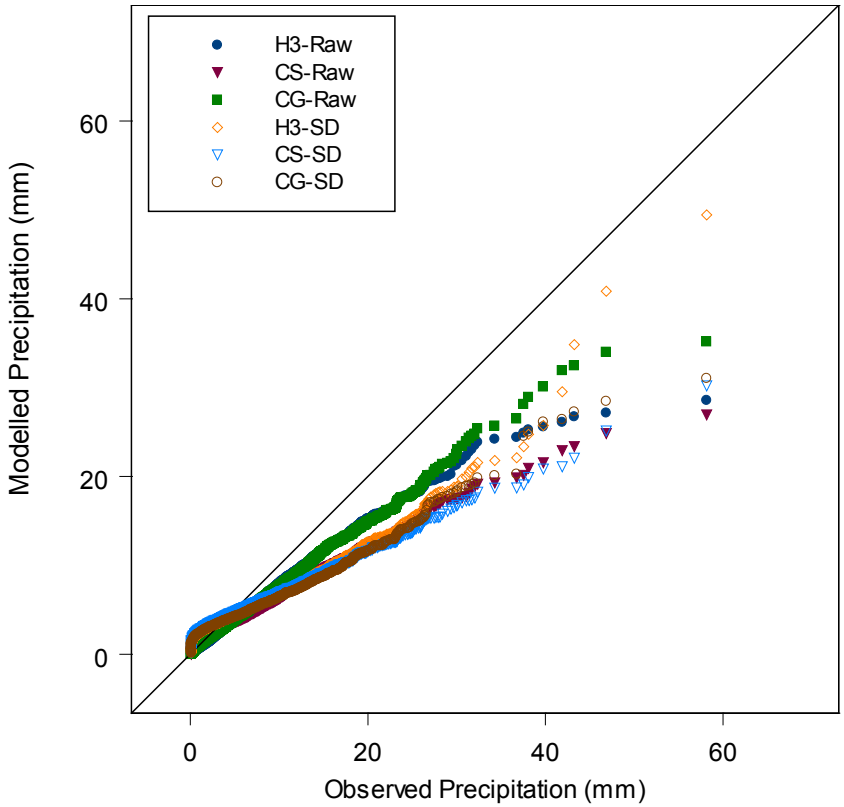

Figure 4.7. Empirical quantile-quantile plots for observed, direct global climate model output (Raw) and statistically downscaled (SD) precipitation at Kilkenny for the period 1961–1990. H3 = HadCM3, CS = CSIRO Mk2 and CG = CGCM2.

Climate models ultimately represent a simplification of what is a very complex system, and deficiencies in their ability to reproduce the statistics of the observed series – particularly that of precipitation – can arise for a number of reasons, such as the omission of a key climate process within the model and the use of a particular parameterisation scheme. Nonetheless, weaknesses also arise because of a dependency of variables (such as precipitation) on climate processes that occur at a scale smaller than can be resolved by the current evolution of GCMs. As a consequence, GCMs tend to produce a 'drizzle effect', where sub-grid scale precipitation such as a convective precipitation event is effectively averaged over the grid box, resulting in low-intensity precipitation being simulated for the grid box.

In a comparison of the shape and scale parameters of an empirical gamma distribution fit to observed, GCM and statistically downscaled precipitation data, GCM grid scale precipitation was found to more closely approximate the statistical properties of the observed data, in spite of the simplifying processes within the GCM structure. Fealy and Sweeney (2008a; 2008b) employed a generalised linear model (GLM) to statistically downscale precipitation for station locations around Ireland as this method assumes that the dependent variable, or predictand, is from a particular distribution of the exponential family, of which the gamma distribution belongs. A comparison of PDFs for the observed, GCM modelled and statistically downscaled data at Valentia and Kilkenny suggests that the statistical downscaling approach overestimates the frequency of the occurrence of precipitation events of around 5 millimetres (mm) at both stations. These differences are likely to arise from the two-step methodology employed in the statistical downscaling approach. Initially, a logistic regression model is used to model precipitation occurrence as a binary sequence. Daily precipitation amounts, modelled using the GLM approach, are then selected on the basis of days on which precipitation is modelled to occur. The optimum predictors differ between both the occurrence and the amounts models as predictors that capture precipitation amounts differ from those that 'trigger' the precipitation event. While differences arise in the shape and scale parameters of the statistically downscaled and observed precipitation, when mean daily precipitation (mm/day) is compared over a seasonal basis, the statistically downscaled data performs much better than the GCM simulations in reproducing the mean, while the GCMs appear to be more skilful in capturing the standard deviation (Tables 4.3 and 4.4).

The development of downscaled scenarios, either through dynamic regional climate modelling or statistical downscaling, will add to the propagation of errors within the modelling framework (Rowell, 2006; Hingray et al., 2007b; Dibike et al., 2008). However, in order to provide information at a scale that is useful for decision-makers, such downscaling efforts continue to remain a crucial step in developing robust adaptation strategies, assuming the various contributions to uncertainty are accounted for adequately.

Table 4.3. Seasonal mean daily precipitation ($\bar{x}$) and standard deviations (s) for Valentia (observed), direct global climate model (GCM) output (global climate model [GCM]) from HadCM3 (H3), CSIRO Mk2 (CS) and CGCM2 (CG), statistically downscaled (SD) for the 1961–1990 period.

	Season	Obs	GCM			SD		
		Valentia	H3	CG	CS	H3-SD	CG-SD	CS-SD
$\bar{x}$	DJF	*5.0*	2.8	3.6	3.0	*4.7*	*5.0*	*5.3*
	MAM	*3.1*	2.4	2.8	2.4	*2.7*	*3.2*	*3.3*
	JJA	*2.9*	2.6	2.2	2.8	*2.7*	*2.0*	*2.8*
	SON	*4.7*	2.7	3.4	3.2	*5.3*	*5.4*	*5.7*
s	DJF	*7.2*	4.2	3.8	3.2	*4.7*	*5.0*	*4.9*
	MAM	*5.3*	3.1	3.1	2.4	*3.3*	*3.1*	*3.2*
	JJA	*5.6*	3.3	3.2	2.3	*3.2*	*2.6*	*3.1*
	SON	*7.6*	4.1	4.3	3.4	*6.1*	*5.7*	*6.3*

Italic shows observed data. DJF = December, January, February; MAM = March, April, May; JJA = June, July, August; SON = September, October, November. (Observed data after Met Éireann; GCM outputs after Wilby and Dawson, 2007; statistically downscaled data after Fealy and Sweeney, 2007; 2008b.)

Table 4.4. Seasonal mean daily precipitation ($\bar{x}$) and standard deviations (s) for Kilkenny (observed), direct global climate model (GCM) output from HadCM3 (H3), CSIRO Mk2 (CS) and CGCM2 (CG), statistically downscaled (SD) for the 1961–1990 period.

	Season	Obs	GCM			SD		
		Kilkenny	H3	CG	CS	H3-SD	CG-SD	CS-SD
$\bar{x}$	DJF	*2.7*	2.8	3.6	3.0	*2.8*	*2.7*	*3.0*
	MAM	*1.9*	2.4	2.8	2.4	*1.6*	*1.8*	*2.1*
	JJA	*1.9*	2.6	2.2	2.8	*1.8*	*1.5*	*1.8*
	SON	*2.6*	2.7	3.4	3.2	*2.9*	*2.9*	*2.8*
s	DJF	*4.5*	4.2	3.8	3.2	*3.0*	*2.8*	*2.9*
	MAM	*3.4*	3.1	3.1	2.4	*2.0*	*2.1*	*2.3*
	JJA	*4.3*	3.3	3.2	2.3	*2.1*	*1.7*	*1.9*
	SON	*4.7*	4.1	4.3	3.4	*3.7*	*3.5*	*3.4*

Italic shows observed data. DJF = December, January, February; MAM = March, April, May; JJA = June, July, August; SON = September, October, November. (Observed data after Met Éireann; GCM outputs after Wilby and Dawson, 2007; statistically downscaled data after Fealy and Sweeney, 2007; 2008b.)

5 Accounting for Uncertainties in Regional Climate Change Projections for Ireland

This section will outline a methodology that can be used to produce probabilistic-based regional climate scenarios for Ireland, taking into account a number of key uncertainties. The methodology is adapted from Hulme and Carter (1999), Jones (2000) and New and Hulme (2000) and applied to two impacts-relevant climate variables, seasonal mean temperature (°C) and precipitation change (%), for a selection of GCMs. The proposed methodology has previously been applied directly to GCM output and RCM output, but is refined here for application to statistically downscaled data for a selection of stations in Ireland (see Appendix II for GCM ΔT and regional response and Appendix III for application of the methodology directly to GCM output for Ireland).

5.1 Application to Statistically Downscaled Data

Fealy and Sweeney (2007; 2008a; 2008b) previously developed statistically downscaled climate scenarios for Ireland for a selection of variables, including temperature and precipitation, based on the output from three GCMs, namely CGCM2, CSIRO Mk2 and HadCM3 for both the A2 and B2 emissions scenarios (Table 5.1). This data exists at a daily resolution for the model-simulated periods of 1961–2099 for all model realisations. While the authors sought to develop a range of scenarios, from which they derived a weighted mean ensemble accounting for uncertainty in the driving GCMs, other uncertainties were ignored, partly due to the limited availability of different GCM-emissions scenarios combinations. Therefore, no probabilities could be attributed to the derived climate projections, which represents a significant, but acknowledged, weakness in the resultant projections for use in impact assessments or policy formulation.

Seasonal means for the 2080s (2070–2099) were derived from the statistically downscaled daily data for each of the 14 synoptic stations modelled by Fealy and Sweeney (2007; 2008a; 2008b). This derived dataset provides the basis for the following analysis. The 2080s was selected as the signal-to-noise ratio is likely to be larger for this period (Jones, 2000).

In a modification of the pattern-scaling methodology outlined previously, the approach employed here applied the technique to the statistically downscaled data. For example, the ratio of global mean temperature change (°C) between the individual GCMs and emissions scenarios (Table 5.1) was employed to scale the statistically downscaled A2 scenario projections for

Table 5.1. List of global climate models employed in analysis and change in global mean surface temperature (°C) for the A1FI, A2, B2 and B1 emissions scenarios.

Model	Institution/country	Reference	Scenario	ΔT_{global}
CGCM2	CCCma, Canada	Flato et al., 2000	A1FI	4.38
			A2	3.55
			B2	2.46
			B1	2.02
CSIRO Mk2	CSIRO, Australia	Hirst et al., 1996, 2000	A1FI	4.86
			A2	3.94
			B2	3.14
			B1	2.59
HadCM3	UKMO, UK	Gordon et al., 2000	A1FI	4.86
			A2	3.93
			B2	3.07
			B1	2.52

Emissions scenarios in italics are those that were available as statistically downscaled projections.

all stations, for both temperature and precipitation for the 2080s, according to Equation 3.1 above:

$$\Delta T_{A1F} = \left\langle \frac{\Delta T_{A1F}}{\Delta T_{A2}} \right\rangle \Delta T_{A2}$$

Where

ΔT_{A1FI}= desired scenario

$<\Delta T_{A1FI}/\Delta T_{A2}>$ = ratio of global mean temperature change for GCMi (Table 5.1)

ΔT_{A2} = projected change in temperature for the 2080s' period

As with the pattern-scaling methodology, this method assumes that some form of a linear relationship exists between the downscaled emissions scenarios for the 14 stations employed in the analysis. As both the A2 and B2 downscaled scenarios for temperature and precipitation were available, this assumption could be tested by scaling the downscaled A2 scenario at each station by the ratio of the A2 and B2 global mean surface temperature change for each GCM, to derive a scaled B2 emissions scenario. If a linear relationship existed, then the assumption was taken as valid.

Figure 5.1 illustrates the seasonal relationship between the statistically downscaled B2 emissions scenario, for both temperature and precipitation, and the B2 response, scaled by the method outlined above for the 2080s. While the assumption of a linear response was found to be valid between driving emissions scenarios, the slope of the equation was found to vary seasonally. Therefore, seasonal linear regression equations were derived to account for the difference between the statistically downscaled B2 and GCM-scaled B2 projections.

This method was applied to the statistically downscaled A2 scenarios for all stations and GCMs to calculate station level changes for the A1FI and B1 emissions scenarios. The results from the application of this method are outlined in Tables 5.2 and 5.3 for the selected stations of Valentia, Malin Head, Casement and Kilkenny for the winter (DJF) and summer (JJA) seasons for the 2080s' period, for both temperature (°C) and precipitation change (%). The projected changes in temperature and precipitation are shown to be sensitive to both emissions scenario and GCM. The greatest difference in projected temperatures between the GCMs is associated with the A1FI scenario. For precipitation, significant intermodel differences are apparent both between and within individual emissions scenarios. Appendix IV contains the scaled responses and statistically downscaled seasonal changes for all 14 of the synoptic stations employed by Fealy and Sweeney (2007; 2008a; 2008b) and for all seasons, for both temperature (°C) and precipitation change (%).

Table 5.2. Global climate model (GCM) scaled temperature change (°C) for selected stations for the 2070–2099 period from three GCMs and the A1FI and B1 emissions scenarios. The A2 and B2 scenario data are directly derived from statistically downscaled data.

GCM	SRES	Valentia		Malin Head		Casement		Kilkenny	
		ΔT_{DJF}	ΔT_{JJA}	ΔT_{DJF}	ΔT_{JJA}	ΔT_{DJF}	ΔT_{JJA}	ΔT_{DJF}	ΔT_{JJA}
CGCM2	A1FI	5.1	3.6	4.3	3.1	5.9	4.2	5.7	4.5
CGCM2	A2	3.0	3.1	2.5	2.6	3.5	3.6	3.4	3.8
CGCM2	B2	2.9	2.0	2.3	1.7	3.3	2.4	3.2	2.4
CGCM2	B1	2.4	1.6	2.0	1.4	2.8	1.9	2.6	2.0
CSIRO Mk2	A1FI	4.4	2.1	3.7	1.9	5.0	2.4	5.0	2.7
CSIRO Mk2	A2	3.7	2.1	3.1	1.8	4.2	2.4	4.2	2.8
CSIRO Mk2	B2	2.9	1.5	2.5	1.3	3.3	1.7	3.3	1.9
CSIRO Mk2	B1	2.4	1.3	2.1	1.1	2.8	1.4	2.8	1.6
HadCM3	A1FI	1.2	2.5	1.1	2.4	1.4	3.1	1.4	3.3
HadCM3	A2	1.4	2.5	1.2	2.4	1.6	3.1	1.6	3.3
HadCM3	B2	0.7	1.6	0.7	1.6	0.9	2.0	0.9	2.1
HadCM3	B1	0.6	1.4	0.5	1.3	0.7	1.7	0.7	1.8

The A1FI and B1 scenarios were derived by scaling the statistically downscaled A2 scenario according to the ratio of ΔT from the parent GCM and relevant emissions scenario for each season. DJF = December, January, February; JJA = June, July, August. SRES = Special Report on Emissions Scenarios (after Fealy and Sweeney, 2008a; 2008b)

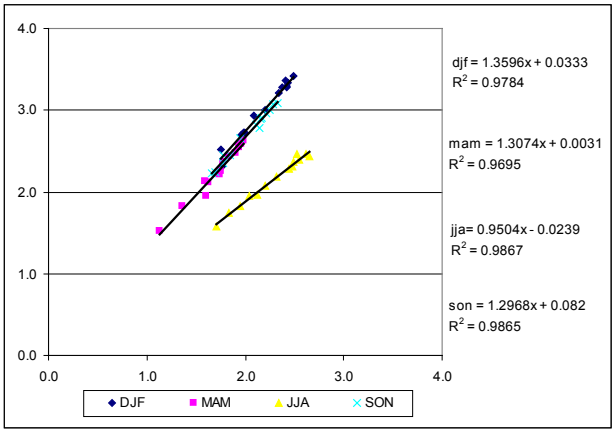

(a) CGCM2 SD vs Scaled ΔT B2 SRES

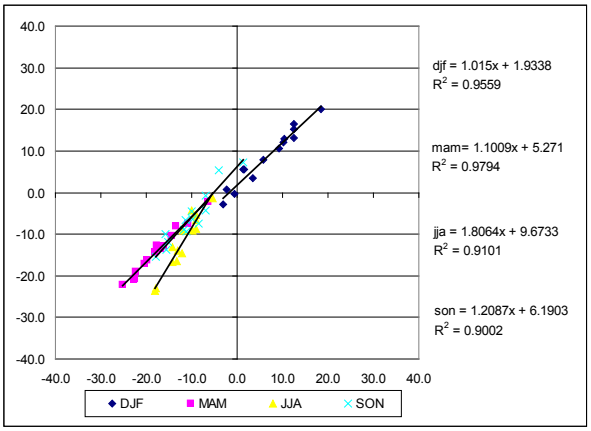

(d) CGCM2 SD vs Scaled ΔP B2 SRES

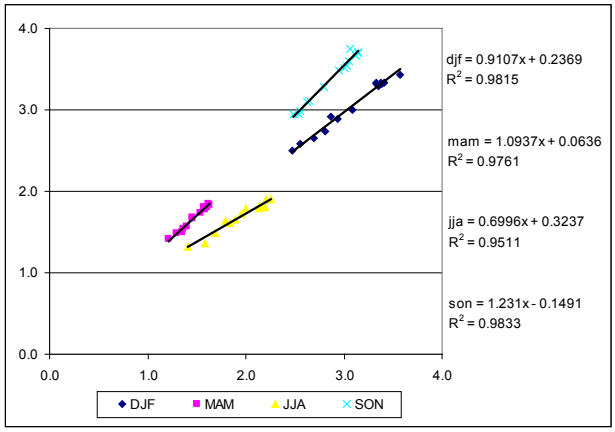

(b) CSIRO Mk2 SD vs Scaled ΔT B2 SRES

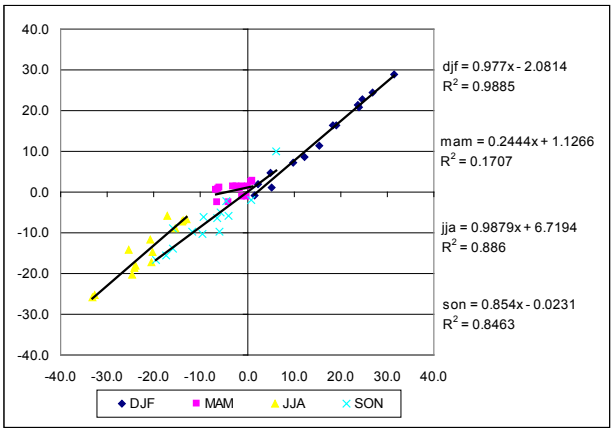

(e) CSIRO Mk2 SD vs Scaled ΔP B2 SRES

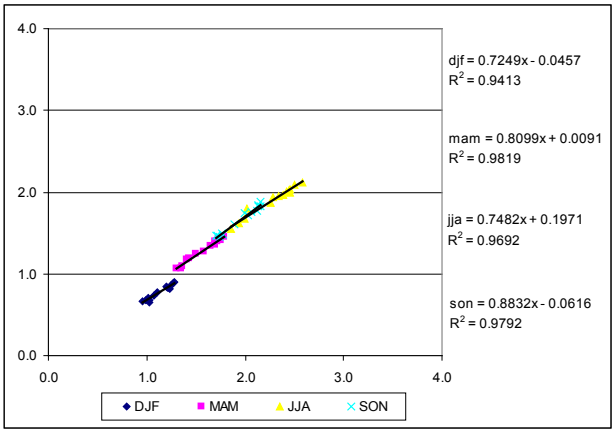

(c) HadCM3 SD vs Scaled ΔT B2 SRES

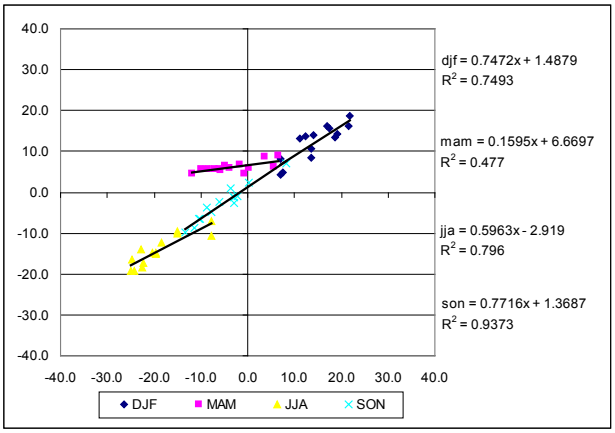

(f) HadCM3 SD vs Scaled ΔP B2 SRES

Figure 5.1. Comparison of statistically downscaled (SD) and scaled B2 temperature (a–c) and precipitation (d–f) based on scaling the statistically downscaled A2 scenario for each global climate model. Regression equations and explained variance for each season illustrate the relationship between the statistically downscaled and scaled B2 scenarios. These seasonally calculated equations were applied as a correction factor for calculating all scaled scenarios. DJF = December, January, February; MAM = March, April, May; JJA = June, July, August; SON = September, October, November. SRES = Special Report on Emissions Scenarios (data after Fealy and Sweeney, 2007; 2008a; 2008b.)

Table 5.3. Global climate model (GCM) scaled percent change in precipitation (%) for selected stations for the 2070–2099 period from three GCMs and the A1FI and B1 emissions scenarios (SRES). The A2 and B2 scenario data are directly derived from statistically downscaled data (after Fealy and Sweeney, 2007; 2008b).

GCM	SRES	Valentia		Malin Head		Casement		Kilkenny	
		ΔP_{DJF}	ΔP_{JJA}	ΔP_{DJF}	ΔP_{JJA}	ΔP_{DJF}	ΔP_{JJA}	ΔP_{DJF}	ΔP_{JJA}
CGCM2	A1FI	-3.8	-29.2	4.5	-22.3	24.5	-47.7	18.7	-19.4
CGCM2	A2	-4.5	-17.4	2.0	-14.3	18.0	-25.7	13.3	-13.0
CGCM2	B2	-2.8	-14.5	5.5	-4.2	13.0	-23.0	10.7	-6.7
CGCM2	B1	-0.7	-8.3	3.1	-5.1	12.3	-16.8	9.7	-3.7
CSIRO Mk2	A1FI	0.1	-24.8	5.5	-13.3	35.1	-31.0	26.6	-19.6
CSIRO Mk2	A2	1.8	-25.9	6.3	-16.5	30.9	-31.0	23.8	-21.6
CSIRO Mk2	B2	-0.8	-17.3	4.6	-6.7	22.7	-20.2	16.3	-5.7
CSIRO Mk2	B1	-0.9	-10.1	2.0	-4.0	17.8	-13.4	13.2	-7.3
HadCM3	A1FI	9.9	-24.3	10.5	-10.1	21.6	-24.6	22.1	-23.9
HadCM3	A2	9.1	-29.0	9.7	-9.8	21.8	-29.3	22.3	-28.5
HadCM3	B2	8.1	-18.4	4.9	-7.0	16.3	-14.0	15.7	-17.4
HadCM3	B1	5.8	-14.0	6.1	-6.7	11.9	-14.1	12.2	-13.8

The A1FI and B1 scenarios were derived by scaling the statistically downscaled A2 scenario according to the ratio of ΔT from the parent GCM and relevant emissions scenario for winter (DJF = December, January, February) and summer (JJA = June, July, August). SRES = Special Report on Emissions Scenarios.

In order to calculate the regional response rate per °C global warming at each station, the projected (statistically downscaled and scaled) warming for each station and season were normalised by the parent GCM/emission scenario change in the global mean surface temperature change from Table 5.1. For example, to calculate the station response per °C global warming (ΔT) for the CGCM2 GCM and the A1FI emissions scenario for the winter season at Valentia, the projected A1FI ΔT at Valentia is 5.1°C, which is then normalised by the global ΔT change from the CGCM2 A1FI of 4.38°C. The resulting normalised value of 1.16°C represents a station response of 1.16°C/°C global warming – that is, for an increase in global mean surface temperature of 1°C, winter seasonal temperatures at Valentia are projected to increase by 1.16°C (ΔTGlobal x ΔTstation), indicating an above average warming rate according to the CGCM2 GCM (see Appendix Va and b for all stations).

The minimum and maximum values for both the temperature and precipitation response/°C ΔT for selected stations (Tables 5.4 and 5.5, see bold and italics) were assumed to represent uncertainty in model output at the regional/station level. While only three GCMs were employed, the projected global ΔT associated with the three GCMs represents an illustrative sub-sample of the full warming range projected by all available GCMs.

In order to produce probabilities of future warming for individual synoptic stations, taking into account some of the key uncertainties associated with the projected warming, including emissions uncertainty and GCM regional response, an MC analysis was employed in conjunction with three different estimates of future warming:

1. ΔT in global mean surface temperature change from the three GCMs employed in the statistical downscaling approach employed by Fealy and Sweeney (2007; 2008a; 2008b) (Table 5.1 – ΔT 2.02 to 4.86°C);

2. Range in ΔT of the estimated transient climate response (TCR), defined as the global surface average temperature (SAT) change at the time of CO_2 doubling in the 1% yr^{-1} transient CO_2 increase experiment (IPCC, 2007). The IPCC (2007) indicates that that the transient climate response is very likely to be greater than 1°C and very unlikely to be greater than 3°C;

3. Estimated equilibrium climate sensitivity with a 5 to 95% probability range of 2.1 to 4.6°C and a median value of 3.2°C with a lognormal distribution (IPCC, 2007).

Table 5.4. Seasonal minimum and maximum temperature response (°C)/°C ΔT_{Global} derived from all global climate models (GCM) and emissions scenarios, based on the statistically downscaled and scaled station level warming.

Temp (°C)	DJF		MAM		JJA		SON	
	Min.	Max.	Min.	Max.	Min.	Max.	Min.	Max.
Valentia	***0.23***	***1.19***	***0.38***	***0.93***	***0.44***	***0.86***	***0.48***	***1.01***
Shannon	0.26	1.33	0.44	1.01	0.51	0.99	0.56	1.15
Dublin	0.21	1.02	0.42	0.86	0.47	0.89	0.55	1.17
Malin Head	***0.21***	***0.99***	***0.35***	***0.85***	***0.38***	***0.75***	***0.47***	***0.94***
Roche's Point	0.22	1.10	0.36	0.74	0.49	0.80	0.47	0.97
Belmullet	0.22	1.11	0.37	0.93	0.48	0.83	0.48	1.01
Clones	0.27	1.35	0.46	1.03	0.55	1.03	0.58	1.17
Rosslare	0.22	1.12	0.35	0.62	0.42	0.70	0.48	1.00
Claremorris	0.27	1.36	0.44	1.07	0.56	1.01	0.57	1.18
Mullingar II	0.27	1.36	0.47	1.05	0.54	1.04	0.59	1.21
Kilkenny	***0.28***	***1.31***	***0.46***	***0.99***	***0.56***	***1.08***	***0.60***	***1.27***
Casement	***0.28***	***1.36***	***0.45***	***0.96***	***0.50***	***1.01***	***0.59***	***1.22***
Cork	0.24	1.23	0.40	0.87	0.54	0.94	0.52	1.08
Birr	0.28	1.39	0.46	1.05	0.57	1.06	0.59	1.25

Stations in bold and italics represent stations employed in the subsequent analysis. DJF = December, January, February; MAM = March, April, May; JJA = June, July, August; SON = September, October, November.

Table 5.5. Seasonal minimum and maximum precipitation response (%)/°C ΔT_{Global} derived from all global climate models (GCM) and emissions scenarios, based on the statistically downscaled and scaled station level warming.

Precip (%)	DJF		MAM		JJA		SON	
	Min.	Max.	Min.	Max.	Min.	Max.	Min.	Max.
Valentia	***-1.28***	***2.64***	***-5.89***	***2.34***	***-7.38***	***-3.91***	***-6.33***	***-2.32***
Shannon	0.66	4.43	-10.22	2.66	-7.72	-4.43	-4.09	-0.24
Dublin	5.59	10.01	-6.59	2.28	-11.07	-5.34	-4.73	-1.20
Malin Head	***0.57***	***2.47***	***-9.24***	***2.94***	***-5.09***	***-1.53***	***-1.62***	***2.20***
Roche's Point	1.37	4.42	-2.78	2.20	-10.58	-4.83	-7.41	-2.81
Belmullet	-0.93	2.32	-6.77	2.44	-4.49	-1.80	-2.83	0.00
Clones	4.42	7.64	-9.08	2.98	-6.55	-2.26	-3.96	-0.17
Rosslare	2.35	4.89	-5.45	2.03	-8.07	-2.37	-4.56	-1.99
Claremorris	3.51	5.84	-7.38	2.87	-4.88	0.81	-4.59	-0.19
Mullingar II	4.20	7.58	-9.12	2.61	-8.26	-3.73	0.53	3.70
Kilkenny	***3.76***	***6.05***	***-8.01***	***2.39***	***-7.25***	***-1.82***	***-6.16***	***-2.10***
Casement	***4.45***	***7.85***	***-7.21***	***2.35***	***-10.89***	***-4.55***	***-3.40***	***-0.81***
Cork	-0.22	4.27	-4.40	2.13	-7.92	-1.81	-6.44	-1.38
Birr	5.07	8.57	-8.26	2.56	-8.24	-3.78	-2.82	0.29

Stations in bold and italics represent stations employed in the subsequent analysis. DJF = December, January, February; MAM = March, April, May; JJA = June, July, August; SON = September, October, November.

The MC analysis was used to randomly sample from the range in ΔT for each of the three methods identified, and the uniform distributions representing the regional response rate in temperature and precipitation change per °C of global warming for each station and season. The resulting ΔT and ΔP therefore take account of uncertainties in the emissions scenarios, by sampling from four marker emissions scenarios (A1FI, A2, B2 and B1), GCM sensitivity and regional response, through the regional response rates per °C global warming at each station. Method III also considers uncertainty in the equilibrium climate sensitivity, through the incorporation of the estimated range in sensitivity from the *Fourth Assessment Report* (IPCC, 2007) (Method III). For all methods, the MC simulation was set to produce 100,000 samples with the initial 10,000 samples excluded from any subsequent analysis.

Method I – As no likelihood could be attributed to the ΔT in global mean surface temperature change from the three GCMs employed in the statistical downscaling approach employed by Fealy and Sweeney (2007; 2008a; 2008b) (Table 5.1 – ΔT 2.02 to 4.86°C), a uniform prior probability distribution (i.e. initially all values within a specified range are treated as having an equal probability of occurrence) was assumed.

Method II – Based on the estimated TCR, defined as the global surface average temperature (SAT) change at the time of CO_2 doubling in the 1% yr^{-1} transient CO_2 increase experiment (IPCC, 2007), which is very likely to be greater than 1°C and very unlikely to be greater than 3°C. A normal distribution was employed as the prior for this method (IPCC, 2007) with a 5 to 95% probability range of 1.5 to 2.8°C (Fig. 5.2).

Method III – Based on the estimated equilibrium climate sensitivity with a 5 to 95% probability range of 2.1 to 4.6°C and a median value of 3.2°C with a lognormal distribution (IPCC, 2007), a distribution of values, conforming to the estimated range and median, was simulated to represent the climate sensitivity (Fig. 5.3).

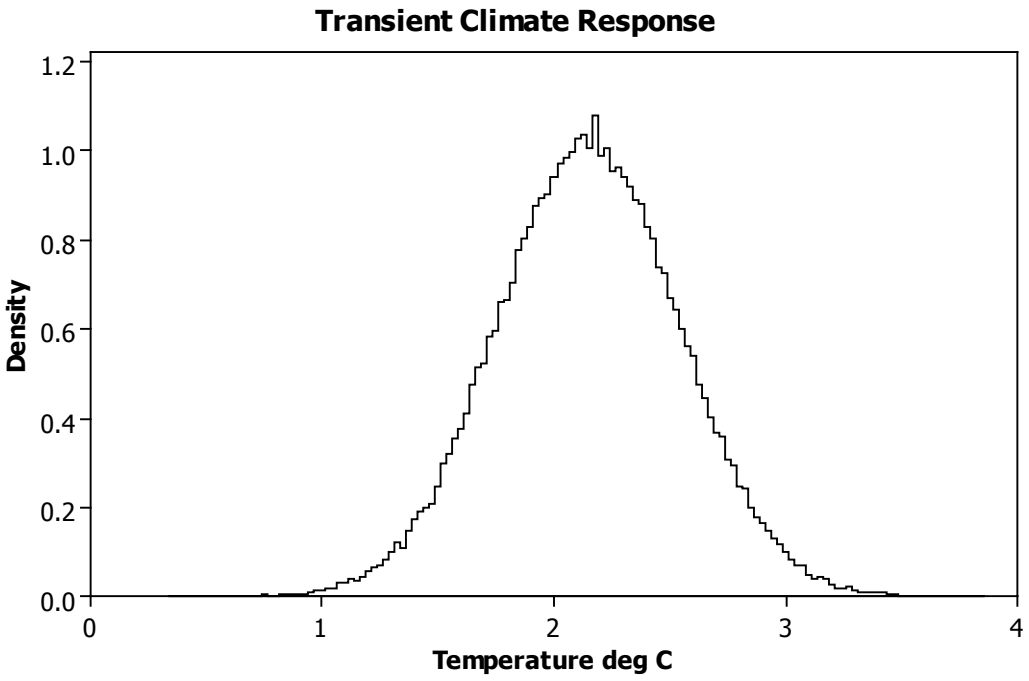

Figure 5.2. Transient climate response (TCR) with a 5 to 95% probability range of 1.5 to 2.8°C (IPCC, 2007).

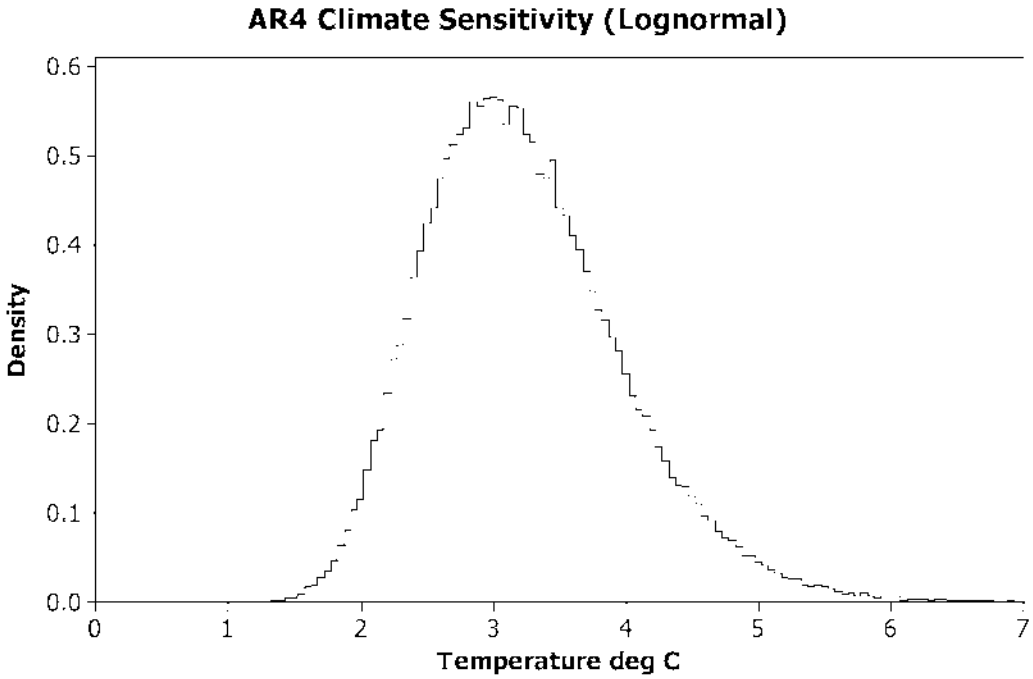

Figure 5.3. Simulation of equilibrium climate sensitivity with a median value of 3.2°C and 5 to 95% probability range of 2.1 to 4.6°C. (The 95% probability range differs from that quoted in the IPCC (2007) range of 2.2 to 4.6˚C, however, this difference is considered negligible.)

5.2 Results

Tables 5.6–5.8 show the results for each of the three different measures of changes in global ΔT (Methods I–III) with the regional response rates at the selected synoptic stations of Valentia, Malin Head, Kilkenny and Casement. The results from Method I are also compared to the ensemble of the statistically downscaled A2 and B2 emissions scenario calculated by Fealy and Sweeney (2007; 2008a; 2008b) employing the IR-CPI (after Wilby and Harris, 2006) (Table 5.9).

However, the results from the three different measures of changes in global ΔT (Methods I–III) are not directly comparable: Method I represents the ΔT in three GCMs for the 2070–2099 period, while Method II reflects changes at the point at which a doubling of CO_2 occurs, which is sensitive to the speed in ocean heat uptake; and Method III represents the change in temperature and precipitation at the point at which the climate has reached a new stable equilibrium, in response to a doubling of CO_2 and is sensitive to the strength of different feedbacks (IPCC, 2007).

Mean changes in all seasons for the four stations are shown in Table 5.9. With the inclusion of the A1FI and B1 scenarios, results for nearly all seasons indicate a greater range in warming for the 2080s period than previously suggested by the statistically downscaled projections of Fealy and Sweeney (2007; 2008a; 2008b), which account only for the A2 and B2 emissions scenario. For projected changes in precipitation, Method I indicates more conservative changes – mainly lower projected decreases – for nearly all stations and seasons when compared to the statistically downscaled ensemble results. Probability distribution functions for changes in temperature and precipitation at each station and season are shown in Figures 5.4 and 5.5. Projected changes in both temperature and precipitation are shown to display a considerable spread in values. For example, winter temperature at Casement suggests an increase from 0.6 to 6.6°C by the 2080s (2070–2099) period. Similarly, with precipitation, both increases and decreases are projected, with an equal likelihood by the 2080s at all stations for spring. Winter precipitation at Valentia and autumn precipitation at Malin Head also display different directions of change with equal likelihoods. Results from the statistically downscaled ensemble, while comparable to the mean changes projected by Method I, take no account of likelihoods or the fact that a projected change could differ in both direction and magnitude.

Table 5.6. Method I seasonal mean temperature (°C) and precipitation change (%) for Valentia, Malin Head, Kilkenny and Casement.

Method I		Temperature						Precipitation					
Station	Season	Mean	Min.	Q1	Med.	Q3	Max.	Mean	Min.	Q1	Med.	Q3	Max.
Valentia	DJF	2.4	0.5	1.5	2.3	3.2	5.8	2.3	-6.2	-1.0	2.2	5.4	12.8
	MAM	2.3	0.8	1.7	2.1	2.8	4.5	-6.1	-28.5	-12.4	-5.7	0.9	11.3
	JJA	2.2	0.9	1.7	2.2	2.7	4.2	-19.4	-35.8	-23.4	-18.8	-14.9	-8.0
	SON	2.6	1.0	1.9	2.5	3.1	4.9	-14.9	-30.7	-18.5	-14.0	-10.7	-4.7
Malin Head	DJF	2.1	0.4	1.3	1.9	2.7	4.8	5.2	1.2	3.4	4.9	6.8	12.0
	MAM	2.1	0.7	1.5	2.0	2.5	4.1	-10.9	-44.8	-20.2	-10.2	-0.4	14.1
	JJA	1.9	0.8	1.5	1.9	2.4	3.6	-11.4	-24.7	-14.5	-10.7	-7.8	-3.1
	SON	2.4	1.0	1.9	2.3	2.9	4.6	1.0	-7.9	-2.2	0.9	4.0	10.7
Kilkenny	DJF	2.7	0.6	1.7	2.6	3.6	6.4	16.9	7.6	13.1	16.6	20.2	29.4
	MAM	2.5	0.9	1.9	2.4	3.0	4.8	-9.7	-38.9	-17.6	-9.2	-0.7	11.5
	JJA	2.8	1.1	2.2	2.7	3.4	5.2	-15.6	-35.2	-20.0	-14.6	-10.3	-3.7
	SON	3.2	1.2	2.4	3.1	3.9	6.2	-14.2	-29.9	-17.8	-13.4	-10.1	-4.3
Casement	DJF	2.8	0.6	1.8	2.7	3.7	6.6	21.2	9.0	16.4	20.6	25.4	38.1
	MAM	2.4	0.9	1.8	2.3	2.9	4.7	-8.3	-34.8	-15.6	-7.8	-0.1	11.4
	JJA	2.6	1.0	2.0	2.5	3.2	4.9	-26.6	-52.7	-32.7	-25.2	-19.7	-9.2
	SON	3.1	1.2	2.4	3.0	3.8	5.9	-7.2	-16.5	-9.4	-6.8	-4.7	-1.7

Also shown are value for minimum (min.), maximum (max.), median (med.) and quartiles (Q1 = 1st quartile; Q3 = 3rd Quartile). DJF = December, January, February; MAM = March, April, May; JJA = June, July, August; SON = September, October, November.

Table 5.7. Method II seasonal mean temperature (°C) and precipitation change (%) for Valentia, Malin Head, Kilkenny and Casement.

Method II		Temperature						Precipitation					
Station	Season	Mean	Min.	Q1	Med.	Q3	Max.	Mean	Min.	Q1	Med.	Q3	Max.
Valentia	DJF	1.5	0.1	1.0	1.5	2.0	4.1	1.5	-4.4	-0.6	1.4	3.4	9.8
	MAM	1.4	0.2	1.1	1.4	1.7	3.3	-3.8	-19.8	-8.0	-3.7	0.6	8.3
	JJA	1.4	0.2	1.1	1.4	1.6	3.2	-12.1	-25.7	-14.2	-11.9	-9.8	-1.6
	SON	1.6	0.3	1.3	1.6	1.9	3.6	-9.3	-22.3	-11.4	-9.0	-6.9	-0.9
Malin Head	DJF	1.3	0.2	0.8	1.2	1.7	3.4	3.3	0.3	2.2	3.2	4.2	8.3
	MAM	1.3	0.2	1.0	1.3	1.6	2.8	-6.8	-30.6	-13.0	-6.6	-0.3	9.8
	JJA	1.2	0.2	1.0	1.2	1.4	2.7	-7.1	-17.5	-9.0	-6.9	-5.0	-1.3
	SON	1.5	0.2	1.2	1.5	1.8	3.3	0.6	-5.3	-1.4	0.6	2.6	7.4
Kilkenny	DJF	1.7	0.2	1.1	1.6	2.2	4.6	10.5	1.8	8.8	10.4	12.1	21.8
	MAM	1.6	0.2	1.2	1.5	1.9	3.7	-6.1	-27.2	-11.3	-5.9	-0.5	8.4
	JJA	1.8	0.3	1.4	1.7	2.1	3.9	-9.7	-27.4	-12.5	-9.4	-6.6	-1.1
	SON	2.0	0.3	1.6	2.0	2.4	4.9	-8.9	-23.7	-11.0	-8.6	-6.5	-1.3
Casement	DJF	1.8	0.2	1.1	1.7	2.3	4.7	13.2	2.1	10.9	13.0	15.4	26.8
	MAM	1.5	0.2	1.2	1.5	1.8	3.4	-5.2	-24.0	-10.0	-5.0	-0.1	7.6
	JJA	1.6	0.3	1.3	1.6	1.9	3.4	-16.6	-39.2	-20.1	-16.2	-12.7	-1.8
	SON	1.9	0.3	1.5	1.9	2.3	4.1	-4.5	-12.4	-5.8	-4.4	-3.0	-0.5

Also shown are values for minimum (min), maximum (max), median (med) and quartiles (Q1 = 1st quartile; Q3 = 3rd Quartile). DJF = December, January, February; MAM = March, April, May; JJA = June, July, August; SON = September, October, November.

Differences between the projected changes from Method I and II stem from the timing of a doubling of atmospheric CO_2. Method I projects changes in temperature and precipitation for a particular timeslice, that of the 2080s, whereas the TCR (Method II) represents the instantaneous response of the climate system at the point in time in which a doubling of CO_2 takes place. The results from Method II are therefore more relevant as a mid-21st century projection, assuming a linear response in the regional warming rate per °C of ΔT global mean surface temperature. Probability distribution functions for the TCR ΔT global are shown in Figures 5.6 and 5.7.

Method III results are based on the estimated equilibrium climate sensitivity with a 5 to 95% probability range of 2.1 to 4.6°C and a lognormal distribution (IPCC, 2007) (Table 5.9; Figs 5.8 and 5.9). These results assume that emissions stabilise after doubling and that the climate system has attained equilibrium, including ocean heat uptake after a doubling of CO_2 has been attained. While the IPCC (2007) states that the equilibrium is very likely to be greater than 1.5°C, due to physical reasons, values substantially higher than 4.5°C cannot be ruled out. Owing to the current inability to constrain the upper tail of the estimated range in values for the equilibrium climate sensitivity, the results from Method III may represent an underestimation of the possible range in, though less likely, values for the regional response at equilibrium CO_2. However, from an adaptation or infrastructure design perspective, the time horizon associated with reaching equilibrium CO_2 is too distant to be of significant importance for adaptation purposes in the medium term.

The ability to produce PDFs, that account explicitly for key uncertainties which propagate from the emissions scenarios to the GCMs employed, represents a significant improvement over traditional statistical downscaling techniques. However, a significant weakness in this approach is that no strict quantification of uncertainty in predictor selection in the statistical downscaling procedure is accounted for. This source of uncertainty is likely to be greatest in cases where a number of optimum predictor sets may exist, but the

Table 5.8. Method III seasonal mean temperature (°C) and precipitation change (%) for Valentia, Malin Head, Kilkenny and Casement.

Method III		Temperature						Precipitation					
Station	Season	Mean	Min.	Q1	Med.	Q3	Max.	Mean	Min.	Q1	Med.	Q3	Max.
Valentia	DJF	2.3	0.3	1.4	2.2	3.0	8.2	2.2	-9.3	-0.9	2.1	5.1	18.4
	MAM	2.1	0.5	1.6	2.0	2.6	6.5	-5.7	-40.7	-11.8	-5.4	0.9	15.6
	JJA	2.1	0.6	1.6	2.0	2.5	5.9	-18.2	-51.5	-21.4	-17.6	-14.3	-5.4
	SON	2.4	0.6	1.9	2.3	2.9	6.9	-14.0	-48.1	-17.1	-13.3	-10.1	-3.2
Malin Head	DJF	1.9	0.3	1.2	1.8	2.5	7.2	4.9	0.9	3.2	4.7	6.3	17.2
	MAM	1.9	0.5	1.4	1.9	2.3	5.7	-10.3	-62.8	-19.2	-9.7	-0.4	18.9
	JJA	1.8	0.5	1.4	1.8	2.2	5.5	-10.7	-34.2	-13.4	-10.2	-7.4	-2.3
	SON	2.3	0.7	1.8	2.2	2.7	6.8	0.9	-10.7	-2.1	0.9	3.8	15.5
Kilkenny	DJF	2.6	0.4	1.6	2.4	3.3	9.2	15.9	5.2	12.8	15.3	18.4	43.5
	MAM	2.3	0.6	1.8	2.3	2.8	6.9	-9.1	-53.8	-16.7	-8.7	-0.7	15.7
	JJA	2.7	0.8	2.1	2.5	3.1	7.4	-14.7	-52.0	-18.7	-13.9	-9.7	-2.7
	SON	3.0	0.8	2.3	2.9	3.6	8.9	-13.4	-43.0	-16.5	-12.7	-9.6	-3.1
Casement	DJF	2.6	0.4	1.7	2.5	3.4	8.8	19.9	5.9	15.8	19.2	23.2	55.2
	MAM	2.3	0.5	1.7	2.2	2.7	6.8	-7.8	-50.2	-14.8	-7.4	-0.1	15.8
	JJA	2.4	0.7	1.9	2.3	2.9	7.8	-25.0	-74.2	-30.2	-23.9	-18.6	-6.6
	SON	2.9	0.9	2.3	2.8	3.5	8.4	-6.8	-24.6	-8.7	-6.5	-4.5	-1.1

Also shown are values for minimum (min.), maximum (max.), median (med.) and quartiles (Q1 = 1st quartile; Q3 = 3rd Quartile). DJF = December, January, February; MAM = March, April, May; JJA = June, July, August; SON = September, October, November.

Table 5.9. Comparison of mean temperature (°C) and precipitation (%) change in the statistically downscaled ensemble (SD-Ens), based on the A2 and B2 emissions scenarios, calculated by Fealy and Sweeney (2007; 2008a; 2008b) employing the IR-CPI and the mean changes calculated from the probability distribution functions (Method I) employing the broader range of emissions scenarios (A1FI, A2 B2, B1).

		Temperature		Precipitation	
Station	**Season**	**SD-Ens**	**PDF**	**SD-Ens**	**PDF**
Valentia	DJF	2.0	2.4	3.5	2.3
	MAM	1.9	2.3	-9.8	-6.1
	JJA	2.1	2.2	-25.6	-19.4
	SON	2.4	2.6	-16.0	-14.9
Malin Head	DJF	1.7	2.1	5.8	5.2
	MAM	1.7	2.1	-11.1	-10.9
	JJA	1.9	1.9	-13.1	-11.4
	SON	2.3	2.4	0.1	1.0
Kilkenny	DJF	2.3	2.7	16.9	16.9
	MAM	2.1	2.5	-12.7	-9.7
	JJA	2.7	2.8	-25.8	-15.6
	SON	3.0	3.2	-16.7	-14.2
Casement	DJF	2.3	2.8	19.2	21.2
	MAM	2.1	2.4	-9.7	-8.3
	JJA	2.6	2.6	-31.8	-26.6
	SON	2.9	3.1	-10.5	-7.2

DJF = December, January, February; MAM = March, April, May; JJA = June, July, August; SON = September, October, November.

resultant downscaled scenarios produce divergent responses. Such a situation can arise when candidate predictors which have a large sensitivity to warming (for example, relative humidity and temperature) contribute separately to two equally optimum sets of predictors. While both sets of predictors may provide a similar level of explanation in the validation of the downscaled data, the future projected change in the desired variable will largely be determined by the sensitivity of the selected predictor set. However, this is a recognised weakness in statistical downscaling and generally the selection of the optimum predictor set seeks to avoid the use of overly sensitive candidate predictors in the selection criteria.

In addition, the ability of the GCM to simulate candidate predictors employed in the statistical downscaling approach (Fig. 2.6) will also contribute to the uncertainty. This source of uncertainty arises from sub-grid scale processes and model parameterisations within the parent GCM. In an analysis of uncertainty in statistically downscaled temperature and precipitation in Northern Canada, Dibike et al. (2008) suggest that the regression-based downscaling approach used in their analysis was able to reproduce the climate regime over highly heterogeneous terrain when driven by accurate GCM predictors. Such findings indicate that the regression-based approach may not contribute as much uncertainty to the cascade as the GCM employed. Similar conclusions have been arrived at for downscaled output using regional climate models.

The method outlined here is considered to be sensitive to the choice of GCMs employed, in that the contribution of an individual model that projects a change in the statistically downscaled temperature or precipitation, which is opposite in sign to all available GCMs, has equal weight in the uniform distribution ascribed as a prior to the regional response rate. While attributing a non-uniform distribution as a prior to the regional response rates is difficult to ascertain objectively, weighting the contribution of projected changes from each GCM is one alternative. Determining the relevant criteria, such as convergence of model output (Giorgi and Mearns, 2002) to derive the weights requires careful consideration.

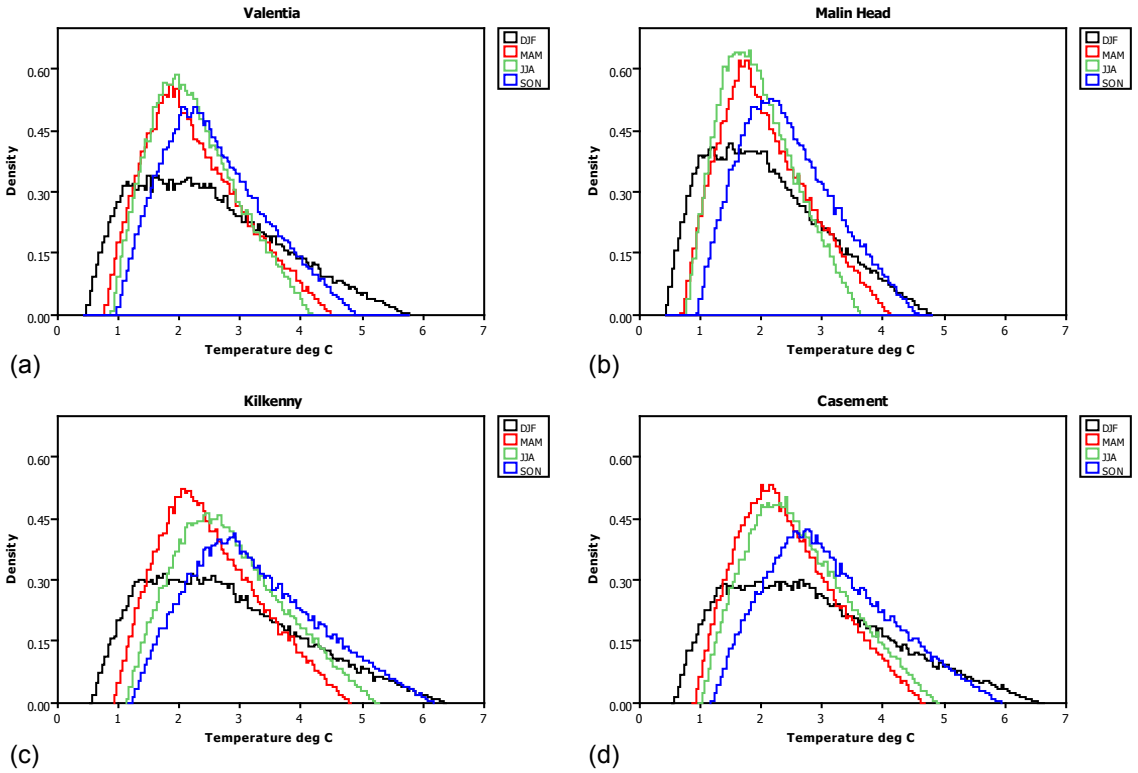

Figure 5.4. Method I probability distribution functions of projected change in seasonal mean temperature (˚C) for (a) Valentia, (b) Malin Head, (c) Kilkenny and (d) Casement for the 2070–2099 period, assuming a uniform distribution for ΔT from three global climate models (GCM) and a uniform distribution for the scaling variables outlined in Table 5.4.

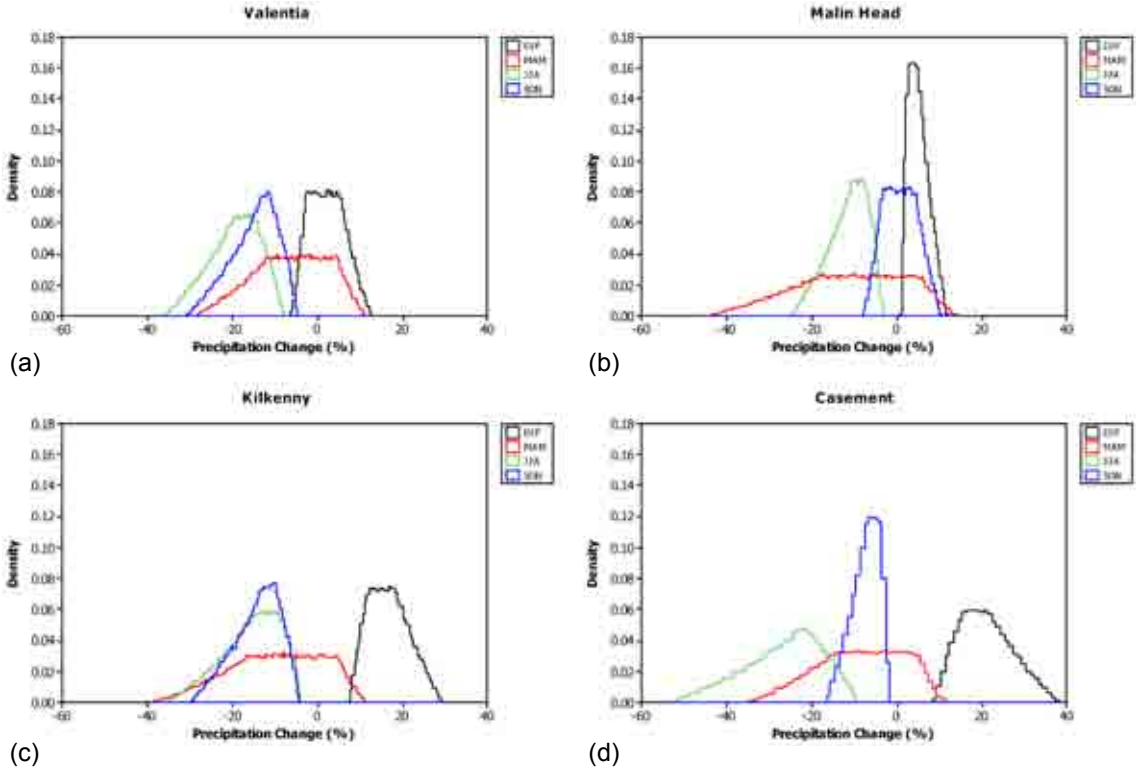

Figure 5.5 Method I probability distribution functions of projected change in seasonal precipitation (%) for (a) Valentia, (b) Malin Head, (c) Kilkenny and (d) Casement for the 2070–2099 period, assuming a uniform distribution for ΔT from three global climate models (GCM) and a uniform distribution for the scaling variables outlined in Table 5.5.

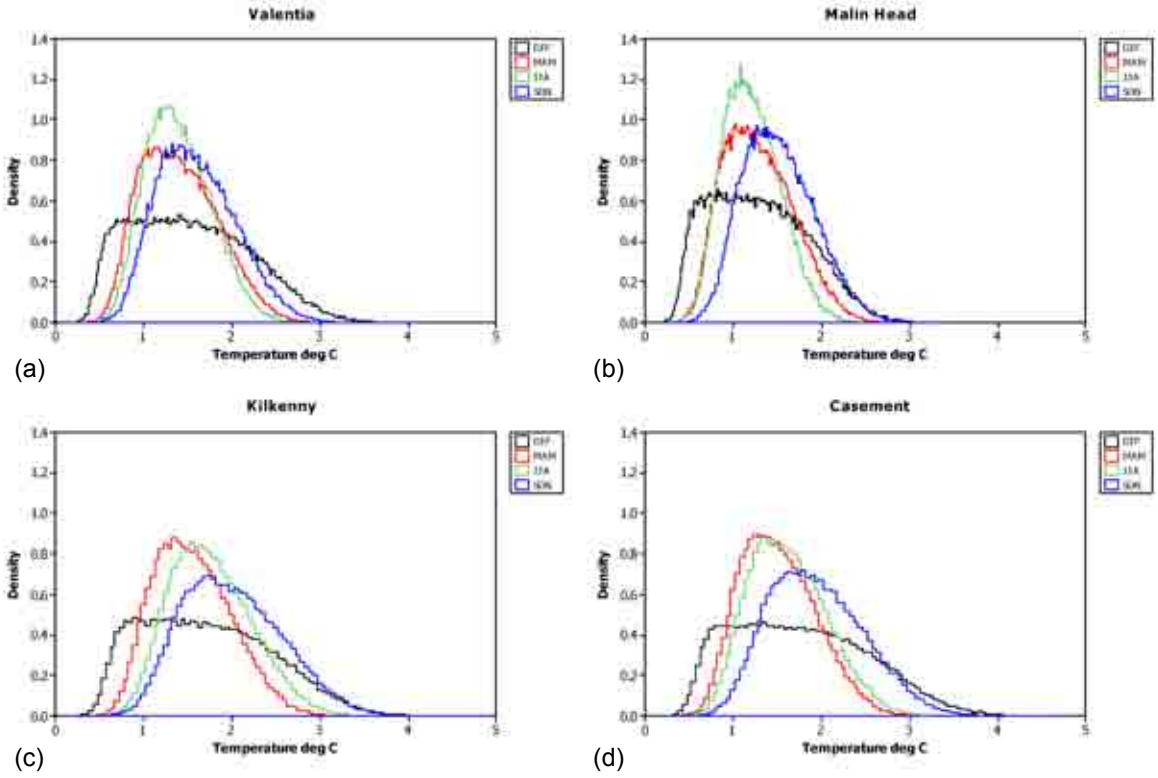

Figure 5.6. Method II probability distribution functions of projected change in seasonal mean temperature (˚C) for (a) Valentia, (b) Malin Head, (c) Kilkenny and (d) Casement for the 2070–2099 period, with a normal distribution for transient climate response (TCR) and a uniform distribution for the scaling variables outlined in Table 5.4.

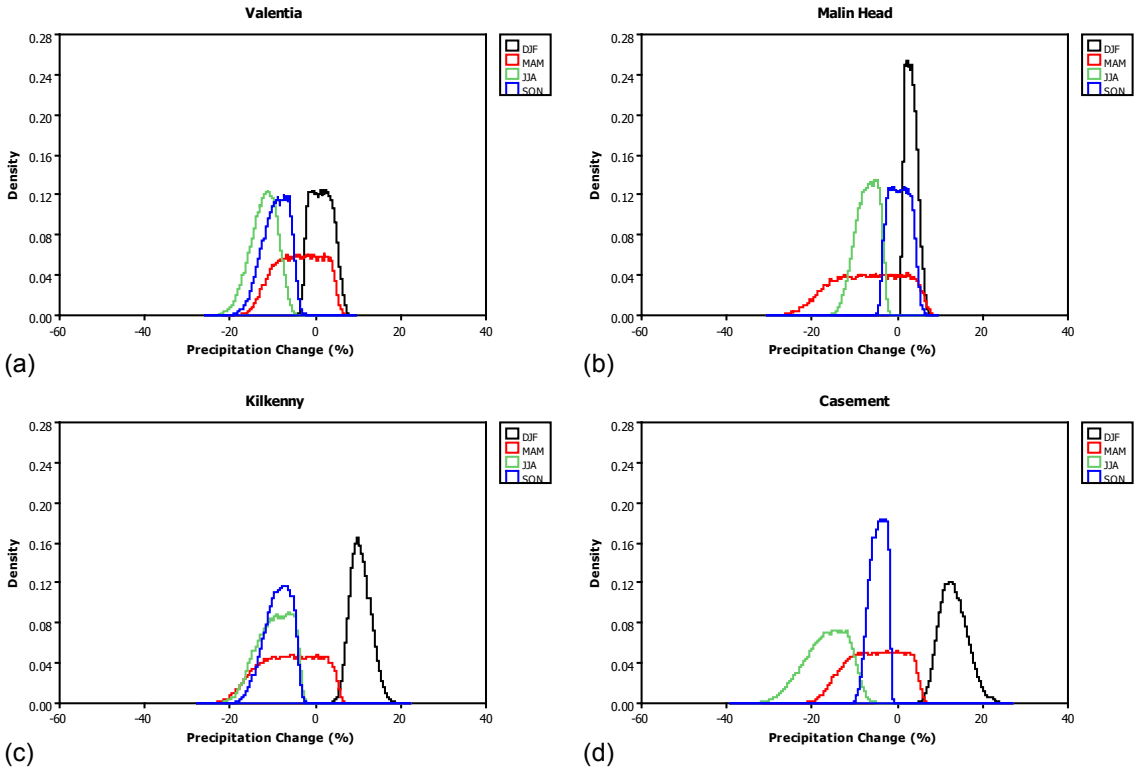

Figure 5.7. Method II probability distribution functions of projected change in seasonal precipitation (%) for Valentia, Malin Head, Kilkenny and Casement for the 2070–2099 period, with a normal distribution for transient climate response (TCR) and a uniform distribution for the scaling variables outlined in Table 5.5.

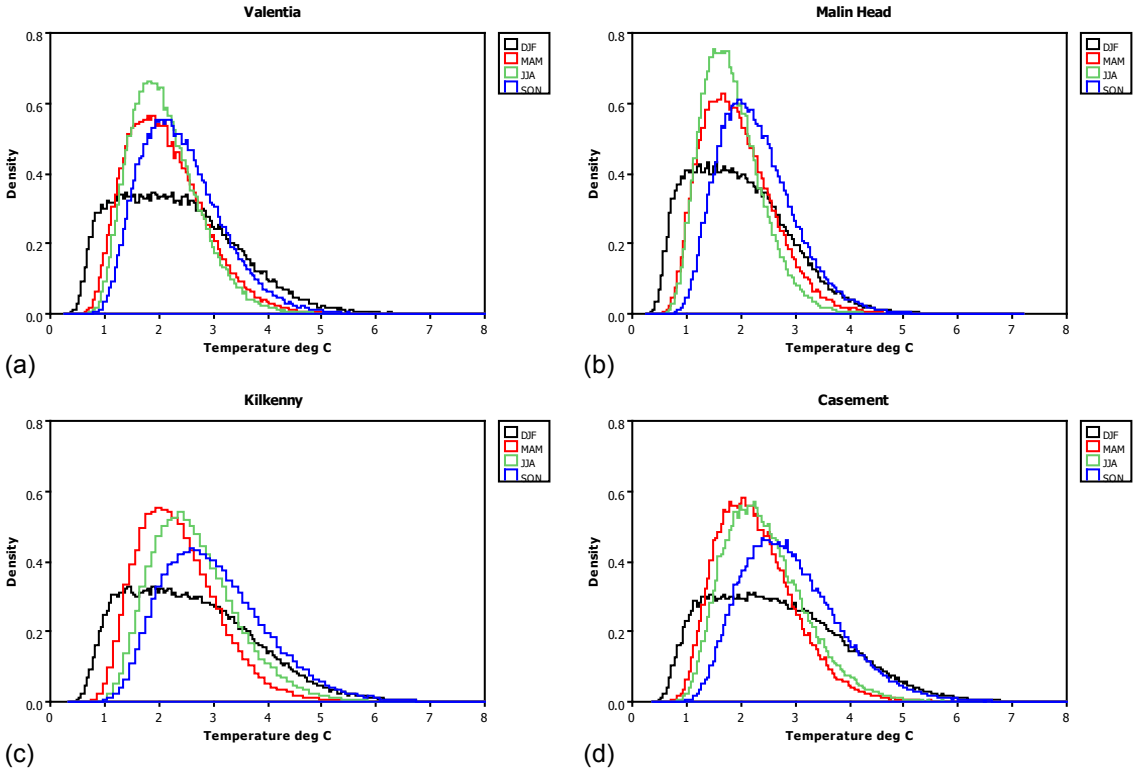

Figure 5.8. Method III probability distribution functions of projected change in seasonal mean temperature (˚C) for Valentia, Malin Head, Kilkenny and Casement for the 2070–2099 period, assuming a lognormal distribution for equilibrium climate sensitivity and a uniform distribution for the scaling variables outlined in Table 5.4.

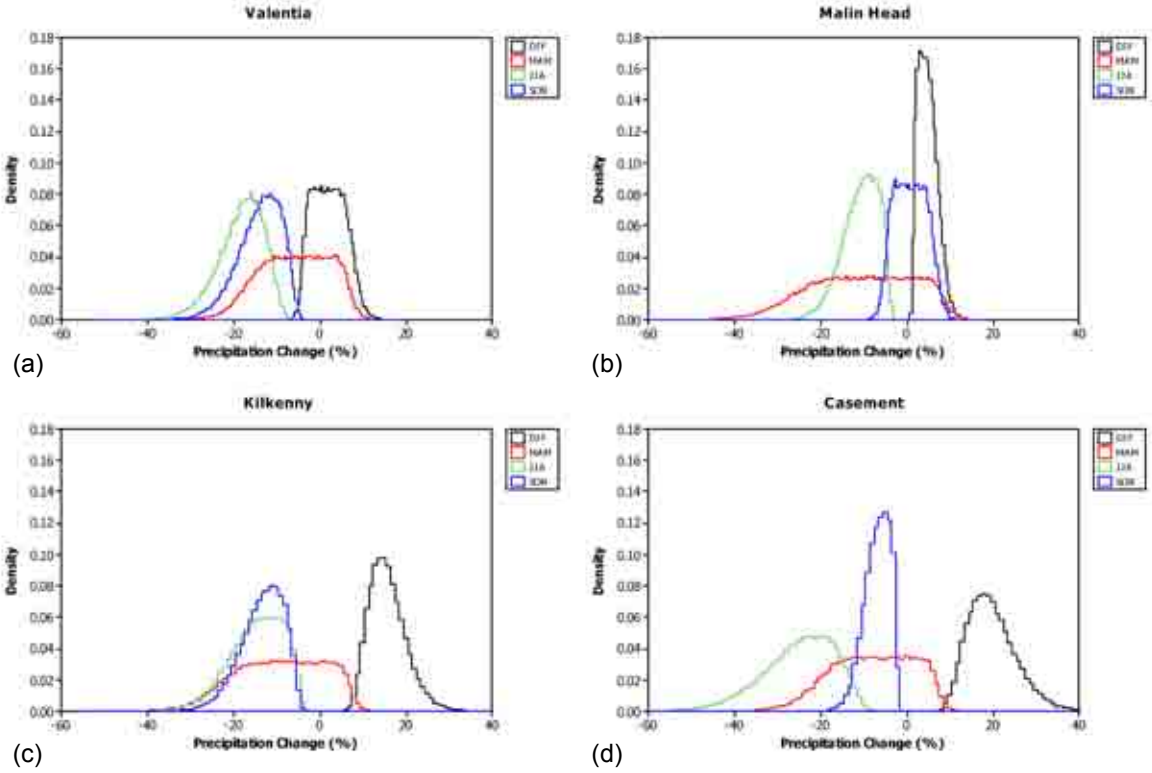

Figure 5.9. Method III probability distribution functions of projected change in seasonal precipitation (%) for Valentia, Malin Head, Kilkenny and Casement for the 2070–2099 period, assuming a lognormal distribution for equilibrium climate sensitivity and a uniform distribution for the scaling variables outlined in Table 5.5.

5.3 Discussion

Kass and Raftery (1995) suggest that 'any approach that selects a single model and then makes inferences conditionally on that model ignores the uncertainty involved in model selection, which can be a big part of overall uncertainty', and 'this leads to underestimation of the uncertainty about quantities of interest, sometimes to a dramatic extent' (Kass & Raftery, 1995, 784, after Katz, 2002). Yet in spite of this early acknowledgement, the climate modelling and impacts community continued to produce and employ single trajectory climate scenarios for use in impact assessments that sought to inform policy-making. While there was a valid historical reason for this, arising from the limited number of centres undertaking global climate modelling because of the computational resources required and associated expense of running such model simulations, the implications for the policy community were significant. Global climate models have been found to produce such divergent scenarios at the regional scale that it is difficult, if not impossible, to develop appropriate adaptation strategies (Stakhiv, 1998) based on one or a few GCMs. Hulme and Carter (1999) consider the practice of employing a limited number of climate scenarios as 'dangerous', as such an approach reflects only a partial assessment of the associated risk involved. Modelling the climate system will always result in a range of possible futures being projected, even when forced with the same emissions scenario (Hulme and Carter, 1999).

While a number of techniques have been developed in order to account for model differences, due to emissions scenarios and GCMs, such as pattern scaling, simple climate models or more recently the incorporation of Earth System models of Intermediate Complexity (EMICs), an inability to produce probabilistic-based projections has proved a limiting factor in enabling the quantification of potential vulnerability impacts in key sectors and hindered the subsequent development of suitable policy responses to reduce or mitigate such impacts.

More recently, this topic has received much attention in the literature, with divergent attitudes and opinions towards the most suitable approach to employ. In spite of such divergence in attitudes, the discussion is vital. Some exciting developments have also emerged, through the PPEs (Murphy et al., 2004) and large-scale experiments such as Climateprediction.net, which included a significant participation of non-climate scientists and the public at large in providing distributed computer resources for climate modelling at the global scale.

The generation of multiple scenarios from different GCMs has received much focus within the statistical downscaling community, largely due to the ease in implementation of statistically based downscaling approaches. Nevertheless, traditional statistical downscaling approaches do not explicitly account for the uncertainties that accrue in the modelling process. Intercomparisons of dynamically based downscaled scenarios have also become feasible through European Union-funded projects such as PRUDENCE and ENSEMBLES, which focused on producing outputs from multiple GCM–RCM combinations for a common domain over Europe. The availability of such data from a number of RCMs has contributed greatly to the development of probabilistic-based approaches at the required scale for policy assessment and decision-making, based on dynamical regional climate models.

The approach outlined within this report adopted a technique widely used in the dynamical modelling community: to pattern scale statistically downscaled projections of temperature and precipitation for selected stations for Ireland for the 2080s. The resulting scenarios, scaled to reproduce the warming from the A1FI and B1 emissions scenarios, were then employed in a probabilistic assessment based on three estimates of future changes in global mean surface temperature, according to (i) three GCMs employed in the original statistical downscaling approach of Fealy and Sweeney (2007; 2008a; 2008b); (ii) the estimated transient response of the climate system to a doubling of CO_2 at the time of doubling (IPCC, 2007), and (iii) the estimated equilibrium climate sensitivity due to a doubling of CO2 (IPCC, 2007).

While the projected mean changes in temperature and precipitation, based on the probabilistic approach, were found to be comparable to the ensemble mean directly derived from the statistically downscaled data, the PDFs indicated a wide range in the distribution of the projected changes. Projections of temperature were found to be consistent in the direction and magnitude of change. However, results for precipitation were found to vary in both direction and magnitude in particular

seasons. While the probabilistic-based mean seasonal projected changes in precipitation was found to be more conservative than that of the ensemble mean from the statistical downscaling approach, the range in projected changes was found to vary. Particular seasons exhibited an equal likelihood of both positive and negative changes associated with precipitation. Such findings suggest that the development of adaptation strategies based on climate scenarios that do not account for uncertainties explicitly could result in maladaptation.

The proposed method represents a technique that allows probabilistic-based climate scenarios to be developed rapidly, even with limited availability of downscaled data. While the results of the technique do not differ significantly from the original, statistically downscaled climate scenarios (Fealy and Sweeney, 2007; 2008a; 2008b), the incorporation of emissions and model uncertainty into the projections represents an important contribution to traditional downscaling techniques. The outcome of this research can be readily employed in conjunction with bottom-up approaches, such as determining the likelihood and timing of exceeding a particular threshold in a sensitivity analysis, to provide decision-makers with the appropriate information – at the relevant scale – needed to develop robust adaptation strategies.

However, a note of caution: information derived from probabilistic-based climate assessments is not independent of the methodology employed (New et al., 2007), so the risk of maladaptation remains. Moreover, the contribution of full end-to-end probabilistic-based climate impact assessments to the decision-making process remains largely untested with the exception of one or two peer-reviewed studies (Wilby et al., 2009).

In parallel to the research reported on here, a web-based statistical downscaling tool has been developed to facilitate the rapid development of statistically downscaled scenarios (Appendix VI). It is anticipated that the availability of such a web-based tool, with outputs that can be incorporated with the method outlined above to provide probabilistic-based scenarios, will facilitate the development and integration of probabilistic-based climate scenarios into the wider stakeholder community.

6 References

Bates, J.R. Feedback and climate sensitivity: A critique, unpublished.

Beven, K.J. (2001) *Rainfall-runoff modelling: The Primer*. Wiley & Sons, Chichester, pp. 217–25.

Bony, S., Colman, R., Kattsov, V.M., Allan, R.P., Bretherton, C.S., Dufresne, J-L., Hall, A., Hallegatte, S., Holland, M.M, Ingram, W., Randall, D.A., Soden, B.J., Tselioudis, G. and Webb, M.J. (2006) How well do we understand and evaluate climate change feedback processes?. *Journal of Climate*, 19 (15): 3445–82.

Broecker, W.S. (2006) Was the Younger Dryas triggered by a flood?. *Science,* 312 (5777): 1146–8.

Broecker, W.S. and Hemming, S. (2001) Climate swings come into focus. *Science,* 294 (5550): 2308–9.

Climateprediction.net http://climateprediction.net/. [Accessed, February 2009.]

Dessai, S. and Hulme, M. (2003) *Does climate policy need probabilities?,* Tyndall Centre Working Paper No. 34.

Dibike, Y.B., Gachon, P., St-Hilaire, A., Ouarda, T.B.M.J. and Nguyen, V.T.-V. (2008) Uncertainty analysis of statistically downscaled temperature and precipitation regimes in Northern Canada. *Theoretical and Applied Climatology*, 91(1–4): 149–70.

Ekström, M., Hingray, B., Mezghani, A. and Jones, P. D.(2007) Regional climate model data used within the SWURVE project – 2: addressing uncertainty in regional climate model data for five European case study areas. *Hydrology and Earth System Sciences*, 11(3): 1085–96.

Fealy, R. and Sweeney, J. (2007) Statistical downscaling of precipitation for a selection of sites in Ireland employing a generalised linear modelling approach, *International Journal of Climatology*, 27(15): 2083–94.

Fealy, R. and Sweeney, J. (2008a) Statistical downscaling of temperature, radiation and potential evapotranspiration to produce a multiple GCM ensemble mean for a selection of sites in Ireland. *Irish Geography*, 41(1): 1–27.

Fealy, R. and Sweeney, J. (2008b) 'Climate Scenarios for Ireland', in Sweeney et al., (2008) *Climate Change– Refining the Impacts for Ireland*, Environmental Protection Agency, Ireland.

Flato, G.M., Boer, G.J., Lee, W.G., McFarlane, N.A., Ramsden, D., Reader, M.C. and Weaver, A.J. (2000) The Canadian Centre for Climate Modelling and Analysis Global Coupled Model and its Climate. *Climate Dynamics*, 16 (6): 451–67.

Gachon P. and Dibike Y. B. (2007) Temperature change signals in northern Canada: Convergence of statistical downscaling results using two driving GCMs. *International Journal of Climatology*, 27(12): 1623–41.

Giorgi, F. and Francisco, R. (2000) Evaluating uncertainties in the prediction of regional climate change. *Geophysical Research Letters*, 27(9): 1295–8.

Giorgi, F. and Mearns, L.O. (2002) Calculation of average, uncertainty range, and reliability of regional climate changes from AOGCM simulations via the 'Reliability Ensemble Averaging' (REA) Method. *Journal of Climate*, 15(10): 1141–58.

Gordon, C., Cooper, C., Senior, C. A., Banks, H., Gregory, J. M., Johns, T. C., Mitchell, J. F. B. and Wood, R. A. (2000) The simulation of SST, sea ice extents and ocean heat transports in a version of the Hadley Centre coupled model without flux adjustments. *Climate Dynamics*, 16 (2/3): 147–68.

Hingray, B., Mezghani, A. and Buishand, T.A. (2007a) Development of probability distributions for regional climate change from uncertain global mean warming and an uncertain scaling relationship. *Hydrology and Earth System Sciences*, 11(3): 1097–114.

Hingray, B., Mouhous, N., Mezghani, A., Bogner, K., Schaefli, B. and Musy, A. (2007b) Accounting for global-mean warming and scaling uncertainties in climate change impact studies: application to a regulated lake system. *Hydrology and Earth System Sciences*, 11(3): 1207–26.

Hirst A.C., O'Farrell S.P. and Gordon H.B. (2000) Comparison of a coupled ocean-atmosphere model with and without oceanic eddy-induced advection. 1. Ocean spin-up and control integrations. *Journal of Climate*, 13(1): 139–63.

Hirst, A.C., Gordon, H. B., and O'Farrell, S.P. (1996) Global warming in a coupled climate model including oceanic eddy-induced advection. *Geophysical Research Letters*, 23(23): 3361–64.

Hulme, M. and Carter, T.R. (1999) Representing uncertainty in climate change scenarios and impact studies, in T. Carter, M. Hulme and D. Viner (eds) *Representing uncertainty in climate change scenarios and impact studies* (Proc. ECLAT-2 Helsinki Workshop, 14–16 April, 1999), Climatic Research Unit, Norwich, UK, 128 pp.

Hulme, M. and Carter, T.R. (2000) 'The changing climate of Europe', in Parry, M.L. (ed.) *Assessment of the Potential Effects of Climate Change in Europe*. Report of the ACACIA Concerted Action, November 2000, UEA, Norwick, UK, 350 pp.

Hulme, M., Jenkins, G.J., Lu, X., Turnpenny, J.R., Mitchell, T.D., Jones, R.G., Lowe, J., Murphy, J.M., Hassell, D., Boorman, P., McDonald,R. and Hill,S. (2002) *Climate Change Scenarios for the United Kingdom: The UKCIP02 Scientific Report*, Tyndall Centre for Climate Change Research, School of Environmental Sciences, University of East Anglia, Norwich, UK, 120pp.

Intergovernmental Panel on Climate Changes (IPCC) (2001a) *Climate Change 2001: The Scientific Basis.* Contribution of Working Group I to the Third Assessment Report of the Intergovernmental Panel on Climate Change (IPCC). Houghton, J. T., Ding, Y., Griggs, D.J., Noguer, M., van der Linden, P. J. and Xiaosu, D. (eds) Cambridge University Press, UK. 944 pp.

IPCC (2001b) *Guidance Notes for Lead Authors of the IPCC Fourth Assessment Report on Addressing Uncertainties*, http://www.ipcc.ch/ipccreports/ar4-wg1.htm. Accessed online, February 2006.

IPCC (2007) *Climate Change 2007: The Physical Science Basis*. Contribution of Working Group I to the Fourth Assessment Report of the Intergovernmental Panel on Climate Change. Solomon, S., Qin, D., Manning, M., Chen, Z., Marquis, M., Averyt, K.B., Tignor, M. and Miller, H.L. (eds.) Cambridge University Press, Cambridge, United Kingdom and New York, NY, USA, 996 pp.

Jones, R.N. (2000) Analysing the risk of climate change using an irrigation demand model, *Climate Research*, 14(2): 89–100.

Jones, R.N. and Mearns, L.O. (2003) Assessing Future Climate Risks, in Lim, B., Carter, I. and al Huq, S. (eds). *Adaptation Policy Framework,* Technical Paper 5, United Nations Development Programme, New York.

Kass, R.E. and Raftery, A.E. (1995) Bayes factors. *Journal of American Statistical Association*, 90: 773–95.

Katz, R.W. (2002) Techniques for estimating uncertainty in climate change scenarios and impact studies. *Climate Research*, 20(2): 167–85.

Kenny, G.J., Warrick, R.A., Campbell, B.D., Sims, G.C., Camilleri, M., Jamieson, P.D., Mitchell, N.D., McPherson, H.G. and Salinger, M.J. (2000) Investigating climate change impacts and thresholds: an application of the CLIMPACTS integrated assessment model for New Zealand agriculture. *Climatic Change*, 46(1/2): 91–113.

Lambert, S.J. and Boer, G.J. (2001) CMIP1 evaluation and intercomparison of coupled climate models. *Climate Dynamics*, 17(2/3): 83–106.

McGrath, R., Nishimura, E., Nolan, P., Semmler, T., Sweeney, C. and Wang, S., (2005) *Climate Change: Regional Climate Model Predictions for Ireland*, Environmental Protection Agency, ERTDI Report Series No. 36, 45 pp.

McWilliams, B.E. (ed.) (1991) *Climate Change: Studies on the implications for Ireland*, Stationery Office, Dublin, Ireland.

Mitchell, J.F.B., Johns, T.C., Eagles, M., Ingram, W.J. and Davis, R.A. (1999) Towards the construction of climate change scenarios. *Climatic Change*, 41(3–4): 547–81.

Mitchell, T. D. (2003) Pattern Scaling: An examination of the accuracy of the technique for describing future climates. *Climatic Change*, 60(3): 217–42.

Mitchell, T.D., Hulme, M., and New, M. (2002) Climate data for political areas, *Area*, 34(1): 109–12.

Moss, R.H. and Schneider, S.H. (2000) 'Uncertainties in the IPCC TAR: Recommendations to Lead Authors for More Consistent Assessment and Reporting', in Pachauri R., T. Taniguchi, and K. Tanaka (eds), *Guidance Papers on the Cross Cutting Issues of the Third Assessment Report of the IPCC*, Geneva, Switzerland: World Meteorological Organization, 33–51.

Murphy, J., Sexton, D., Barnett, D., Jones, G., Webb, M., Collins, M. and Stainforth, D. (2004) Quantification of modelling uncertainties in a large ensemble of climate change simulations, *Nature*, 430(7001): 768–72.

Næss, L.O., Bang, G., Eriksen, S. and Vevatne, J. (2005) Institutional adaptation to climate change: Flood responses at the municipal level in Norway. Global Environmental Change, 15A(2): 125–38.

Nakicenovic, N., Alcamo, J., Davis, G., de Vries, B., Fenhann, J., Gaffin, S., Gregory, K., Gr, A., Yong Jung, T., Kram, T., La Rovere, E.L., Michaelis, L., Mori, S., Morita, T., Pepper, W., Pitcher, H., Price, L., Riahi, K., Roehrl, A., Rogner, H-H., Sankovski, A., Schlesinger, M., Shukla, P., Smith, S., Swart, R., van Rooijen, S., Victor, N. and Dadi Z. (2000). *Special Report on Emissions Scenarios: A Special Report of Working Group III of the Intergovernmental Panel on Climate Change*, Cambridge University Press, Cambridge, UK, 599pp.

New, M. and Hulme, M. (2000) Representing uncertainty in climate change scenarios: a Monte-Carlo approach. *Integrated Assessment*, 1 (3): 203–13.

New, M., Lopez, A., Dessai, S. and Wilby, R. (2007) Challenges in using probabilistic climate change information for impact assessments: an example from the water sector. *Philosophical Transactions of the Royal Society A*, 365 (1857): 2117–131.

Nychka, D. and Tebaldi, C. (2003) Comments on 'Calculation of average, uncertainty range, and reliability of regional climate changes from AOGCM simulations via the 'Reliability Ensemble Averaging' (REA) Method'. *Journal of Climate*, 16(5): 883–4.

Oberkampf, W.L., DeLand, S.M., Rutherford, B.M., Diegert, K.V. and Alvin, K.F. (2002) Error and uncertainty in modelling and simulation. *Reliability Engineering and System Safety*, 75(3): 333–57.

Parry, M.L., Carter, T.R. and Hulme, M. (1996) What is a dangerous climate change? *Global Environmental Change*, 6(1): 1–6.

Paté-Cornell, M.E. (1996) Uncertainties in risk analysis: Six levels of treatment, *Reliability Engineering and System Safety*, 54(2): 95–111.

Pulwarty R.S. and Melis T.S. (2001) Climate extremes and adaptive management on the Colorado River: Lessons from the 1997–1998 ENSO event. *Journal of Environmental Management*, 63 (3): 307–24.

Räisänen, J. (2001) CO_2-induced climate change in CMIP2 experiments: Quantification of agreement and role of internal variability. *Journal of Climate*, 14(9): 2088–104.

Räisänen, J. and Palmer, T.N. (2001) A probability and decision-model analysis of a multimodel ensemble of climate change simulations. *Journal of Climate*, 14(15): 3212–26.

Risbey, J.S. (1998) Sensitivities of water supply planning decisions to streamflow and climate scenario uncertainties. *Water Policy*, 1(3): 321–40.

Roe, G.H. and Baker, M.B. (2007) Why is climate sensitivity so unpredictable? *Science*, 318(5850): 629–32.

Rowell, D. P. (2006) A demonstration of the uncertainty in projections of UK climate change resulting from regional model formulation. *Climatic Change*, 79(3): 243–57.

Ruosteenoja, K., Carter, T.R., Jylhä, K. and Tuomenvirta, H. (2003) *Future climate in world regions: an intercomparison of model-based projections for the new IPCC emissions scenarios*. The Finnish Environment 644, Finnish Environment Institute, 83pp.

Ruosteenoja, K., Tuomenvirta, H. and Jylhä, K. (2007) GCM-based regional temperature and precipitation change estimates for Europe under four SRES scenarios applying a super-ensemble pattern-scaling method. *Climatic Change*, 81(3/4): 193–208.

Santer, B.D., Wigley, T.M.L., Schlesinger, M.E. and Mitchell, J.F.B. (1990) *Developing Climate Scenarios from Equilibrium GCM results*. Report No. 47, Max-Planck-Institut-für-Meteorologie, Hamburg, 29 pp.

Schneider, S.H., 1983: CO_2, climate and society: a brief overview, in Chen R.S., E.M. Boulding, and S.H. Schneider, (eds), *Social Science Research and Climatic Change: An Interdisciplinary Appraisal*, Dordrecht, The Netherlands: D. Reidel Publishing, 9–15.

Stakhiv, E.Z. (1998) Policy implications of climate change impacts on water resources management. *Water Policy*, 1(2): 159–75.

Stephenson, D.B. and Pavan, V. (2003) The North Atlantic Oscillation in coupled climate models: a CMIP1 evaluation. *Climate Dynamics*, 20(4): 381–99.

Sweeney, J. and Fealy, R. (2002) Future Climate Scenarios for Ireland using High Resolution Statistical Downscaling Techniques, *Proceedings of the Rio+10 Conference*, University College, Dublin, 2001.

Sweeney, J. and Fealy, R. (2003a) Establishing reference climate scenarios for Ireland, in Sweeney, J., Brereton, T., Byrne, C., Charlton, R., Emblow, C., Fealy, R., Holden, N., Jones, M., Donnelly, A., Moore, S., Purser, P., Byrne, K., Farrell, E., Mayes, E., Minchin, D., Wilson, J. and Wilson, J. (2003) *Climate Change Scenarios and Impacts for Ireland.* Report to the Environmental Protection Agency, Johnstown Castle, Wexford.

Sweeney, J. and Fealy, R. (2003b) A preliminary Investigation of future climate scenarios for Ireland. *Biology and Environment*, Proceedings of the Royal Irish Academy, Special Issue, 102B(3): 121–8.

Tans, P. (2009) Trends in Atmospheric Carbon Dioxide – Mauna Loa [online] NOAA/ESRL www.esrl.noaa.gov/gmd/ccgg/trends [Accessed: 19 November 2009].

Tebaldi, C. and Knutti, R. (2007) The use of the multimodel ensemble in probabilistic climate projections. *Philosophical Transactions of the Royal Society A*, 365(1857): 2053–75.

Thomas, D.S.G., Twyman, C., Osbahr, H. and Hewitson, B. (2007) Adaptation to climate change and variability: farmer responses to intra-seasonal precipitation trends in South Africa. *Climatic Change* 83(3): 301–22.

Washington, W.M., Weatherly, J.W., Meehl, G.A., Semtner Jr., A.J., Bettge, T.W., Craig, A.P., Strand Jr., W.G., Arblaster, J.M., Wayland, V.B., James, R. and Zhang, Y. (2000) Parallel climate model (PCM) control and transient simulations. *Climate Dynamics*, 16(10–11): 755–74.

Webb, M. J., Senior, C. A., Sexton, D. M. H., Ingram, W. J., Williams, K. D., Ringer, M. A., McAvaney, B. J., Colman, R., Soden, B. J., Gudgel, R., Knutson, T., Emori, S., Ogura, T., Tsushima, Y., Andronova, N., Li, B., Musat, I., Bony, S. and Taylor K. E. (2006) On the contribution of local feedback mechanisms to the range of climate sensitivity in two GCM ensembles. *Climate Dynamics*, 27(1): 17–38.

Wigley, T.M.L. and Raper, S.C.B. (2001) Interpretations of high projections for global-mean warming, *Science*, 293: 451–4.

Wilby, R. L., Troni, J., Biot, Y., Tedd, L., Hewitson, B.C., Smith, D. M. and Sutton, R.T. (2009) A review of climate risk information for adaptation and development planning. *International Journal of Climatology*, 29 (9):1193–215.

Wilby, R.L. (2005) Uncertainty in water resource model parameters used for climate change impact assessment. *Hydrological Processes*, 19(16): 3201–19.

Wilby, R.L. and Dawson, C.W. (2007) *SDSM 4.2 — A decision support tool for the assessment of regional climate change impacts*, User Manual prepared on behalf of the Environment Agency, https://co-public.lboro.ac.uk/cocwd/SDSM/SDSMManual.pdf. [Accessed online June 2007].

Wilby, R.L. and Harris, I. (2006) A framework for assessing uncertainties in climate change impacts: low flow scenarios for the River Thames. *Water Resources Research*, 42 (2): W02419

Williams, K. D., Ringer, M. A., Senior, C. A., Webb, M. J., McAvaney, B. J., Andronova, N., Bony, S., Dufresne, J.-L., Emori, S., Gudgel, R., Knutson, T., Li, B., Lo, K., Musat, I., Wegner, J., Slingo, A., Mitchell, J. F. B. (2006) Evaluation of a component of the cloud response to climate change in an intercomparison of climate models. *Climate Dynamics*, 26(2–3): 145–65.

Acronyms and Annotations

AMIP	Atmospheric Model Intercomparison Project
AOGCMs	Atmosphere-ocean global climate models
CDFs	Cumulative distribution functions
CMIPI-5	Coupled Model Intercomparison Project
CPI	Climate Prediction Index
GCM	Global climate model
GLM	Generalised linear model
IPCC	Intergovernmental Panel on Climate Change
IR-CPI	Impacts Relevant Climate Prediction Index
LGM	Last Glacial Maximum
MAGICC	Model of the Assessment of Greenhouse gas Induced Climate Change
MC	Monte Carlo approach
MMD	Multi-model data (MMD)
NAO	North Atlantic Oscillation
NCEP	National Centres for Environmental Prediction
PDFs	Probability distribution functions
PPE	Perturbed physics ensemble
ppmv	Parts per million volume
RCMs	Regional climate models
REA	Reliability Ensemble Averaging
SAT	Surface average temperature
SRES	Special Report on Emissions Scenarios
SSTs	Sea surface temperatures
TAR	Third Assessment Report
TCR	Transient climate response
THC	Thermohaline circulation
TOA	Top of the atmosphere
Wm-s	Watts per square meter

Appendix I

Probability Distribution Functions of Precipitation (1961–1990)

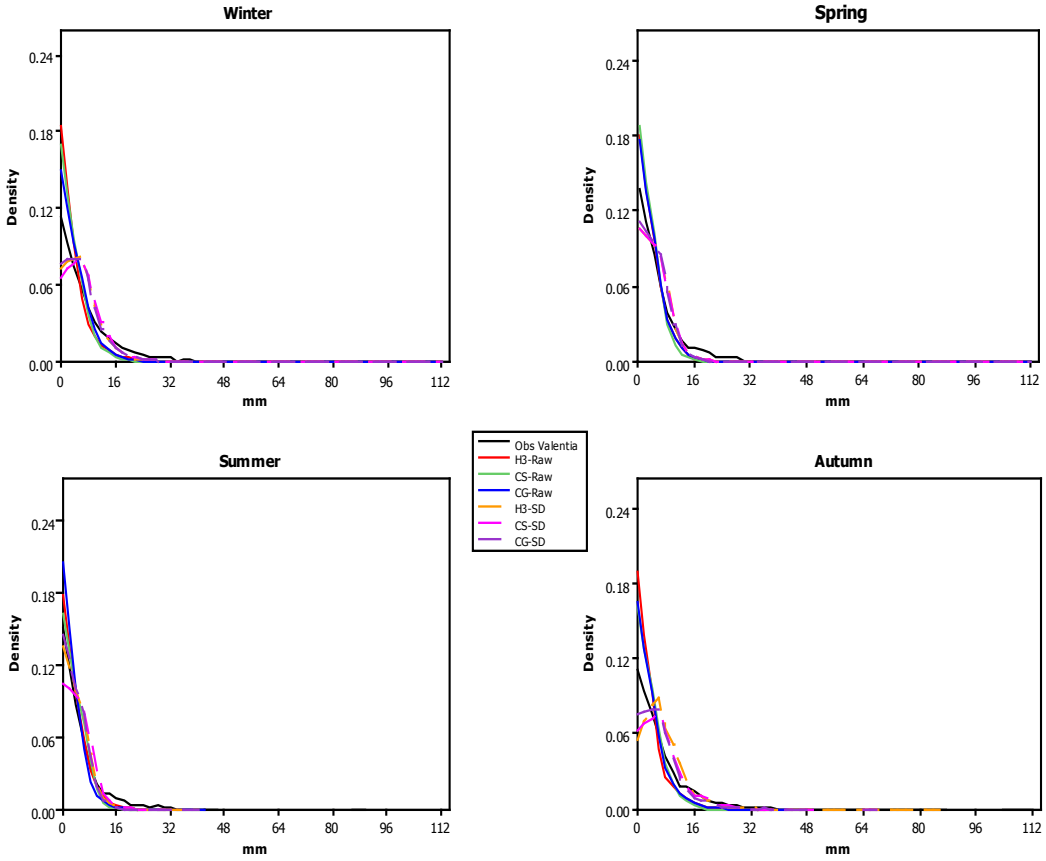

Figure A.I 1. Probability distribution functions (PDFs) of daily observed precipitation at Valentia, direct global climate model (GCM) daily precipitation (Raw) and bias corrected statistically downscaled (SD) daily precipitation for the 1960–1990 period for the A2 emissions scenario (observed data from Met Éireann; GCM data after Wilby and Dawson, 2007; statistically downscaled data after Fealy and Sweeney, 2007; 2008b).

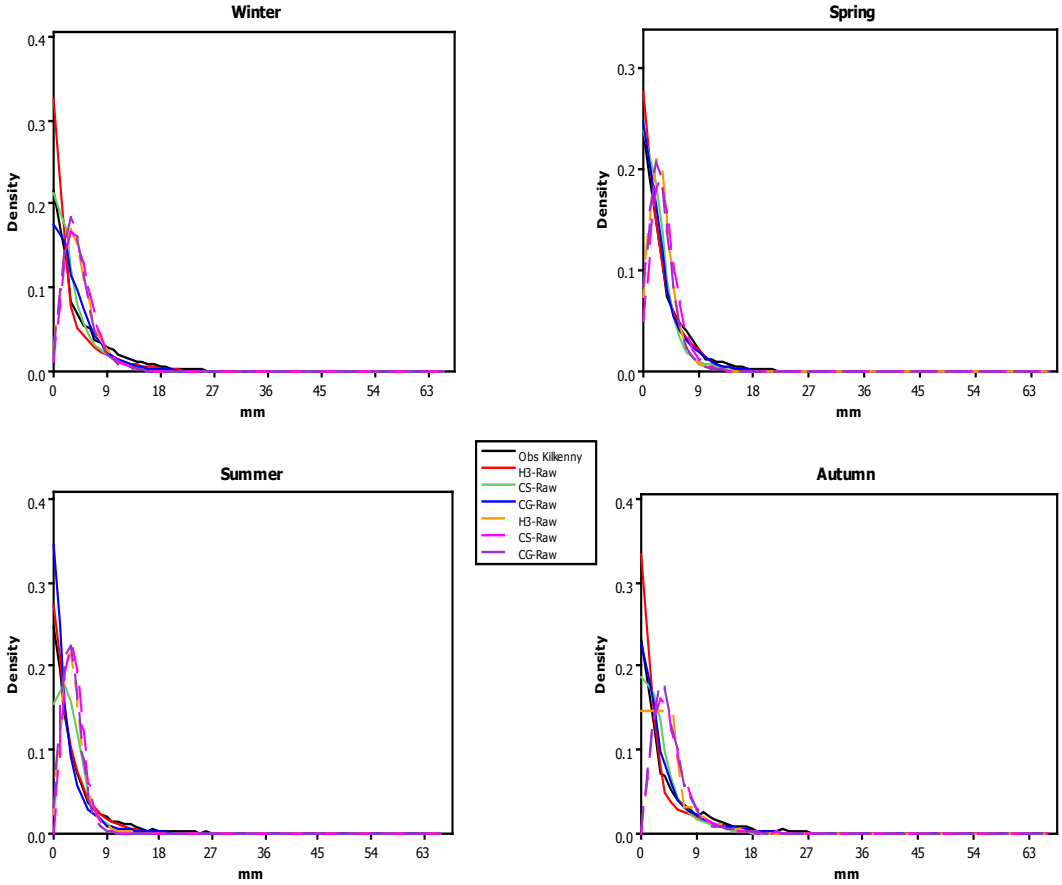

Figure A.I 2. Probability distribution functions (PDFs) of daily observed precipitation at Kilkenny, direct global climate model (GCM) daily precipitation (Raw) and bias corrected statistically downscaled (SD) daily precipitation for the 1960–1990 period for the A2 emissions scenario (observed data from Met Éireann; GCM data after Wilby and Dawson, 2007; statistically downscaled data after Fealy and Sweeney, 2007; 2008b).

Appendix II

Table A.II. Global (ΔTglobal) and regional (Irish grid box from respective global climate model (GCM)) (ΔT_{DJF}, ΔT_{MAM},ΔT_{JJA}, ΔT_{SON}, ΔT_{ANN}) temperature (°C) and (ΔP_{DJF}, ΔP_{MAM}, ΔP_{JJA}, ΔP_{SON}, ΔP_{ANN}) precipitation change (%) from four GCMs and four marker emissions scenarios.

GCM	Scenario	ΔT_{GLOBAL}	ΔT_{DJF}	ΔT_{MAM}	ΔT_{JJA}	ΔT_{SON}	ΔT_{ANN}	ΔP_{DJF}	ΔP_{MAM}	ΔP_{JJA}	ΔP_{SON}	ΔP_{ANN}
CGCM2	A1F1	4.382	2.7	2.2	3.3	2.9	2.8	18.2	9.3	0	-1.4	7.0
CGCM2	A2	3.548	2.1	1.8	2.7	2.3	2.2	14.7	7.5	0	-1.1	5.6
CGCM2	B2	2.462	1.6	1.6	2.0	1.9	1.7	7.3	12.2	0.4	4.7	6.2
CGCM2	B1	2.023	1.3	1.3	1.6	1.5	1.4	6.0	10.0	0.3	3.9	5.1
CSIRO Mk2	A1F1	4.855	2.9	1.9	2.8	3.0	2.7	18.3	7.7	-9.0	6.7	7.3
CSIRO Mk2	A2	3.938	3.1	2.0	2.7	3.1	2.7	21.1	11.7	-0.9	6.3	10.4
CSIRO Mk2	B2	3.139	2.6	1.5	2.2	2.4	2.2	21.9	7.5	-2.1	8.4	10.2
CSIRO Mk2	B1	2.592	2.2	1.4	2.1	2.4	2.0	6.1	11.7	5.3	8.4	7.8
HadCM3	A1F1	4.863	2.7	2.8	3.1	3.3	3.0	25.0	3.7	-35.2	9.9	4.2
HadCM3	A2	3.931	2.3	2.1	2.3	2.7	2.4	20.8	7.1	-27.0	5.2	3.9
HadCM3	B2	3.07	1.4	1.5	1.5	1.8	1.5	7.3	7.4	-17.4	2.8	1.1
HadCM3	B1	2.521	1.6	1.4	1.5	1.7	1.5	14.4	5.3	-21.9	5.3	2.7
PCM	A1F1	3.045	2.3	2.2	1.7	3.1	2.3	8.4	24.8	3.3	2.8	9.2
PCM	A2	2.462	1.9	1.8	1.4	2.5	1.9	6.8	20.1	2.6	2.3	7.5
PCM	B2	1.894	1.5	1.6	0.9	2.0	1.5	7.1	16.3	7.3	0.1	7.0
PCM	B1	1.541	1.2	1.3	0.7	1.6	1.2	5.7	13.2	5.9	0.1	5.7

Source: data from Mitchell et al., 2002.

Appendix III

Quantifying Uncertainty in Global Climate Model Projections at the Regional Scale

Global climate model (GCM) data for the grid box domain representing Ireland was obtained for four GCMs and four emissions scenarios (data obtained from Mitchell et al., 2002). The data for all the models employed exists on a common grid for the Irish domain (Mitchell et al., 2002). The four models, namely the CGCM2, CSIRO Mk2, HadCM3 and NCAR PCM and their respective equilibrium climate sensitivity, are listed in Table A.III 1. While GCM selection was determined solely on data availability, all four have been used extensively and appear in a range of peer-reviewed literature, and they represent a sample of the spread in estimated climate sensitivity.

The regional data, derived from the grid box for Ireland, for each model and emissions scenario (Table A.III 2), was first standardised or normalised according to its respective GCM global mean temperature change (ΔTglobal) for that particular emissions scenario. This normalisation is akin to normalising the regional change signal in the pattern scaling methodology, outlined previously, in order to derive a regional 'response pattern'. The normalised, regional values, of temperature and precipitation change reflect a regional response per °C global warming for the 2080s' period (Table A.III 3).

Table A.III 1. List of global climate models (GCM) employed in analysis, institution, equilibrium climate sensitivity and reference for each GCM.

GCM Name	Institution/country	$2xCO_2$ ΔT	Reference
CGCM2	CCCma, Canada	3.5°C	Flato et al., 2000
CSIRO Mk2	CSIRO, Australia	4.3°C	Hirst et al., 1996, 2000
HadCM3	UKMO, UK	3.3°C	Gordon et al., 2000
NCAR PCM	NCAR, USA	2.1°C	Washington et al., 2000

Table A.III 2. Global (ΔTglobal) and regional (Irish grid box(es) from respective global climate model (GCM)) (Δt_{JJA}, Δt_{DJF}, Δt_{ANN}) temperature (°C) and (Δp_{JJA}, Δp_{DJF}, Δp_{ANN}) precipitation change (%) from four GCMs and four marker emissions scenarios (Data from Mitchell et al., 2002).

Model	Scenario	ΔT_{global}	Δt_{JJA}	Δt_{DJF}	Δt_{ANN}	Δp_{JJA}	Δp_{DJF}	Δp_{ANN}
CGCM2	A1FI	4.38	3.3	2.7	2.8	0	18.2	7.0
CGCM2	A2	3.55	2.7	2.1	2.2	0	14.7	5.6
CGCM2	B2	2.46	2.0	1.6	1.7	0.4	7.3	6.2
CGCM2	B1	2.02	1.6	1.3	1.4	0.3	6.0	5.1
CSIRO Mk2	A1FI	4.86	2.8	2.9	2.7	-9.0	18.3	7.3
CSIRO Mk2	A2	3.94	2.7	3.1	2.7	-0.9	21.1	10.4
CSIRO Mk2	B2	3.14	2.2	2.6	2.2	-2.1	21.9	10.2
CSIRO Mk2	B1	2.59	2.1	2.2	2.0	5.3	6.1	7.8
HadCM3	A1FI	4.86	3.1	2.7	3.0	-35.2	25.0	4.2
HadCM3	A2	3.93	2.3	2.3	2.4	-27.0	20.8	3.9
HadCM3	B2	3.07	1.5	1.4	1.5	-17.4	7.3	1.1
HadCM3	B1	2.52	1.5	1.6	1.5	-21.9	14.4	2.7
PCM	A1FI	3.05	1.7	2.3	2.3	3.3	8.4	9.2
PCM	A2	2.46	1.4	1.9	1.9	2.6	6.8	7.5
PCM	B2	1.89	0.9	1.5	1.5	7.3	7.1	7.0
PCM	B1	1.54	0.7	1.2	1.2	5.9	5.7	5.7

Table A.III 3. Normalised regional temperature (°C) and precipitation (%) responses for the 2070–2099 period for Ireland derived from the global climate model (GCM) and emissions combinations outlined in Table A.III 2.

Variable	Regional			
	DJF	MAM	JJA	SON
Temperature ($\Delta T_{REGIONAL}/\Delta T_{GLOBAL}$)	0.46 – 0.85	0.39 – 0.84	0.45 – 0.81	0.59 – 1.06
Precipitation ($\Delta P_{REGIONAL}/\Delta T_{GLOBAL}$)	+2.35 – +6.98	+0.76 – +8.61	-8.69 – +3.85	-0.32 – +3.24

DJF = December, January, February; MAM = March, April, May; JJA = June, July, August; SON = September, October, November (data from Mitchell et al., 2002).

In addition to the regional uncertainty signal (i.e. the regional rate of warming derived from the four GCMs), these regional ranges encompass four Special Report on Emissions Scenarios (SRES) emissions marker scenarios, which in turn account for approximately 80% of the range of future emissions contained in the full range of 40 emissions scenarios storylines. Table A.III 4 illustrates the range in projected values for global temperature and regional temperature and precipitation the 2080s. While projected changes in temperature are similar in direction, they differ in magnitude, in contrast to the projected changes in precipitation, which differ in both magnitude and direction.

Following Jones (2000), three sources of uncertainty are considered: (i) emissions scenarios; (ii) climate sensitivity; and (iii) regional variability, for two 'impact critical' climate variables, temperature and precipitation, for the winter and summer seasons for the 2080. The 2080s was selected as the signal-to-noise ratio is likely to be larger for this period. However, no measure of natural variability is considered.

The data from Table A.III 3 was then used in conjunction with the estimated climate sensitivity range of 2.1 to 4.6°C (5 to 95% probability for lognormal distribution), with a median value of 3.2°C. While the IPCC (2007) attaches a likelihood to the estimated range in equilibrium climate sensitivity, no such likelihoods are attached to the regional response per °C. Consequently, a uniform distribution was assumed as a prior, attributing an equal probability to all values within the regional response ranges.

Based on the range in equilibrium climate sensitivity estimated in the Second Assessment Report (0.7 to 2.1°C) (IPCC, 1996), Jones (2000) attributed a uniform distribution to both the climate sensitivity and regional response, derived from five GCMs. It has been shown that if two probabilities have a uniform distribution and are considered to be independent of each other, when they are multiplied together, the resultant distribution will have a peak around its average value (Jones, 2000). However, the *Fourth Assessment Report* has attributed a probability distribution to the revised estimates for equilibrium climate sensitivity, which is employed here (Fig. A.III 1).

In order to produce probabilities of future warming for Ireland, taking into account some of the key uncertainties associated with the projected warming,

Table A.III 4. Range from lowest to highest in projected global temperature change (ΔT) (°C) regional temperature (°C) and precipitation change (%) for Ireland from the global climate model (GCM) and emissions combinations outlined in Table A.III 2.

Variable	Global	Regional			
		DJF	MAM	JJA	SON
Temperature (ΔT)	1.54 – 4.86	1.2 – 3.1	1.3 – 2.8	0.7 – 3.3	1.5 – 3.3
Precipitation (ΔP)		+5.7 – +25.0	+3.7 – +24.8	-35.2 – +7.3	-1.4 – +9.9

DJF = December, January, February; MAM = March, April, May; JJA = June, July, August; SON = September, October, November (data from Mitchell et al., 2002).

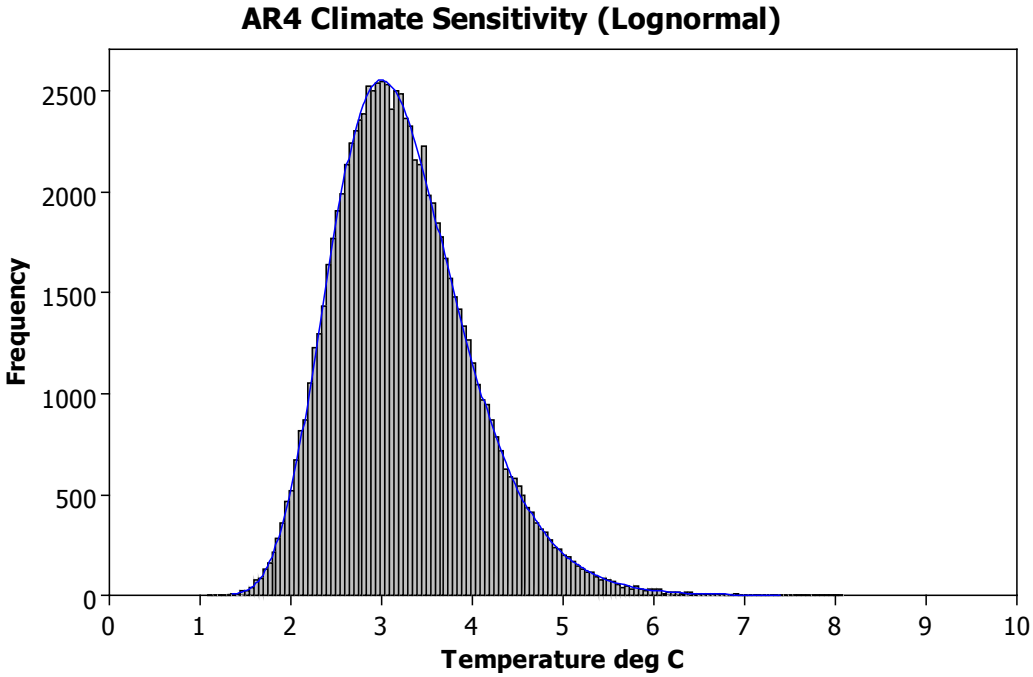

Figure A.III 1. Monte Carlo simulation of equilibrium climate sensitivity with a median value of 3.2˚C and 5 to 95% probability range of 2.1 to 4.6˚C. (The 95% probability range differs from that quoted in the IPCC (2007) range of 2.2 to 4.6˚C, however, this difference is considered negligible).

a Monte Carlo (MC) analysis was employed. The MC was used to randomly sample from both the lognormal, representing equilibrium climate sensitivity, and uniform, representing the regional response rate in temperature and precipitation per degree of global warming, distributions. The resulting ΔT and ΔP therefore represent or take account of uncertainties in the emissions scenarios, by sampling from four marker emissions scenarios A1FI, A2, B2 and B1; climate sensitivity, through the incorporation of the estimated range in sensitivity from the Fourth Assessment Report (IPCC, 2007); GCM climate sensitivity and the regional GCM response, through the response rates per °C global warming. The MC simulation was set to produce 100,000 samples using a burn in of 10,000 samples, which were subsequently deleted, the results of which are shown in Figures A.III 2 and A.III 3.

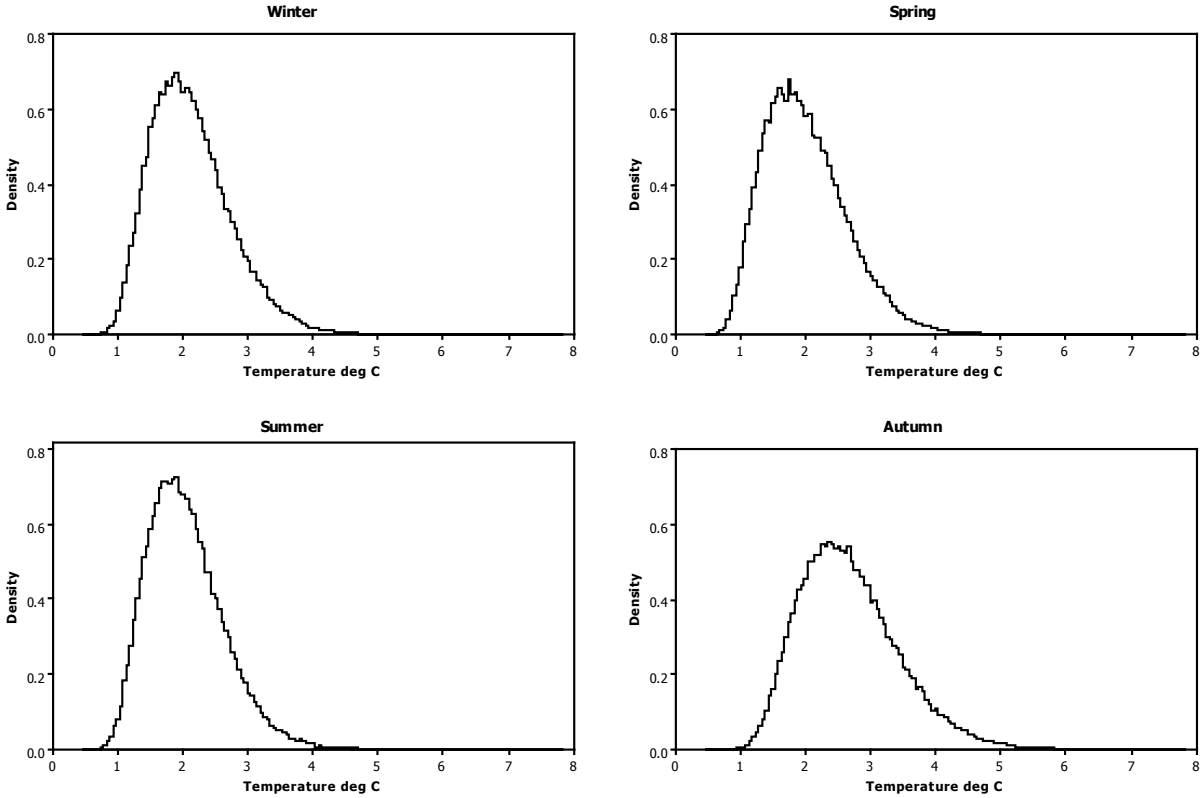

Figure A.III 2. Probability distribution of seasonal mean temperature change (°C) based on the *Fourth Assessment Report* estimated equilibrium climate sensitivity (lognormal) and regional response rates for the Ireland grid box.

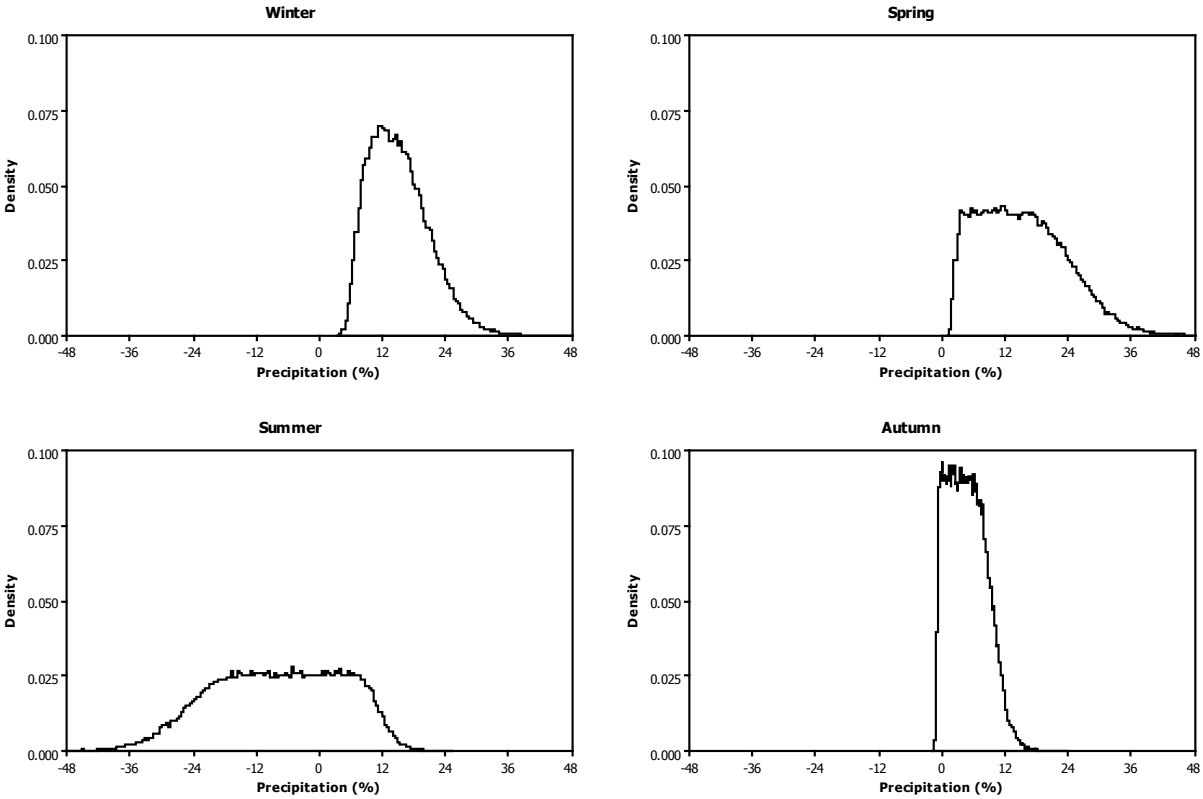

Figure A.III 3. Probability distribution of seasonal precipitation change (%) based on the *Fourth Assessment Report* estimated equilibrium climate sensitivity (lognormal) and regional response rates for the Ireland grid box.

Table A.III 5. Distributional parameters of the PDFs of temperature and precipitation derived from the Monte Carlo analysis for the 2080s (2070–2099).

Variable	Season	Mean	SE Mean	St Dev	Q1	Median	Q3	Min.	Max.
ΔT (°C)	DJF	2.11	0.00	0.62	1.66	2.04	2.48	0.53	5.95
ΔT (°C)	MAM	1.99	0.00	0.63	1.52	1.91	2.37	0.48	6.12
ΔT (°C)	JJA	2.04	0.00	0.58	1.61	1.97	2.38	0.64	5.74
ΔT (°C)	SON	2.67	0.00	0.76	2.11	2.57	3.12	0.83	7.78
ΔP (%)	DJF	15.08	0.02	5.66	10.71	14.41	18.61	3.39	48.82
ΔP (%)	MAM	15.16	0.03	8.29	8.38	14.41	20.83	1.11	63.06
ΔP (%)	JJA	-7.87	0.04	12.21	-17.19	-7.46	2.23	-60.09	25.22
ΔP (%)	SON	4.71	0.01	3.59	1.73	4.46	7.28	-1.94	23.69

DJF = December, January, February; MAM = March, April, May; JJA = June, July, August; SON = September, October, November.

Table A.III 5 shows the change in mean temperature (°C) and precipitation (%) for the 2070 to 2099 period.

Appendix IV

Table A.IV 1. Scaled temperature change (°C) for selected stations for the 2070–2099 period from three global climate model (GCM) and four emissions scenarios (SRES) for December, January and February (DJF).

GCM	SRES	Valentia	Shannon	Dublin	Malin Head	Roche's Point	Belmullet	Clones	Rosslare	Claremorris	Mullingar	Kilkenny	Casement	Cork	Birr
CGCM2	A1FI	5.1	5.8	4.3	4.3	4.8	4.8	5.9	4.9	5.9	5.9	5.7	5.9	5.4	6.0
CGCM2	A2	3.0	3.4	2.5	2.5	2.8	2.9	3.5	2.9	3.5	3.5	3.4	3.5	3.2	3.6
CGCM2	B2	2.9	3.3	2.5	2.3	2.7	2.7	3.3	2.7	3.4	3.3	3.2	3.3	3.0	3.4
CGCM2	B1	2.4	2.7	2.0	2.0	2.2	2.2	2.7	2.3	2.7	2.7	2.6	2.8	2.5	2.8
CSIRO	A1FI	4.4	4.9	3.8	3.7	4.2	4.3	5.0	4.0	5.0	4.9	5.0	5.0	4.6	5.3
CSIRO	A2	3.7	4.2	3.2	3.1	3.5	3.6	4.2	3.4	4.3	4.2	4.2	4.2	3.9	4.5
CSIRO	B2	2.9	3.3	2.6	2.5	2.7	2.9	3.3	2.7	3.3	3.3	3.3	3.3	3.0	3.4
CSIRO	B1	2.4	2.7	2.2	2.1	2.4	2.4	2.8	2.3	2.8	2.7	2.8	2.8	2.6	2.9
HadCM3	A1FI	1.2	1.3	1.1	1.1	1.1	1.1	1.4	1.1	1.3	1.4	1.4	1.4	1.2	1.4
HadCM3	A2	1.4	1.5	1.3	1.2	1.3	1.3	1.6	1.3	1.6	1.6	1.6	1.6	1.4	1.6
HadCM3	B2	0.7	0.8	0.6	0.7	0.7	0.7	0.8	0.7	0.8	0.8	0.9	0.9	0.8	0.9
HadCM3	B1	0.6	0.7	0.6	0.5	0.6	0.6	0.7	0.5	0.7	0.7	0.7	0.7	0.6	0.7

The A2 and B2 scenario data are directly derived from statistically downscaled data (after Fealy and Sweeney, 2008). The A1FI and B1 scenarios were derived by scaling the statistically downscaled A2 scenario according to the ratio of ΔT from the parent GCM and relevant emissions scenario for each season. SRES = Special Report on Emissions Scenarios.

Table A.IV 2. Scaled temperature change (°C) for selected stations for the 2070–2099 period from three global climate models (GCM) and four emissions scenarios (SRES) for March, April and May (MAM).

GCM	SRES	Valentia	Shannon	Dublin	Malin Head	Roche's Point	Belmullet	Clones	Rosslare	Claremorris	Mullingar	Kilkenny	Casement	Cork	Birr
CGCM2	A1FI	4.1	4.4	3.7	3.7	3.2	4.1	4.5	2.6	4.6	4.6	4.3	4.1	3.8	4.5
CGCM2	A2	2.5	2.7	2.3	2.3	2.0	2.5	2.8	1.6	2.9	2.8	2.6	2.6	2.3	2.8
CGCM2	B2	2.2	2.5	2.1	1.9	1.8	2.3	2.5	1.5	2.6	2.6	2.4	2.4	2.1	2.6
CGCM2	B1	1.9	2.0	1.7	1.7	1.5	1.9	2.1	1.2	2.1	2.1	2.0	1.9	1.8	2.1
CSIRO	A1FI	2.4	2.7	2.5	2.4	2.2	2.4	2.8	2.1	2.7	2.8	2.7	2.7	2.5	2.8
CSIRO	A2	1.7	1.9	1.8	1.7	1.6	1.8	2.0	1.5	2.0	2.0	2.0	2.0	1.8	2.0
CSIRO	B2	1.5	1.7	1.7	1.5	1.5	1.6	1.8	1.4	1.8	1.8	1.8	1.8	1.7	1.8
CSIRO	B1	1.3	1.5	1.4	1.3	1.2	1.3	1.5	1.2	1.5	1.5	1.5	1.5	1.4	1.5
HadCM3	A1FI	1.8	2.1	2.0	1.7	1.8	1.8	2.3	1.7	2.2	2.3	2.2	2.2	1.9	2.2
HadCM3	A2	1.8	2.1	2.0	1.7	1.7	1.8	2.2	1.7	2.2	2.3	2.2	2.2	1.9	2.2
HadCM3	B2	1.2	1.3	1.3	1.1	1.1	1.2	1.4	1.1	1.4	1.4	1.4	1.4	1.3	1.4
HadCM3	B1	1.0	1.1	1.1	0.9	0.9	0.9	1.2	0.9	1.1	1.2	1.2	1.1	1.0	1.2

The A2 and B2 scenario data are directly derived from statistically downscaled data (after Fealy and Sweeney, 2008). The A1FI and B1 scenarios were derived by scaling the statistically downscaled A2 scenario according to the ratio of ΔT from the parent GCM and relevant emissions scenario for each season. SRES = Special Report on Emissions Scenarios.

Table A.IV 3. Scaled temperature change (°C) for selected stations for the 2070–2099 period from three global climate models (GCMs) and four emissions scenarios (SRES) for June, July and August (JJA). The A2 and B2 scenario data are directly derived from statistically downscaled data (after Fealy and Sweeney, 2008).

GCM	SRES	Valentia	Shannon	Dublin	Malin Head	Roche's Point	Belmullet	Clones	Rosslare	Claremorris	Mullingar	Kilkenny	Casement	Cork	Birr
CGCM2	A1FI	3.6	4.1	3.7	3.1	3.3	3.4	4.3	2.9	4.2	4.3	4.5	4.2	3.9	4.4
CGCM2	A2	3.1	3.5	3.2	2.6	2.8	2.9	3.6	2.5	3.6	3.7	3.8	3.6	3.3	3.8
CGCM2	B2	2.0	2.3	2.1	1.7	1.8	1.9	2.5	1.6	2.3	2.4	2.4	2.4	2.2	2.5
CGCM2	B1	1.6	1.9	1.7	1.4	1.5	1.6	2.0	1.3	1.9	2.0	2.0	1.9	1.8	2.0
CSIRO	A1FI	2.1	2.5	2.3	1.9	2.4	2.3	2.7	2.0	2.7	2.6	2.7	2.4	2.6	2.8
CSIRO	A2	2.1	2.5	2.2	1.8	2.4	2.3	2.7	2.0	2.8	2.7	2.8	2.4	2.7	2.8
CSIRO	B2	1.5	1.8	1.6	1.3	1.7	1.6	1.8	1.4	1.8	1.8	1.9	1.7	1.8	1.9
CSIRO	B1	1.3	1.5	1.4	1.1	1.4	1.4	1.6	1.2	1.6	1.6	1.6	1.4	1.6	1.6
HadCM3	A1FI	2.5	2.9	3.0	2.4	3.1	2.6	3.0	2.6	2.9	3.1	3.3	3.1	3.2	3.1
HadCM3	A2	2.5	2.9	3.0	2.4	3.1	2.6	3.0	2.6	2.9	3.1	3.3	3.1	3.2	3.1
HadCM3	B2	1.6	1.9	2.0	1.6	2.0	1.7	2.0	1.8	1.9	2.0	2.1	2.0	2.1	2.0
HadCM3	B1	1.4	1.6	1.7	1.3	1.7	1.4	1.6	1.4	1.6	1.7	1.8	1.7	1.7	1.7

The A1FI and B1 scenarios were derived by scaling the statistically downscaled A2 scenario according to the ratio of ΔT from the parent GCM and relevant emissions scenario for each season. SRES = Special Report on Emissions Scenarios.

Table A.IV 4. Scaled temperature change (°C) for selected stations for the 2070–2099 period from three global climate models (GCMs) and four emissions scenarios (SRES) for September, October and November (SON).

GCM	SRES	Valentia	Shannon	Dublin	Malin Head	Roche's Point	Belmullet	Clones	Rosslare	Claremorris	Mullingar	Kilkenny	Casement	Cork	Birr
CGCM2	A1FI	4.3	4.9	5.0	4.0	4.2	3.9	5.1	4.2	5.1	5.2	5.5	5.3	4.6	5.4
CGCM2	A2	2.7	3.0	3.1	2.4	2.6	2.4	3.1	2.6	3.1	3.2	3.4	3.2	2.8	3.3
CGCM2	B2	2.5	2.8	2.8	2.2	2.4	2.2	2.9	2.5	2.9	3.0	3.1	3.0	2.7	3.1
CGCM2	B1	2.0	2.3	2.4	1.9	2.0	1.9	2.4	2.0	2.4	2.4	2.6	2.5	2.2	2.5
CSIRO	A1FI	4.7	5.6	5.5	4.6	4.7	4.9	5.7	4.8	5.6	5.8	5.8	5.7	5.2	5.8
CSIRO	A2	3.2	3.8	3.7	3.1	3.2	3.3	3.8	3.3	3.8	3.9	3.9	3.8	3.5	3.9
CSIRO	B2	3.0	3.5	3.5	2.9	2.9	3.1	3.6	3.1	3.5	3.7	3.7	3.7	3.3	3.7
CSIRO	B1	2.5	2.9	2.8	2.4	2.4	2.5	2.9	2.5	2.9	3.0	3.0	3.0	2.7	3.0
HadCM3	A1FI	2.4	2.8	2.7	2.3	2.3	2.4	2.9	2.4	2.8	2.9	3.0	2.9	2.6	2.9
HadCM3	A2	2.3	2.6	2.6	2.2	2.2	2.2	2.7	2.3	2.6	2.7	2.8	2.7	2.4	2.8
HadCM3	B2	1.5	1.7	1.7	1.5	1.5	1.5	1.8	1.5	1.8	1.8	1.9	1.8	1.6	1.8
HadCM3	B1	1.2	1.4	1.4	1.2	1.2	1.2	1.5	1.2	1.4	1.5	1.5	1.5	1.3	1.5

The A2 and B2 scenario data are directly derived from statistically downscaled data (after Fealy and Sweeney, 2008). The A1FI and B1 scenarios were derived by scaling the statistically downscaled A2 scenario according to the ratio of ΔT from the parent GCM and relevant emissions scenario for each season. SRES = Special Report on Emissions Scenarios.

Table A.IV 5. Scaled percent change in precipitation (%) for selected stations for the 2070–2099 period from three global climate models (GCMs) and four emissions scenarios (SRES) for December, January and February (DJF).

GCM	SRES	Valentia	Shannon	Dublin	Malin Head	Roche's Point	Belmullet	Clones	Rosslare	Claremorris	Mullingar	Kilkenny	Casement	Cork	Birr
CGCM2	A1FI	-3.8	4.9	35.3	4.5	8.0	-2.2	24.6	12.4	20.5	20.6	18.7	24.5	1.0	24.5
CGCM2	A2	-4.5	2.3	26.6	2.0	4.9	-3.3	18.1	8.3	14.8	14.9	13.3	18.0	-0.8	18.0
CGCM2	B2	-2.8	5.7	20.1	5.5	3.4	0.8	16.6	7.9	12.1	12.8	10.7	13.0	-0.4	15.2
CGCM2	B1	-0.7	3.3	17.3	3.1	4.8	0.0	12.4	6.8	10.5	10.5	9.7	12.3	1.5	12.3
CSIRO	A1FI	0.1	16.4	45.4	5.5	12.6	1.5	34.1	21.1	25.6	33.9	26.6	35.1	5.7	38.5
CSIRO	A2	1.8	15.3	39.4	6.3	12.2	3.0	30.1	19.3	23.0	29.8	23.8	30.9	6.5	33.7
CSIRO	B2	-0.8	8.6	28.8	4.6	7.2	1.9	20.9	11.5	16.4	21.4	16.3	22.7	1.2	24.6
CSIRO	B1	-0.9	7.8	23.3	2.0	5.8	-0.2	17.3	10.3	12.7	17.1	13.2	17.8	2.1	19.6
HadCM3	A1FI	9.9	17.6	27.2	10.5	16.2	9.9	23.7	18.2	17.7	24.1	22.1	21.6	14.6	27.1
HadCM3	A2	9.1	17.4	27.8	9.7	15.9	9.1	24.1	18.1	17.5	24.4	22.3	21.8	14.2	27.7
HadCM3	B2	8.1	8.6	18.6	4.9	13.6	4.3	13.6	14.1	10.8	14.4	15.7	16.3	13.1	16.1
HadCM3	B1	5.8	9.8	14.8	6.1	9.1	5.8	13.0	10.1	9.9	13.2	12.2	11.9	8.3	14.8

The A2 and B2 scenario data are directly derived from statistically downscaled data (after Fealy and Sweeney, 2008). The A1FI and B1 scenarios were derived by scaling the statistically downscaled A2 scenario according to the ratio of ΔT from the parent GCM and relevant emissions scenario for each season. SRES = Special Report on Emissions Scenarios.

Table A.IV 6. Scaled percent change in precipitation (%) for selected stations for the 2070–2099 period from global climate models (GCMs) and four emissions scenarios (SRES) for March, April and May (MAM).

GCM	SRES	Valentia	Shannon	Dublin	Malin Head	Roche's Point	Belmullet	Clones	Rosslare	Claremorris	Mullingar	Kilkenny	Casement	Cork	Birr
CGCM2	A1FI	-23.1	-44.0	-26.5	-39.3	-7.1	-27.4	-38.5	-21.0	-30.3	-38.7	-33.4	-29.5	-15.9	-34.6
CGCM2	A2	-20.9	-36.3	-23.4	-32.8	-9.1	-24.0	-32.2	-19.3	-26.2	-32.4	-28.4	-25.6	-15.6	-29.3
CGCM2	B2	-10.5	-22.2	-12.9	-20.8	-2.3	-13.5	-18.9	-8.2	-14.3	-20.7	-16.3	-12.6	-7.5	-17.1
CGCM2	B1	-7.8	-17.5	-9.4	-15.3	-0.5	-9.8	-14.9	-6.9	-11.2	-15.0	-12.6	-10.8	-4.5	-13.1
CSIRO	A1FI	-1.3	0.7	0.3	1.1	-1.1	0.7	0.5	-1.2	-0.4	1.4	-0.1	1.6	-1.4	1.2
CSIRO	A2	-8.1	-1.5	-2.8	-0.1	-7.5	-1.5	-2.0	-7.7	-5.0	0.9	-3.9	1.5	-8.3	0.3
CSIRO	B2	-2.4	1.4	1.3	-1.1	1.2	-1.1	0.7	0.9	-2.5	2.6	1.3	2.8	0.4	1.4
CSIRO	B1	-0.2	0.9	0.7	1.1	-0.1	0.9	0.8	-0.1	0.3	1.3	0.5	1.4	-0.2	1.2
HadCM3	A1FI	5.2	6.7	4.9	8.1	4.5	5.7	8.3	3.7	7.6	6.5	5.4	5.2	4.2	6.2
HadCM3	A2	-7.7	0.3	-9.1	7.1	-10.9	-5.0	8.3	-15.2	4.7	-0.8	-6.3	-7.3	-12.7	-2.2
HadCM3	B2	5.7	5.8	5.8	6.3	5.5	6.1	9.0	4.6	8.8	4.5	6.4	5.5	5.6	6.8
HadCM3	B1	5.9	6.7	5.7	7.4	5.6	6.2	7.5	5.1	7.1	6.6	6.0	5.9	5.4	6.4

The A2 and B2 scenario data are directly derived from statistically downscaled data (after Fealy and Sweeney, 2008). The A1FI and B1 scenarios were derived by scaling the statistically downscaled A2 scenario according to the ratio of ΔT from the parent GCM and relevant emissions scenario for each season. SRES = Special Report on Emissions Scenarios.

Table A.IV 7. Scaled percent change in precipitation (%) for selected stations for the 2070–2099 period from global climate models (GCMs) and four emissions scenarios (SRES) for June, July and August (JJA).

GCM	SRES	Valentia	Shannon	Dublin	Malin Head	Roche's Point	Belmullet	Clones	Rosslare	Claremorris	Mullingar	Kilkenny	Casement	Cork	Birr
CGCM2	A1FI	-29.2	-32.9	-48.5	-22.3	-32.4	-19.2	-28.7	-21.7	-7.7	-36.2	-19.4	-47.7	-19.2	-36.1
CGCM2	A2	-17.4	-19.1	-26.1	-14.3	-18.9	-12.9	-17.2	-14.1	-7.8	-20.6	-13.0	-25.7	-13.0	-20.5
CGCM2	B2	-14.5	-16.5	-23.6	-4.2	-14.0	-5.3	-9.2	-9.1	-1.3	-13.2	-6.7	-23.0	-8.6	-16.7
CGCM2	B1	-8.3	-10.0	-17.2	-5.1	-9.8	-3.6	-8.0	-4.8	1.6	-11.5	-3.7	-16.8	-3.7	-11.5
CSIRO	A1FI	-24.8	-30.3	-43.2	-13.3	-44.0	-14.8	-16.9	-32.0	-14.3	-25.2	-19.6	-31.0	-29.8	-24.2
CSIRO	A2	-25.9	-30.4	-41.0	-16.5	-41.6	-17.7	-19.4	-31.8	-17.2	-26.2	-21.6	-31.0	-29.9	-25.4
CSIRO	B2	-17.3	-18.5	-25.4	-6.7	-25.8	-7.3	-9.0	-14.2	-7.0	-11.7	-5.7	-20.2	-18.0	-14.8
CSIRO	B1	-10.1	-13.0	-20.0	-4.0	-20.4	-4.8	-5.9	-13.9	-4.5	-10.3	-7.3	-13.4	-12.8	-9.8
HadCM3	A1FI	-24.3	-21.5	-26.2	-10.1	-26.5	-10.2	-17.0	-20.3	-17.1	-21.4	-23.9	-24.6	-25.9	-22.1
HadCM3	A2	-29.0	-25.2	-31.5	-9.8	-32.0	-9.9	-19.1	-23.5	-19.2	-25.1	-28.5	-29.3	-31.2	-26.0
HadCM3	B2	-18.4	-15.2	-16.4	-7.0	-19.1	-10.6	-10.2	-12.2	-9.7	-14.7	-17.4	-14.0	-19.3	-14.8
HadCM3	B1	-14.0	-12.6	-15.0	-6.7	-15.2	-6.7	-10.2	-11.9	-10.3	-12.5	-13.8	-14.1	-14.8	-12.9

The A2 and B2 scenario data are directly derived from statistically downscaled data (after Fealy and Sweeney, 2008). The A1FI and B1 scenarios were derived by scaling the statistically downscaled A2 scenario according to the ratio of ΔT from the parent GCM and relevant emissions scenario for each season. SRES = Special Report on Emissions Scenarios.

Table A.IV 8. Scaled percent change in precipitation (%) for selected stations for the 2070–2099 period from global climate models (GCMs) and four emissions scenarios (SRES) for September, October and November (SON).

GCM	SRES	Valentia	Shannon	Dublin	Malin Head	Roche's Point	Belmullet	Clones	Rosslare	Claremorris	Mullingar	Kilkenny	Casement	Cork	Birr
CGCM2	A1FI	-27.3	-15.5	-18.9	-2.4	-32.5	-8.8	-14.8	-17.9	-18.1	9.0	-26.4	-11.8	-27.9	-8.8
CGCM2	A2	-22.4	-14.5	-16.8	-5.7	-25.9	-10.0	-14.0	-16.2	-16.3	1.9	-21.9	-12.1	-22.9	-10.0
CGCM2	B2	-13.8	-4.5	-9.0	5.4	-15.5	-0.8	-6.3	-9.4	-6.6	7.3	-11.8	-7.5	-9.9	-4.4
CGCM2	B1	-9.3	-3.8	-5.4	2.2	-11.7	-0.7	-3.5	-5.0	-5.0	7.5	-8.9	-2.1	-9.6	-0.7
CSIRO	A1FI	-23.0	-8.4	-12.8	1.2	-25.8	-6.1	-7.6	-15.7	-12.5	8.2	-21.0	-8.0	-21.0	-5.5
CSIRO	A2	-21.9	-7.9	-12.1	1.2	-24.5	-5.8	-7.2	-14.9	-11.9	7.8	-19.9	-7.5	-19.9	-5.2
CSIRO	B2	-15.5	-6.5	-10.2	-1.8	-16.6	-2.3	-5.0	-9.7	-6.1	10.0	-14.0	-9.7	-8.9	-5.9
CSIRO	B1	-12.3	-4.5	-6.8	0.6	-13.8	-3.3	-4.1	-8.4	-6.7	4.3	-11.2	-4.3	-11.2	-2.9
HadCM3	A1FI	-12.6	-2.4	-9.4	1.6	-14.9	-1.3	-2.1	-11.0	-2.2	11.4	-11.5	-6.2	-8.0	-2.9
HadCM3	A2	-14.6	-4.0	-11.2	0.2	-17.1	-2.8	-3.7	-12.9	-3.8	10.5	-13.5	-7.9	-9.8	-4.5
HadCM3	B2	-8.7	-0.9	-3.7	2.4	-9.9	-1.0	-1.4	-6.4	-2.6	6.9	-6.6	-2.5	-4.7	0.9
HadCM3	B1	-5.9	-0.6	-4.2	1.5	-7.1	0.0	-0.4	-5.0	-0.5	6.6	-5.3	-2.5	-3.5	-0.9

The A2 and B2 scenario data are directly derived from statistically downscaled data (after Fealy and Sweeney, 2008). The A1FI and B1 scenarios were derived by scaling the statistically downscaled A2 scenario according to the ratio of ΔT from the parent GCM and relevant emissions scenario for each season. SRES = Special Report on Emissions Scenarios.

Appendix Va

Scaling Factors for Statistically Downscaled Temperature (2070–2099)

Table A.Va 1. A1FI scaling factors for statistically downscaled temperature (2070–2099).

SRES	Station	CGCM2				CSIRO Mk2				HadCM3			
		DJF	MAM	JJA	SON	DJF	MAM	JJA	SON	DJF	MAM	JJA	SON
A1FI	Valentia	1.16	0.93	0.81	0.99	0.90	0.49	0.44	0.97	0.24	0.38	0.51	0.50
A1FI	Shannon	1.32	1.01	0.94	1.13	1.02	0.55	0.51	1.15	0.27	0.44	0.60	0.57
A1FI	Dublin	0.97	0.85	0.84	1.15	0.79	0.52	0.47	1.13	0.23	0.42	0.62	0.56
A1FI	Malin Head	0.98	0.85	0.70	0.91	0.77	0.49	0.38	0.94	0.22	0.35	0.49	0.48
A1FI	Roche's Point	1.09	0.72	0.75	0.95	0.87	0.46	0.49	0.97	0.23	0.36	0.64	0.48
A1FI	Belmullet	1.10	0.93	0.78	0.89	0.88	0.50	0.48	1.01	0.23	0.37	0.53	0.49
A1FI	Clones	1.34	1.03	0.97	1.15	1.03	0.57	0.55	1.16	0.28	0.46	0.61	0.60
A1FI	Rosslare	1.11	0.60	0.66	0.95	0.83	0.44	0.42	1.00	0.22	0.36	0.53	0.50
A1FI	Claremorris	1.34	1.05	0.95	1.16	1.04	0.56	0.56	1.16	0.28	0.45	0.59	0.58
A1FI	Mullingar II	1.35	1.04	0.98	1.18	1.01	0.58	0.54	1.20	0.28	0.47	0.63	0.60
A1FI	Kilkenny	1.30	0.97	1.02	1.25	1.02	0.56	0.56	1.20	0.29	0.46	0.67	0.61
A1FI	Casement	1.35	0.95	0.96	1.20	1.03	0.56	0.50	1.17	0.29	0.45	0.64	0.60
A1FI	Cork	1.22	0.87	0.89	1.05	0.94	0.52	0.54	1.07	0.25	0.40	0.65	0.53
A1FI	Birr	1.38	1.03	1.00	1.22	1.09	0.58	0.57	1.19	0.29	0.46	0.64	0.61

DJF = December, January, February; MAM = March, April, May; JJA = June, July, August; SON = September, October, November.

Table A.Va 2. A2 scaling factors for statistically downscaled temperature (2070–2099).

SRES	Station	CGCM2				CSIRO Mk2				HadCM3			
		DJF	MAM	JJA	SON	DJF	MAM	JJA	SON	DJF	MAM	JJA	SON
A2	Valentia	0.85	0.71	0.86	0.75	0.93	0.43	0.54	0.82	0.35	0.47	0.63	0.58
A2	Shannon	0.96	0.77	0.99	0.86	1.06	0.49	0.64	0.96	0.39	0.54	0.74	0.66
A2	Dublin	0.71	0.65	0.89	0.87	0.81	0.46	0.57	0.94	0.33	0.51	0.78	0.65
A2	Malin Head	0.71	0.65	0.75	0.69	0.79	0.43	0.45	0.79	0.31	0.42	0.60	0.56
A2	Roche's Point	0.80	0.55	0.79	0.72	0.90	0.41	0.61	0.81	0.33	0.44	0.80	0.56
A2	Belmullet	0.80	0.71	0.83	0.67	0.91	0.44	0.59	0.84	0.33	0.46	0.65	0.57
A2	Clones	0.98	0.79	1.03	0.87	1.08	0.51	0.69	0.97	0.40	0.57	0.76	0.69
A2	Rosslare	0.81	0.46	0.70	0.72	0.86	0.39	0.50	0.84	0.32	0.44	0.66	0.58
A2	Claremorris	0.98	0.80	1.01	0.88	1.09	0.50	0.70	0.97	0.40	0.55	0.73	0.67
A2	Mullingar II	0.99	0.80	1.04	0.90	1.06	0.52	0.68	1.00	0.40	0.58	0.79	0.69
A2	Kilkenny	0.95	0.75	1.08	0.95	1.07	0.50	0.71	1.00	0.41	0.56	0.84	0.70
A2	Casement	0.99	0.72	1.01	0.91	1.08	0.50	0.62	0.98	0.41	0.55	0.80	0.70
A2	Cork	0.89	0.66	0.94	0.79	0.98	0.46	0.68	0.89	0.36	0.49	0.82	0.62
A2	Birr	1.01	0.79	1.06	0.93	1.14	0.51	0.72	0.99	0.42	0.56	0.80	0.70

DJF = December, January, February; MAM = March, April, May; JJA = June, July, August; SON = September, October, November.

Table A.Va 3. B2 Scaling factors for statistically downscaled temperature (2070–2099).

SRES	Station	CGCM2				CSIRO Mk2				HadCM3			
		DJF	MAM	JJA	SON	DJF	MAM	JJA	SON	DJF	MAM	JJA	SON
B2	Valentia	1.19	0.90	0.80	1.00	0.92	0.49	0.48	0.95	0.24	0.39	0.53	0.48
B2	Shannon	1.33	1.00	0.93	1.15	1.06	0.55	0.57	1.12	0.27	0.44	0.63	0.56
B2	Dublin	1.02	0.86	0.84	1.13	0.82	0.54	0.52	1.11	0.21	0.42	0.64	0.57
B2	Malin Head	0.94	0.79	0.71	0.91	0.80	0.48	0.42	0.94	0.22	0.35	0.50	0.48
B2	Roche's Point	1.10	0.74	0.74	0.95	0.87	0.48	0.53	0.94	0.23	0.36	0.65	0.48
B2	Belmullet	1.11	0.92	0.79	0.91	0.93	0.50	0.51	0.99	0.22	0.38	0.55	0.48
B2	Clones	1.34	1.03	1.00	1.17	1.06	0.58	0.57	1.15	0.27	0.46	0.64	0.58
B2	Rosslare	1.11	0.62	0.64	1.00	0.85	0.45	0.43	0.99	0.22	0.35	0.58	0.49
B2	Claremorris	1.36	1.07	0.94	1.18	1.06	0.57	0.57	1.13	0.27	0.44	0.61	0.57
B2	Mullingar II	1.33	1.05	0.97	1.20	1.06	0.58	0.57	1.18	0.27	0.47	0.65	0.59
B2	Kilkenny	1.31	0.99	0.99	1.25	1.05	0.58	0.61	1.18	0.29	0.46	0.69	0.61
B2	Casement	1.35	0.96	0.96	1.22	1.06	0.58	0.55	1.19	0.28	0.45	0.66	0.60
B2	Cork	1.22	0.86	0.89	1.08	0.96	0.53	0.58	1.05	0.25	0.41	0.68	0.52
B2	Birr	1.39	1.05	1.00	1.25	1.09	0.59	0.60	1.17	0.29	0.46	0.66	0.60

DJF = December, January, February; MAM = March, April, May; JJA = June, July, August; SON = September, October, November.

Table A.Va 4. B1 Scaling factors for statistically downscaled temperature (2070–2099).

SRES	Station	CGCM2				CSIRO Mk2				HadCM3			
		DJF	MAM	JJA	SON	DJF	MAM	JJA	SON	DJF	MAM	JJA	SON
B1	Valentia	1.17	0.93	0.81	1.01	0.94	0.50	0.50	0.95	0.23	0.38	0.55	0.49
B1	Shannon	1.33	1.01	0.93	1.15	1.06	0.56	0.57	1.12	0.26	0.44	0.63	0.56
B1	Dublin	0.98	0.85	0.84	1.17	0.83	0.53	0.52	1.10	0.22	0.42	0.66	0.55
B1	Malin Head	0.99	0.85	0.70	0.93	0.81	0.50	0.44	0.92	0.21	0.35	0.53	0.47
B1	Roche's Point	1.10	0.72	0.74	0.97	0.91	0.47	0.55	0.94	0.22	0.36	0.68	0.47
B1	Belmullet	1.11	0.93	0.78	0.91	0.92	0.51	0.53	0.98	0.22	0.37	0.56	0.48
B1	Clones	1.35	1.03	0.96	1.17	1.07	0.59	0.61	1.14	0.27	0.47	0.65	0.59
B1	Rosslare	1.12	0.60	0.65	0.98	0.87	0.45	0.48	0.97	0.22	0.36	0.57	0.48
B1	Claremorris	1.35	1.05	0.95	1.18	1.08	0.57	0.62	1.13	0.27	0.45	0.63	0.57
B1	Mullingar II	1.36	1.04	0.97	1.21	1.06	0.59	0.60	1.17	0.27	0.48	0.67	0.59
B1	Kilkenny	1.31	0.98	1.01	1.27	1.06	0.58	0.62	1.17	0.28	0.46	0.71	0.60
B1	Casement	1.36	0.95	0.95	1.22	1.07	0.57	0.56	1.15	0.28	0.45	0.68	0.59
B1	Cork	1.23	0.87	0.88	1.07	0.99	0.53	0.60	1.04	0.24	0.40	0.69	0.52
B1	Birr	1.39	1.03	1.00	1.24	1.13	0.59	0.63	1.17	0.28	0.46	0.67	0.59

DJF = December, January, February; MAM = March, April, May; JJA = June, July, August; SON = September, October, November.

Appendix Vb

Scaling Factors for Statistically Downscaled Precipitation (2070–2099)

Table A.Vb 1. A1FI scaling factors for statistically downscaled precipitation (2070–2099).

SRES	Station	CGCM2				CSIRO Mk2				HadCM3			
		DJF	MAM	JJA	SON	DJF	MAM	JJA	SON	DJF	MAM	JJA	SON
A1FI	Valentia	-0.86	-5.28	-6.66	-6.23	0.03	-0.27	-5.12	-4.74	2.03	1.06	-5.00	-2.58
A1FI	Shannon	1.11	-10.05	-7.50	-3.53	3.37	0.14	-6.24	-1.73	3.61	1.39	-4.43	-0.50
A1FI	Dublin	8.05	-6.06	-11.07	-4.30	9.36	0.06	-8.91	-2.63	5.59	1.00	-5.39	-1.92
A1FI	Malin Head	1.02	-8.97	-5.09	-0.54	1.14	0.23	-2.74	0.25	2.15	1.66	-2.09	0.33
A1FI	Roche's Point	1.83	-1.63	-7.40	-7.41	2.60	-0.23	-9.06	-5.31	3.33	0.93	-5.45	-3.07
A1FI	Belmullet	-0.50	-6.25	-4.38	-2.01	0.31	0.14	-3.05	-1.26	2.03	1.17	-2.10	-0.26
A1FI	Clones	5.62	-8.79	-6.55	-3.37	7.03	0.11	-3.47	-1.57	4.88	1.71	-3.50	-0.44
A1FI	Rosslare	2.82	-4.80	-4.95	-4.10	4.35	-0.25	-6.59	-3.23	3.74	0.75	-4.17	-2.25
A1FI	Claremorris	4.68	-6.92	-1.76	-4.13	5.28	-0.08	-2.94	-2.58	3.63	1.56	-3.51	-0.46
A1FI	Mullingar II	4.70	-8.84	-8.26	2.06	6.98	0.29	-5.19	1.68	4.95	1.34	-4.40	2.34
A1FI	Kilkenny	4.26	-7.62	-4.42	-6.03	5.48	-0.01	-4.04	-4.32	4.54	1.12	-4.92	-2.36
A1FI	Casement	5.58	-6.73	-10.89	-2.70	7.24	0.33	-6.39	-1.64	4.45	1.07	-5.05	-1.27
A1FI	Cork	0.22	-3.64	-4.39	-6.37	1.18	-0.28	-6.13	-4.32	3.01	0.86	-5.33	-1.64
A1FI	Birr	5.58	-7.89	-8.24	-2.00	7.94	0.25	-4.99	-1.13	5.57	1.28	-4.54	-0.61

DJF = December, January, February; MAM = March, April, May; JJA = June, July, August; SON = September, October, November.

Table A.Vb 2. A2 scaling factors for statistically downscaled precipitation (2070–2099).

SRES	Station	CGCM2				CSIRO Mk2				HadCM3			
		DJF	MAM	JJA	SON	DJF	MAM	JJA	SON	DJF	MAM	JJA	SON
A2	Valentia	-1.28	-5.89	-4.91	-6.33	0.47	-2.07	-6.58	-5.55	2.31	-1.95	-7.38	-3.71
A2	Shannon	0.66	-10.22	-5.37	-4.09	3.89	-0.38	-7.72	-2.02	4.43	0.09	-6.42	-1.01
A2	Dublin	7.49	-6.59	-7.35	-4.73	10.01	-0.70	-10.42	-3.08	7.07	-2.32	-8.03	-2.86
A2	Malin Head	0.57	-9.24	-4.04	-1.62	1.60	-0.01	-4.18	0.30	2.47	1.82	-2.49	0.06
A2	Roche's Point	1.37	-2.57	-5.32	-7.30	3.10	-1.90	-10.58	-6.22	4.04	-2.78	-8.14	-4.34
A2	Belmullet	-0.93	-6.77	-3.64	-2.83	0.76	-0.37	-4.49	-1.47	2.31	-1.27	-2.51	-0.71
A2	Clones	5.10	-9.08	-4.85	-3.96	7.64	-0.52	-4.92	-1.84	6.12	2.12	-4.87	-0.93
A2	Rosslare	2.35	-5.45	-3.96	-4.56	4.89	-1.97	-8.07	-3.78	4.60	-3.87	-5.98	-3.29
A2	Claremorris	4.17	-7.38	-2.20	-4.59	5.84	-1.28	-4.37	-3.01	4.45	1.19	-4.88	-0.96
A2	Mullingar II	4.20	-9.12	-5.79	0.53	7.58	0.24	-6.66	1.98	6.22	-0.21	-6.38	2.67
A2	Kilkenny	3.76	-8.01	-3.67	-6.16	6.05	-0.99	-5.49	-5.05	5.67	-1.60	-7.25	-3.43
A2	Casement	5.07	-7.21	-7.25	-3.40	7.85	0.38	-7.87	-1.92	5.55	-1.86	-7.46	-2.00
A2	Cork	-0.22	-4.40	-3.65	-6.44	1.64	-2.10	-7.61	-5.05	3.62	-3.23	-7.92	-2.49
A2	Birr	5.07	-8.26	-5.78	-2.82	8.57	0.07	-6.45	-1.31	7.05	-0.55	-6.61	-1.15

DJF = December, January, February; MAM = March, April, May; JJA = June, July, August; SON = September, October, November.

Table A.Vb 3. B2 scaling factors for statistically downscaled precipitation (2070–2099).

SRES	Station	CGCM2				CSIRO Mk2				HadCM3			
		DJF	MAM	JJA	SON	DJF	MAM	JJA	SON	DJF	MAM	JJA	SON
B2	Valentia	-1.15	-4.26	-5.89	-5.61	-0.27	-0.77	-5.51	-4.94	2.64	1.84	-5.99	-2.83
B2	Shannon	2.30	-9.01	-6.71	-1.83	2.74	0.43	-5.91	-2.08	2.79	1.90	-4.94	-0.30
B2	Dublin	8.17	-5.24	-9.60	-3.64	9.18	0.43	-8.08	-3.25	6.06	1.89	-5.34	-1.20
B2	Malin Head	2.22	-8.46	-1.71	2.20	1.46	-0.35	-2.15	-0.59	1.58	2.05	-2.27	0.79
B2	Roche's Point	1.37	-0.92	-5.70	-6.28	2.31	0.40	-8.23	-5.28	4.42	1.81	-6.23	-3.21
B2	Belmullet	0.33	-5.50	-2.14	-0.31	0.60	-0.35	-2.34	-0.72	1.39	1.98	-3.44	-0.31
B2	Clones	6.72	-7.68	-3.73	-2.56	6.66	0.22	-2.87	-1.58	4.42	2.92	-3.32	-0.45
B2	Rosslare	3.19	-3.32	-3.71	-3.83	3.66	0.28	-4.51	-3.10	4.58	1.49	-3.99	-2.08
B2	Claremorris	4.91	-5.80	-0.52	-2.68	5.22	-0.80	-2.23	-1.95	3.51	2.87	-3.16	-0.85
B2	Mullingar II	5.20	-8.40	-5.36	2.96	6.80	0.83	-3.73	3.20	4.68	1.46	-4.78	2.26
B2	Kilkenny	4.35	-6.63	-2.72	-4.79	5.20	0.41	-1.82	-4.46	5.13	2.08	-5.66	-2.16
B2	Casement	5.30	-5.14	-9.36	-3.06	7.24	0.89	-6.42	-3.09	5.32	1.79	-4.55	-0.81
B2	Cork	-0.15	-3.04	-3.50	-4.04	0.37	0.14	-5.74	-2.83	4.27	1.82	-6.30	-1.54
B2	Birr	6.17	-6.94	-6.80	-1.78	7.83	0.43	-4.72	-1.89	5.24	2.21	-4.82	0.29

DJF = December, January, February; MAM = March, April, May; JJA = June, July, August; SON = September, October, November.

Table A.Vb 4. B1 scaling factors for statistically downscaled precipitation (2070–2099).

SRES	Station	CGCM2				CSIRO Mk2				HadCM3			
		DJF	MAM	JJA	SON	DJF	MAM	JJA	SON	DJF	MAM	JJA	SON
B1	Valentia	-0.34	-3.88	-4.08	-4.59	-0.34	-0.07	-3.91	-4.75	2.32	2.34	-5.56	-2.32
B1	Shannon	1.62	-8.65	-4.93	-1.89	2.99	0.34	-5.03	-1.73	3.90	2.66	-4.98	-0.24
B1	Dublin	8.56	-4.65	-8.49	-2.66	8.98	0.26	-7.70	-2.64	5.87	2.28	-5.94	-1.66
B1	Malin Head	1.53	-7.57	-2.52	1.10	0.76	0.43	-1.53	0.25	2.44	2.94	-2.64	0.59
B1	Roche's Point	2.35	-0.23	-4.83	-5.76	2.23	-0.03	-7.86	-5.32	3.61	2.20	-6.01	-2.81
B1	Belmullet	0.02	-4.85	-1.80	-0.36	-0.06	0.34	-1.85	-1.26	2.32	2.44	-2.66	0.00
B1	Clones	6.13	-7.39	-3.97	-1.72	6.66	0.31	-2.26	-1.58	5.16	2.98	-4.06	-0.17
B1	Rosslare	3.34	-3.39	-2.37	-2.45	3.98	-0.05	-5.38	-3.24	4.02	2.03	-4.72	-1.99
B1	Claremorris	5.19	-5.52	0.81	-2.48	4.90	0.12	-1.73	-2.58	3.92	2.83	-4.07	-0.19
B1	Mullingar II	5.21	-7.43	-5.68	3.70	6.60	0.49	-3.98	1.68	5.24	2.61	-4.96	2.60
B1	Kilkenny	4.77	-6.21	-1.85	-4.39	5.10	0.19	-2.83	-4.33	4.83	2.39	-5.48	-2.10
B1	Casement	6.10	-5.33	-8.32	-1.05	6.86	0.53	-5.19	-1.65	4.74	2.35	-5.61	-1.00
B1	Cork	0.74	-2.23	-1.81	-4.73	0.80	-0.08	-4.92	-4.32	3.29	2.13	-5.88	-1.38
B1	Birr	6.10	-6.49	-5.66	-0.35	7.57	0.45	-3.78	-1.13	5.85	2.56	-5.10	-0.35

DJF = December, January, February; MAM = March, April, May; JJA = June, July, August; SON = September, October, November.

Appendix VI

PRediction Of Surface Point Environmental Changes over Time (PROSPECT)

PROSPECT was developed at the National University of Ireland Maynooth by Ciaran McCarthy, Thomas Murphy, Mark Clerkin, Rowan Fealy and Phil Maguire in a collaboration between the Departments of Geography and Computer Science.

Screen shot – Title page

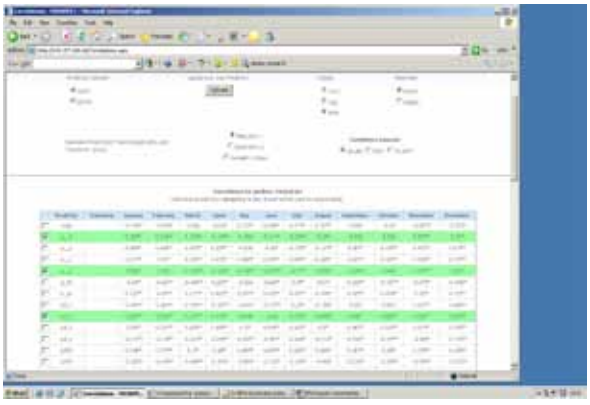

Screen shot – Correlation Analysis

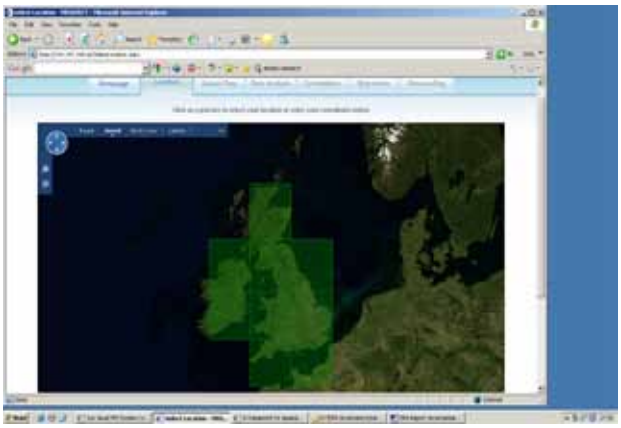

Screen shot – Select Location

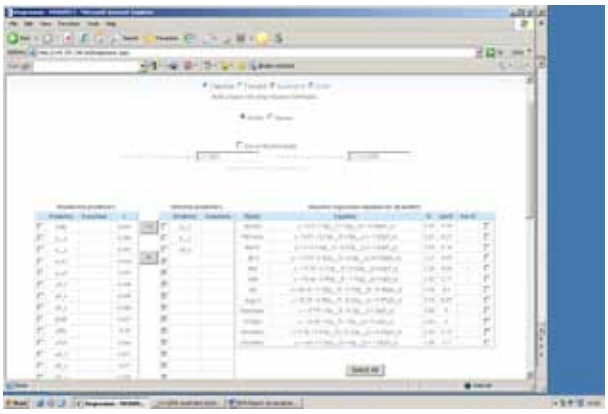

Screen Shot – Regression Analysis

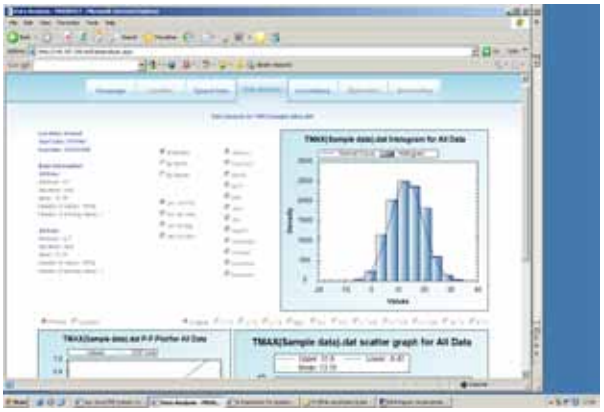

Screen shot – Data Analysis

An Ghníomhaireacht um Chaomhnú Comhshaoil

Is í an Gníomhaireacht um Chaomhnú Comhshaoil (EPA) comhlachta reachtúil a chosnaíonn an comhshaol do mhuintir na tíre go léir. Rialaímid agus déanaimid maoirsiú ar ghníomhaíochtaí a d'fhéadfadh truailliú a chruthú murach sin. Cinntímid go bhfuil eolas cruinn ann ar threochtaí comhshaoil ionas go nglactar aon chéim is gá. Is iad na príomh-nithe a bhfuilimid gníomhach leo ná comhshaol na hÉireann a chosaint agus cinntiú go bhfuil forbairt inbhuanaithe.

Is comhlacht poiblí neamhspleách í an Ghníomhaireacht um Chaomhnú Comhshaoil (EPA) a bunaíodh i mí Iúil 1993 faoin Acht fán nGníomhaireacht um Chaomhnú Comhshaoil 1992. Ó thaobh an Rialtais, is í an Roinn Comhshaoil agus Rialtais Áitiúil a dhéanann urraíocht uirthi.

ÁR bhFREAGRACHTAÍ

CEADÚNÚ

Bíonn ceadúnais á n-eisiúint againn i gcomhair na nithe seo a leanas chun a chinntiú nach mbíonn astuithe uathu ag cur sláinte an phobail ná an comhshaol i mbaol:

- áiseanna dramhaíola (m.sh., líonadh talún, loisceoirí, stáisiúin aistrithe dramhaíola);
- gníomhaíochtaí tionsclaíocha ar scála mór (m.sh., déantúsaíocht cógaisíochta, déantúsaíocht stroighne, stáisiúin chumhachta);
- diantalmhaíocht;
- úsáid faoi shrian agus scaoileadh smachtaithe Orgánach Géinathraithe (GMO);
- mór-áiseanna stórais peitreail.
- Scardadh dramhuisce

FEIDHMIÚ COMHSHAOIL NÁISIÚNTA

- Stiúradh os cionn 2,000 iniúchadh agus cigireacht de áiseanna a fuair ceadúnas ón nGníomhaireacht gach bliain.
- Maoirsiú freagrachtaí cosanta comhshaoil údarás áitiúla thar sé earnáil - aer, fuaim, dramhaíl, dramhuisce agus caighdeán uisce.
- Obair le húdaráis áitiúla agus leis na Gardaí chun stop a chur le gníomhaíocht mhídhleathach dramhaíola trí comhordú a dhéanamh ar líonra forfheidhmithe náisiúnta, díriú isteach ar chiontóirí, stiúradh fiosrúcháin agus maoirsiú leigheas na bhfadhbanna.
- An dlí a chur orthu siúd a bhriseann dlí comhshaoil agus a dhéanann dochar don chomhshaol mar thoradh ar a ngníomhaíochtaí.

MONATÓIREACHT, ANAILÍS AGUS TUAIRISCIÚ AR AN GCOMHSHAOL

- Monatóireacht ar chaighdeán aeir agus caighdeáin aibhneacha, locha, uiscí taoide agus uiscí talaimh; leibhéil agus sruth aibhneacha a thomhas.
- Tuairisciú neamhspleách chun cabhrú le rialtais náisiúnta agus áitiúla cinntí a dhéanamh.

RIALÚ ASTUITHE GÁIS CEAPTHA TEASA NA HÉIREANN

- Cainníochtú astuithe gáis ceaptha teasa na hÉireann i gcomhthéacs ár dtiomantas Kyoto.
- Cur i bhfeidhm na Treorach um Thrádáil Astuithe, a bhfuil baint aige le hos cionn 100 cuideachta atá ina mór-ghineadóirí dé-ocsaíd charbóin in Éirinn.

TAIGHDE AGUS FORBAIRT COMHSHAOIL

- Taighde ar shaincheisteanna comhshaoil a chomhordú (cosúil le caighdéan aeir agus uisce, athrú aeráide, bithéagsúlacht, teicneolaíochtaí comhshaoil).

MEASÚNÚ STRAITÉISEACH COMHSHAOIL

- Ag déanamh measúnú ar thionchar phleananna agus chláracha ar chomhshaol na hÉireann (cosúil le pleananna bainistíochta dramhaíola agus forbartha).

PLEANÁIL, OIDEACHAS AGUS TREOIR CHOMHSHAOIL

- Treoir a thabhairt don phobal agus do thionscal ar cheisteanna comhshaoil éagsúla (m.sh., iarratais ar cheadúnais, seachaint dramhaíola agus rialacháin chomhshaoil).
- Eolas níos fearr ar an gcomhshaol a scaipeadh (trí cláracha teilifíse comhshaoil agus pacáistí acmhainne do bhunscoileanna agus do mheánscoileanna).

BAINISTÍOCHT DRAMHAÍOLA FHORGHNÍOMHACH

- Cur chun cinn seachaint agus laghdú dramhaíola trí chomhordú An Chláir Náisiúnta um Chosc Dramhaíola, lena n-áirítear cur i bhfeidhm na dTionscnamh Freagrachta Táirgeoirí.
- Cur i bhfeidhm Rialachán ar nós na treoracha maidir le Trealamh Leictreach agus Leictreonach Caite agus le Srianadh Substaintí Guaiseacha agus substaintí a dhéanann ídiú ar an gcrios ózóin.
- Plean Náisiúnta Bainistíochta um Dramhaíl Ghuaiseach a fhorbairt chun dramhaíl ghuaiseach a sheachaint agus a bhainistiú.

STRUCHTÚR NA GNÍOMHAIREACHTA

Bunaíodh an Ghníomhaireacht i 1993 chun comhshaol na hÉireann a chosaint. Tá an eagraíocht á bhainistiú ag Bord lánaimseartha, ar a bhfuil Príomhstiúrthóir agus ceithre Stiúrthóir.

Tá obair na Gníomhaireachta ar siúl trí ceithre Oifig:

- An Oifig Aeráide, Ceadúnaithe agus Úsáide Acmhainní
- An Oifig um Fhorfheidhmiúchán Comhshaoil
- An Oifig um Measúnacht Comhshaoil
- An Oifig Cumarsáide agus Seirbhísí Corparáide

Tá Coiste Comhairleach ag an nGníomhaireacht le cabhrú léi. Tá dáréag ball air agus tagann siad le chéile cúpla uair in aghaidh na bliana le plé a dhéanamh ar cheisteanna ar ábhar imní iad agus le comhairle a thabhairt don Bhord.

NDP
National Development Plan 2007 - 2013

Science, Technology, Research and Innovation for the Environment (STRIVE) 2007-2013

The Science, Technology, Research and Innovation for the Environment (STRIVE) programme covers the period 2007 to 2013.

The programme comprises three key measures: Sustainable Development, Cleaner Production and Environmental Technologies, and A Healthy Environment; together with two supporting measures: EPA Environmental Research Centre (ERC) and Capacity & Capability Building. The seven principal thematic areas for the programme are Climate Change; Waste, Resource Management and Chemicals; Water Quality and the Aquatic Environment; Air Quality, Atmospheric Deposition and Noise; Impacts on Biodiversity; Soils and Land-use; and Socio-economic Considerations. In addition, other emerging issues will be addressed as the need arises.

The funding for the programme (approximately €100 million) comes from the Environmental Research Sub-Programme of the National Development Plan (NDP), the Inter-Departmental Committee for the Strategy for Science, Technology and Innovation (IDC-SSTI); and EPA core funding and co-funding by economic sectors.

The EPA has a statutory role to co-ordinate environmental research in Ireland and is organising and administering the STRIVE programme on behalf of the Department of the Environment, Heritage and Local Government.

epa
Environmental Protection Agency
An Ghníomhaireacht um Chaomhnú Comhshaoil

ENVIRONMENTAL PROTECTION AGENCY
PO Box 3000, Johnstown Castle Estate, Co. Wexford, Ireland
t 053 916 0600 f 053 916 0699
LoCall 1890 33 55 99
e info@epa.ie w http://www.epa.ie

SSTI
Strategy for Science, Technology and Innovation

Comhshaol, Oidhreacht agus Rialtas Áitiúil
Environment, Heritage and Local Government